2011

Mechanisms contributing to the deep chlorophyll maximum in Lake Superior

Marcel L. Dijkstra
Michigan Technological University

MECHANISMS CONTRIBUTING TO THE DEEP CHLOROPHYLL MAXIMUM IN LAKE SUPERIOR

By

Marcel L. Dijkstra

A THESIS

Submitted in partial fulfillment of the requirements for the degree of

MASTER OF SCIENCE

(Environmental Engineering)

MICHIGAN TECHNOLOGICAL UNIVERSITY

2011

This thesis, “Mechanisms Contributing to the Deep Chlorophyll Maximum in Lake Superior,” is hereby approved in partial fulfillment of the requirements for the Degree of MASTER OF SCIENCE IN ENVIRONMENTAL ENGINEERING.

Department of Civil and Environmental Engineering

Signatures:

Thesis Advisor _____

Dr. Martin Auer

Department Chair _____

Dr. David Hand

Date _____

Contents

List of Figures

List of Tables

Acknowledgements

It was during the Surface Water Quality Modeling class that Dr. Marty Auer intrigued me with stories about unexplained sub-surface chlorophyll peaks in Lake Superior. After reviewing preliminary modeling results our interest in this mystery became unbearable and further exploration resulted in this thesis. I am very grateful he saw enough in me to give me the opportunity to explore this topic with him and let me become part of his research team. As my advisor, Marty kept me from wandering off into the woods and his insight, experience and drive were instrumental to bring this project to a satisfactory end. I look forward to our continued work on the Great Lakes.

This research would not have been possible without data and results from work done by Laura A. Bub (Lake Superior phytoplankton temperature and light response experiments), Kimberly D. Elenbaas (Heterotrophic Bacterioplankton biologs). EPA data received from Dr. Rick Barbiero (Lake Superior chlorophyll profiles) and Dr. Peder M. Yurista (Lake Superior zooplankton profile) and data received from Dr. Robert W. Sterner (Lake Superior production profiles). Sampling in 2011 for the GLRI project Predicting Ecosystem Changes in Lake Superior provided me with practical insights in the dynamics of Lake Superior as well as valuable water column profiles.

I want to thank my advising committee: Dr. Nancy Auer and Dr. David Watkins for taking time out of their over full schedules to review my work and offer suggestions. Their contribution resulted in a deeper and better understanding of the material covered in this thesis.

Numerous fellow students listened to my new discoveries and little victories as well as gave feedback on ideas and work in progress, in particular Aaron Dayton, Renn Lambert, Sue Larson and especially my office partner Rasika Gawde. Her clear insight in mathematical equations and enthusiasm for modeling kept me going when inertia could have taken over.

I am very thankful for my parents, brother and sister, although far away, through internet and phone calls they kept up with my progress and supported me where possible.

It is a great joy to come home and hear three excited voices shouting: daddy is home, daddy is home! My children; Anna-Irene, Mathijs and Thomas inspired me daily to give my best effort and to be a good example. They also helped me to relax and take a step back when I most needed it; fishing, biking or skating rejuvenated and energized me, thank you for being part of my world.

However nothing would have been possible without my wife's support, Chris is my strength and never failed to keep me focused. Her heroic efforts made it possible to continue when the world seemed to fall apart, her attitude, flexibility and faith have kept our family strong and full of love. Her value is truly beyond measure and words cannot express what she means to me, dank je wel schat, ik hou van jou!

Abstract

The seasonal appearance of a deep chlorophyll maximum (DCM) in Lake Superior is a striking phenomenon that is widely observed; however its mechanisms of formation and maintenance are not well understood. As this phenomenon may be the reflection of an ecological driver, or a driver itself, a lack of understanding its driving forces limits the ability to accurately predict and manage changes in this ecosystem. Key mechanisms generally associated with DCM dynamics (i.e. ecological, physiological and physical phenomena) are examined individually and in concert to establish their role. First the prevailing paradigm, “the DCM is a great place to live”, is analyzed through an integration of the results of laboratory experiments and field measurements. The analysis indicates that growth at this depth is severely restricted and thus not able to explain the full magnitude of this phenomenon. Additional contributing mechanisms like photoadaptation, settling and grazing are reviewed with a one-dimensional mathematical model of chlorophyll and particulate organic carbon.

Settling has the strongest impact on the formation and maintenance of the DCM, transporting biomass to the metalimnion and resulting in the accumulation of algae, i.e. a peak in the particulate organic carbon profile. Subsequently, shade adaptation becomes manifest as a chlorophyll maximum deeper in the water column where light conditions particularly favor the process. Shade adaptation mediates the magnitude, shape and vertical position of the chlorophyll peak. Growth at DCM depth shows only a marginal contribution, while grazing has an adverse effect on the extent of the DCM. The observed separation of the

carbon biomass and chlorophyll maximum should caution scientists to equate the DCM with a large nutrient pool that is available to higher trophic levels.

The ecological significance of the DCM should not be separated from the underlying carbon dynamics. When evaluated in its entirety, the DCM becomes the projected image of a structure that remains elusive to measure but represents the foundation of all higher trophic levels.

These results also offer guidance in examine ecosystem perturbations such as climate change. For example, warming would be expected to prolong the period of thermal stratification, extending the late summer period of suboptimal (phosphorus-limited) growth and attendant transport of phytoplankton to the metalimnion. This reduction in epilimnetic algal production would decrease the supply of algae to the metalimnion, possibly reducing the supply of prey to the grazer community. This work demonstrates the value of modeling to challenge and advance our understanding of ecosystem dynamics, steps vital to reliable testing of management alternatives.

1.0 Introduction

A number of striking physical, chemical and biological signals, occurring across time and space and in both freshwater and marine environments, have attracted the interest of the research community. In Lake Superior, these signals include the thermal bar (Auer and Gatzke 2004), the benthic nepheloid layer (Urban et al. 2004) and heterogeneity in the vertical distribution of zooplankton (Yurista 2009). One of the most widely observed signals in Lake Superior and others of the Laurentian Great Lakes is the deep chlorophyll maximum observed as a sub-surface peak in chlorophyll-a concentrations (DCM; Barbiero and Tuchman 2001). Each of these signals can serve as both a driving force and reflection of ecological processes.

The DCM has been most commonly observed in oligotrophic systems that thermally stratify. With the onset of stratification, metalimnetic chlorophyll levels increase, and a DCM becomes manifest there within a few days. Over time, the location of peak chlorophyll concentration deepens, and the amount of chlorophyll resident within that peak increases, resulting in a well defined, characteristic shape (Figure 1.1). Deepening of the peak in the DCM continues through the stratified interval, potentially reaching the metalimnetic-hypolimnetic boundary, and the peaked nature of the signal becomes less pronounced. At turnover, stability is lost, and vertical mixing redistributes the chlorophyll over the entire water column (Reynolds 1994).

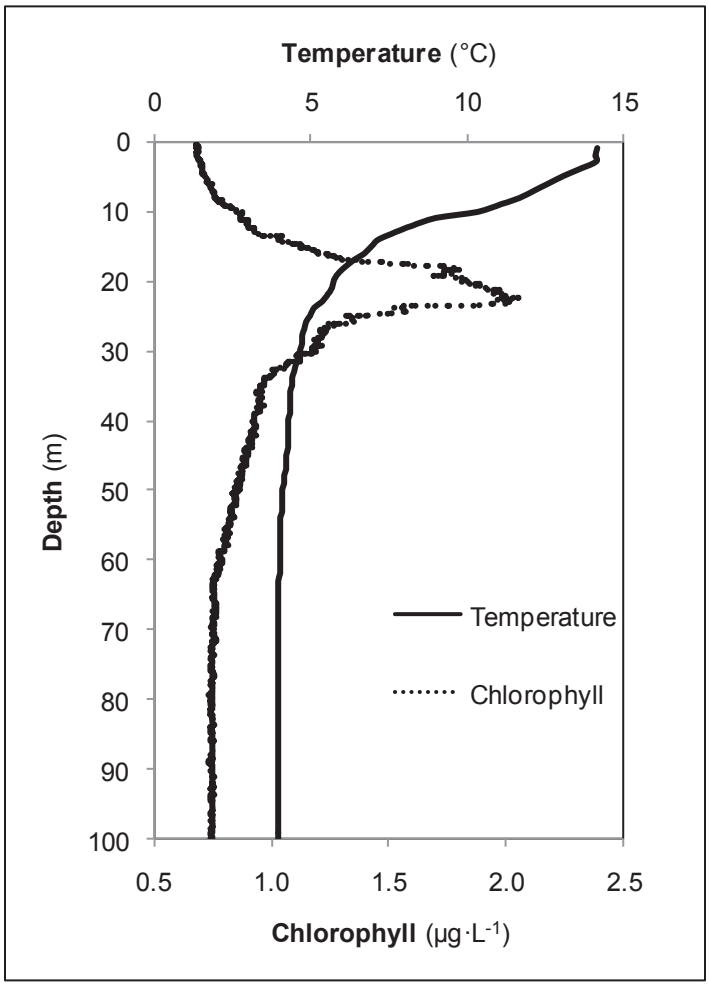

Figure 1.1 Profile of chlorophyll-a concentration and temperature in Lake Superior on July 28, 2011(data from GLRI-Predicting Ecosystem Changes in Lake Superior project)

The DCM is a prominent feature of many dimictic lakes in temperate freshwater environments and oligotrophic oceans, but has also been observed in polymictic (Bahia de Punto, a tropical lake, Vincent et al. 1986) and permanently stratified waters (tropical Pacific Ocean; Vaillancourt et al. 2003); near sea level (fresh waters and Antarctic saline; Holm-Hansen and Hewes 2004, Burnett et al. 2006) and at alpine elevations (>3000 meters; Saros et al. 2005); and in shallow waters (~2 meters, an oxbow lake in Hungary; Grigorszky et al. 2003) and at great depth (150 meters, Ionean Sea in the eastern Mediterranean; Casotti et al. 2003). The DCM has been shown to be ephemeral (persisting for as little as a few days; Abbott et al. 1984), as well as permanent in character (lasting for years; Duteil et al. 2009). The development, maintenance and dissipation of the deep chlorophyll maximum may thus be considered a phenomenon of global interest (Priscu and Goldman 1983, Duteil et al. 2009).

More attention has been focused on describing the spatial and temporal structure of the DCM and its mechanisms of formation than on the ecological significance of the phenomenon. Research driven by climate change concerns has indicated that algae, while representing only 0.2% of global primary producer biomass, are responsible for nearly half of global primary production (due to their rapid turnover times; Field et al. 1998). At the peak of its development, chlorophyll present in the DCM can represent on the order of 60% of that in the photic zone. If the organisms present within the DCM are photosynthetically active, this layer may make an important contribution to net water column primary production. For example, Williamson et al. (2010) have recently described an

approach, based on satellite imaging, for estimating depth-integrated (i.e. including the DCM) production in marine environments.

In a more general sense, an understanding of the role of the DCM in ecosystem function and the forcing conditions mediating its behavior are important in developing predictive ecosystem models, especially for oligotrophic environments. As the DCM is one of the most striking signals in oligotrophic waters (where seasonal dynamics tend to be slow and modest in magnitude), study of this phenomenon offers an excellent opportunity to challenge and advance our conceptual understanding. Finally, it is only when we can adequately model such strong signals, irrespective of their ecological significance, that we can achieve the requisite confidence of our ability to simulate the ecosystem at large.

The DCM has been known for more than 100 years, with some of the earliest observations being derived from reports of metalimnetic oxygen maxima (e.g. Elkhart Lake, Wisconsin, Birge and Juday 1911). *In situ* chlorophyll profiles later provided direct evidence of the DCM (North Pacific Ocean, Anderson 1969; experimental lakes area northwestern Ontario; Fee 1976). Observations of the presence and spatiotemporal dynamics of the DCM in widely differing environments have challenged scientists to identify the factors and processes responsible for its formation, maintenance and dissipation. The majority of studies have focused on biological factors, e.g. growth-favorable habitat, photo-adaptation and the vertical distribution of zooplankton grazing pressure, while others have concentrated on physical mechanisms such as sedimentation.

However, after decades of research there is no generally-accepted mechanism leading to DCM formation (Sterner 2010), nor is there consensus regarding its ecological importance (e.g. Barbiero and Tuchman 2004). Thus, the long-standing failure of the scientific community to reach agreement on the ecological significance (i.e. home or graveyard) of the DCM and the factors mediating its temporal and spatial dynamics serves as an appropriate starting point for further investigation. This work explores the relative importance of mechanisms of DCM formation, maintenance and dissipation in Lake Superior using results from laboratory experiments, field measurements and model simulations.

1.1 The DCM in Lake Superior

Lake Superior is a deep (maximum, 400 m), clear (compensation depth at times >40 m; Sterner 2010), oligotrophic (total phosphorus 0.4 – 1.0 $\mu g \cdot L^{-1}$, Anagnostou and Sherrell 2008) system. The lake is dimictic, generally stratifying for approximately four months beginning in late June. The thermocline, resident at ~20 m in August, deepens progressively to ~40 m towards fall turnover (Auer and Bub 2004). This vertical progression of thermal structure over the stratified interval is similar to that noted for other temperate lakes where the DCM is observed. In Lake Superior, the DCM forms with the onset of stratification and persists until turnover. Inter-annual climatic fluctuations impact its temporal and spatial nature (e.g. Auer and Bub, 2004, Barbiero and Tuchman 2004, Sterner 2010). Peak chlorophyll concentrations of 0.9 – 4.2 $\mu g \cdot L^{-1}$ are located at depths of 20 to 40 m (Barbiero and Tuchman 2001) and markedly exceed surface water

concentrations (0.4 – 1.0 $\mu g \cdot L^{-1}$; Sterner 2010). The phytoplankton community of Lake Superior is typically dominated by cryptophytes and diatoms (Fahnenstiel and Glime 1983, Munawar and Munawar 2009). Single taxon dominance of the DCM has been reported (e.g. *Cyclotella stelligera*; Fahnenstiel and Glime 1983); however, other investigators detail a decidedly diverse community within that layer (Munawar and Munawar 1978, Barbiero and Tuchman 2004). The characterization of the DCM in Lake Superior presented here, particularly its structure and the timing of its formation and dissipation, is consistent with that reported in both early (Olsen and Odlaug 1966, Watson et al. 1975, Moll and Stoermer 1982, Fahnenstiel and Glime 1983) and more contemporary (Barbiero and Tuchman 2004, Sterner 2010) research efforts.

1.2 Objective and Approach

The objective of this research is to understand, in a quantitative fashion, the various mechanisms contributing to the formation, maintenance and dissipation of the deep chlorophyll maximum in Lake Superior. This will be achieved through an integration of the results of laboratory experiments and field measurements with a one-dimensional mathematical model of chlorophyll and particulate organic carbon. In applying that model, key mechanisms generally associated with DCM dynamics (i.e. ecological, physiological and physical phenomena) will be examined individually and in concert to establish their role.

2.0 A Widely-Accepted Paradigm

It is widely accepted that the DCM represents an environment favorable for supporting phytoplankton growth. This point of view may have evolved from observations of the distribution of photosynthetic purple sulfur bacteria in lakes, residing as a thin layer at depths where the availability of both light and chemical resources (sulfide) is insured (e.g. Takahushi and Ichimura 1970, Guerrero et al. 1985). In a parallel fashion, optimization of limiting resources, e.g. light from the surface and nutrients recycled from the hypolimnion, has been offered as an explanation for development of the DCM (Moll and Stoermer 1982, Fahnenstiel and Glime 1983, Abbott et al. 1984, Varela et. al. 1992, Klausmeier and Litchman 2001, Holm-Hansen and Hewes 2004, Saros et al. 2005, Huisman et al. 2006, Hanson et al. 2007, Viličić et al. 2008, Nõges et al. 2010, Mellard et al. 2011). Simply stated, the paradigm suggests that the DCM represents a niche environment where requirements for light, temperature and/or nutrient supply are near-optimal for single species or larger assemblages. A detailed evaluation of the paradigm serves as an appropriate point of departure for consideration of factors mediating the formation, maintenance and dissipation of the DCM in Lake Superior. Here, we seek to accomplish this by characterizing the light, temperature and phosphorus environment of the DCM within the context of requirements for phytoplankton growth in Lake Superior.

2.1 Light

The degree to which solar radiation is attenuated within the water column serves to regulate the vertical distribution of primary production. The extent to which light availability impacts algal growth is tested here through application of an algorithm relating primary production and irradiance (P-I curve, Platt et al. 1980),

$$P^B = P^B_{Max}\left(1 - e^{\frac{-\alpha^{Chl}\cdot I}{P^B_{Max}}}\right)\cdot e^{\frac{-\beta^{Chl}\cdot I}{P^B_{Max}}} \qquad (1)$$

where

P^B =	Growth rate as a function of irradiance	mgC·mgChl^{-1}·hr^{-1}
P^B_{Max} =	Maximum growth rate chlorophyll specific	DCM: 0.15-0.35 hr^{-1}
α^{chl}=	Chlorophyll specific curve fitting parameter photo adaptation	DCM: 0.03-0.009
β^{chl}=	Chlorophyll specific Curve fitting parameter photo inhibition	DCM: 0.0003-0.00004
I =	Irradiance	µE m^{-2} · s^{-1}

The equation is in the form of a parabola with ascending and descending arms of differing slope. The coefficient α describes the slope of the ascending limb (growth response at low light intensities), and the coefficient β describes the slope of the descending limb (growth response at high light intensities, i.e. photo-inhibition). P-I curves were developed by Bub (2001) on a site-specific basis using the DCM phytoplankton assemblage from Lake Superior. Chlorophyll-specific primary production (mgC·mgChl^{-1}·hr^{-1}) was measured over a range of

irradiance values (0 - 1200, μE $m^{-2} \cdot s^{-1}$) and fit to Equation (1) (Platt et al. 1980 as cited by Fahnenstiel et al. 1989). The optimum irradiance for growth of the DCM assembly was found to be ~150 $\mu E \cdot m^{-2} \cdot s^{-1}$, an important finding as light levels in the DCM (~20 $\mu E \cdot m^{-2} \cdot s^{-1}$) are well below that optimum (Figure 2.1).

This finding is consistent with reports by others that the DCM is largely coincident with the compensation depth (DCM <1% of surface irradiance, Olson and Odlaug 1966; DCM irradiance 1.4 - 7.1%, Barbiero and Tuchman 2004) (Figure 2.2).

In summary, no evidence is found that phytoplankton at DCM depth in Lake Superior display a capacity for robust growth at the light levels characteristic of that environment.

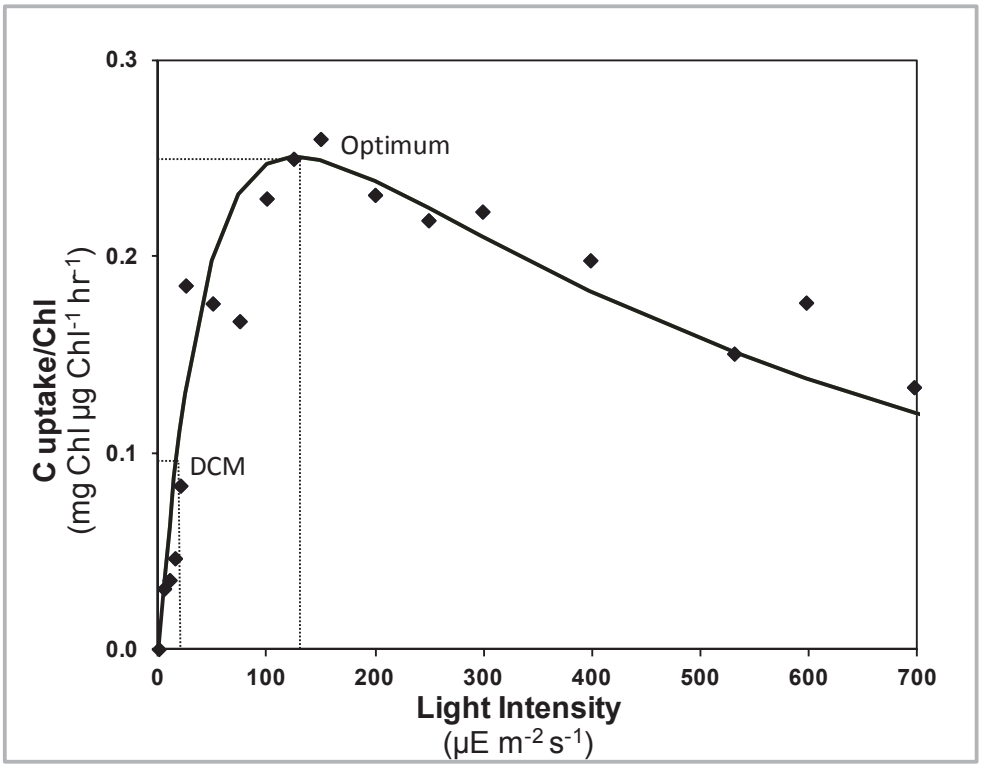

Figure 2.1 Growth measured as carbon uptake Chl^{-1} for DCM algae at HN 210 8-25-2000, adapted from Bub (2001)

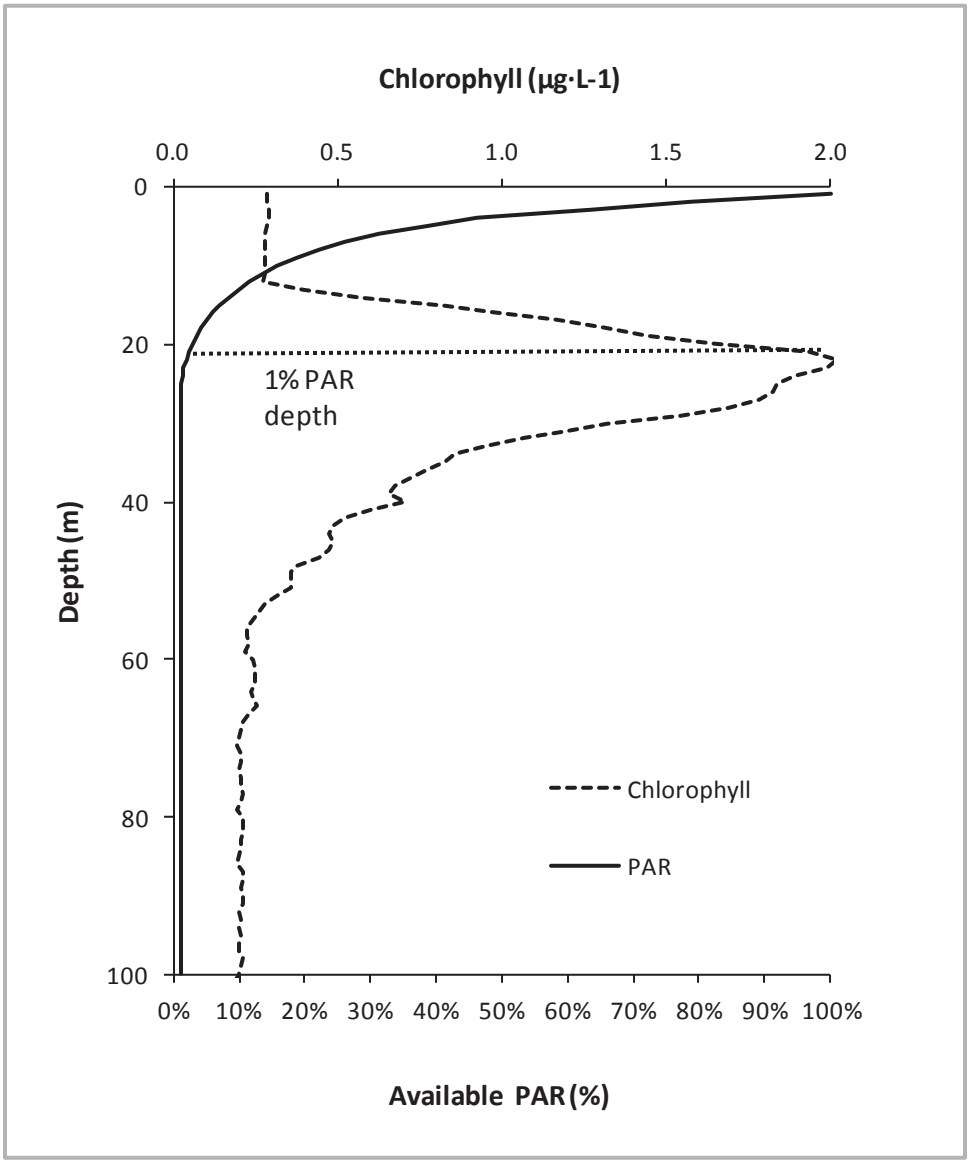

Figure 2.2 Photosynthetic available radiance (PAR) and chlorophyll profile at HN130, 7-30-2001 (Data adapted from Bub 2001)

2.2 Temperature

Temperature also plays a role in mediating seasonality in the phytoplankton community and might well be similarly invoked as a condition influencing DCM formation and structure, i.e. temperatures within the DCM are particularly favorable for supporting phytoplankton growth. Bub (2001) investigated this with an approach similar to that used above for light effects, by measuring chlorophyll-specific primary production over a range of temperatures and fitting the results to the model proposed by Cerco and Cole (1994),

$$K_{g,T} = k_{g,opt} e^{-k_1 (T - T_{opt})^2} \qquad T \le T_{opt}$$

and

$$K_{g,T} = k_{g,opt} e^{-k_2 (T - T_{opt})^2} \qquad T > T_{opt} \qquad (2)$$

where

$K_{g,T}$ =	Growth rate as the result of temperature attenuation	d^{-1}
$K_{g,opt}$ =	growth rate at an optimal temperature (°C)	d^{-1}
t_{opt} =	optimal temperature	(°C)
k_1 and k_2 =	fitting parameters	dimensionless

The result is a bell-shaped curve, with the rate of primary production equal to zero at some minimum temperature, increasing to a maximum at an optimum temperature and then decreasing as temperature rises above that optimum (Figure 2.3). The optimum temperature for the Lake Superior phytoplankton assemblage (surface samples collected in late August) was ~14 °C (Figure 2.3).

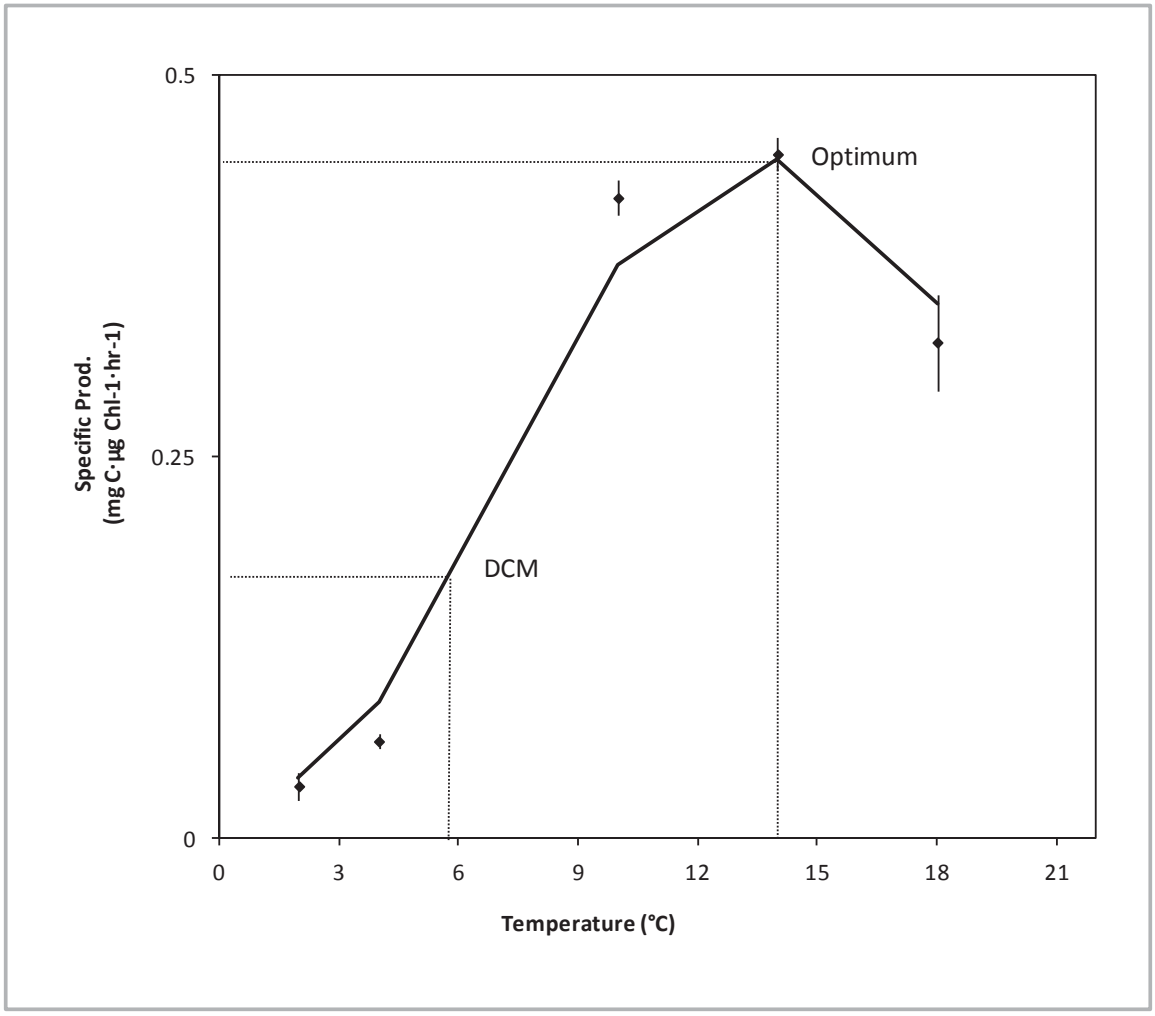

Figure 2.3 Specific production by algae taken from the DCM depth is optimum at ~14 °C (station HN210 8-25-2000, data adapted from Bub 2001)

Temperatures in the DCM, 5-6 °C in August (1997-2001; data of Barbiero and Tuchman 2004), are well below this optimum. It is concluded, therefore, that temperature conditions in the DCM are sub-optimal for supporting phytoplankton growth.

2.3 Nutrients (Phosphorus)

Phytoplankton populations in Lake Superior are phosphorus limited (Rose and Axler 1998, Sterner et al. 2004, Ivanikova et al. 2007). The paradigm invokes a nutrient (here phosphorus) supply to the DCM originating from the mineralization of particulate organic matter delivered to the hypolimnion. This phenomenon would be manifested as a vertical phosphorus gradient, and such signals have been reported from several systems (Letelier et al. 2004, Camacho 2006). However, observations of vertical gradients are rare in the Great Lakes (Eadie et al. 1984, Barbiero and Tuchman 2001). Advances in measurement techniques for phosphorus (e.g. MAGIC, Anagnostou and Sherrell 2008; persulfate oxidation, Baehr and McManus 2003) make it possible to reliably document the presence or absence of gradients, even at the low phosphorus levels characteristic of Lake Superior. Here, concentrations of soluble reactive phosphorus (SRP) have been shown to be both low (0.01 - 0.16 $\mu g \cdot L^{-1}$, Anagnostou and Sherrell 2008; 0.3 - 0.7 $\mu g \cdot L^{-1}$, Baehr and McManus 2003) and vertically homogenous (Baehr and McManus 2003, Heinen and McManus 2004, Anagnostou and Sherrell 2008 (Figure 2.4)). Total dissolved phosphorus (TDP) concentrations are similarly distributed with depth, ranging from 0.4 – 1.0 $\mu g \cdot L^{-1}$

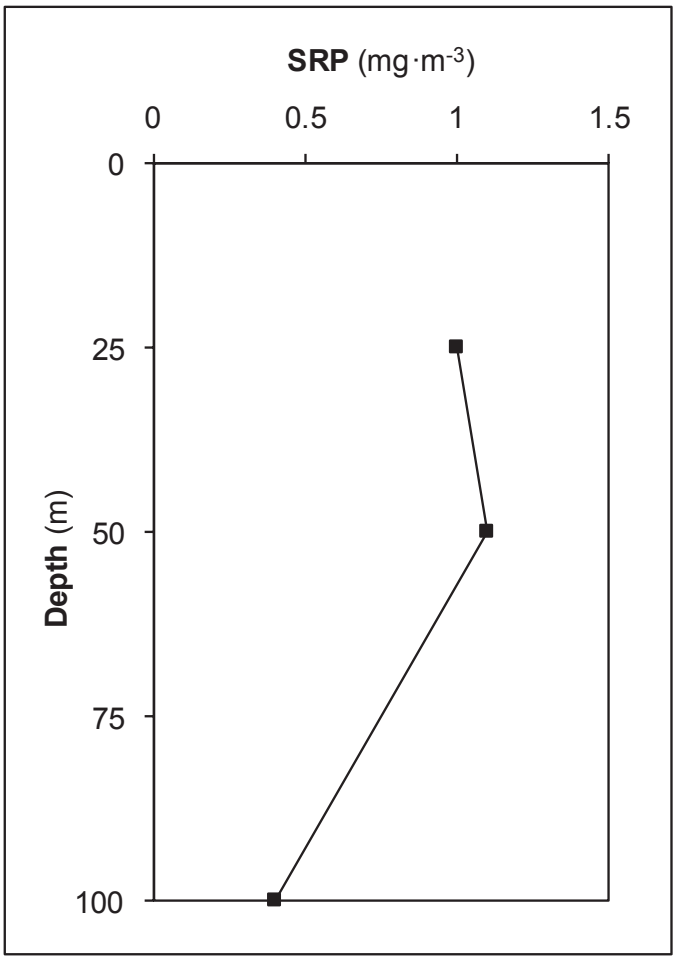

Figure 2.4 Lake Superior SRP profile showing the absence of an upward (limiting) nutrient flux (data from Anagnostou and Sherrell 2008)

(Anagnostou and Sherrell 2008). It cannot be concluded, based on these results, that the DCM offers a nutrient environment particularly favorable for supporting phytoplankton growth.

Indirect measures of the phosphorus status of the phytoplankton community have been considered in this regard as well. Barbiero and Tuchman (2001, 2004) examined C:P ratios in Lake Superior phytoplankton and observed that those in the DCM were less phosphorus stressed (lower C:P ratios) than those in the epilimnion. These authors suggest that the observed reduction in P stress in the DCM reflected an 'undetected flux' from the hypolimnion. An alternative explanation is, however, available. The DCM phytoplankton community may experience less P-stress simply because there is little demand placed on algal phosphorus reserves, as growth is limited at the sub-optimal light and temperature conditions found there.

Alkaline phosphatase activity (APA) represents another indirect measure of P status in algae. At limiting levels of SRP, algal cells may mobilize the enzyme alkaline phosphatase to cleave orthophosphorus from dissolved organic P molecules (Pettersson 1980, Rose and Axler 1997). Alkaline phosphatase activity in the Lake Superior phytoplankton community was examined using two analytical approaches: determination of the rate of hydrolysis of the artificial phosphorus substrate 4-methylumbelliferyl phosphate (APA v_{max} μM/min, 4-MUP $\rightarrow$ MUP; Pettersson and Jansson 1978) and a presence-absence assay using a molecular probe (enzyme-labeled fluorescence, ELF; Gonzáles-Gil et al. 1998, Rengefors et al. 2003). Rates of enzymatic hydrolysis were more than 4 times

greater in the epilimnion than in the DCM indicating greater levels of P stress in surface waters (Figure 2.5). Similar results were observed with the ELF assay where alkaline phosphatase activity was detected in ~25% less cells than in the epilimnion (Figure 2.5). In both cases, DCM phytoplankton populations exhibited less P stress, a response that is attributed to phosphorus reserves unused due to light limitation (Malkin et al. 2008, Auer et al. 2010).

Finally, favorable conditions with respect to phosphorus may be reflected in the water column drawdown of other nutrients utilized for growth (e.g. nitrate, silicon; Urban 2009). In Lake Superior, a modest drawdown of nitrate is observed in surface waters, but there is no such response within the DCM (McManus et al. 2003, Ivanikova et al. 2007). Thus, there is no convincing evidence, either directly (water column P levels) or indirectly (algal P status) that the DCM offers a nutrient environment particularly favorable for supporting algal growth.

2.4 Evidence from Primary Production Profiles

Individual analysis of the primary forcing factors for phytoplankton growth (light, temperature and nutrients) provided no support for a paradigm in which the DCM represents a favored niche. However, these factors are considered to be multiplicative in nature (Droop 1983), and further certainty may be achieved by inspection of laboratory-derived profiles of primary production in Lake Superior (Figure 2.6). Here, the primary production maximum is evident at a depth of ~10 m and is separated from the DCM by ~20 m. An essentially identical result was

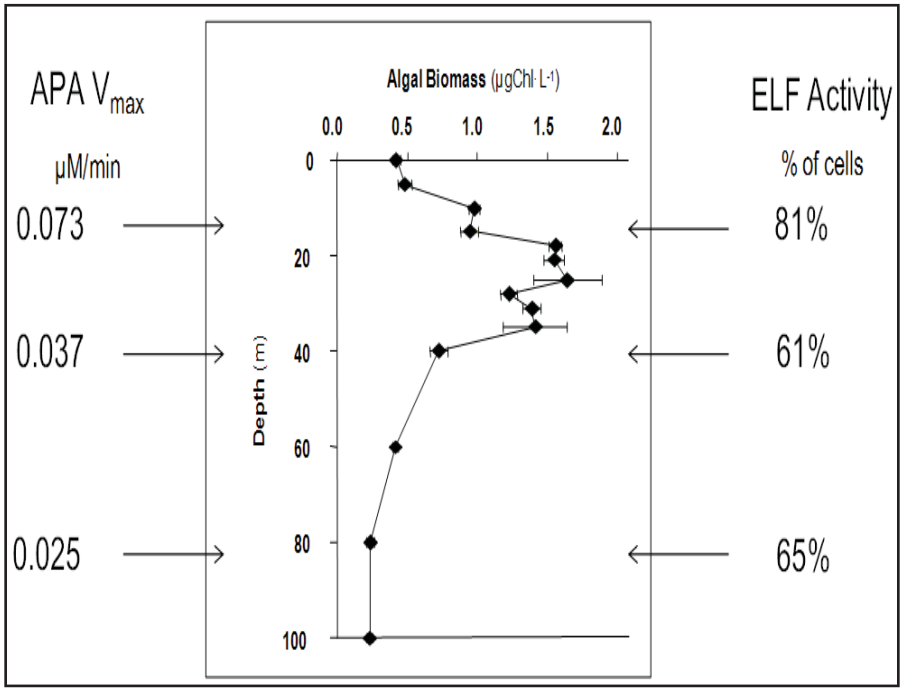

Figure 2.5 Activity of nutrient sequestration based on APA and ELF (Data from Elenbaas 2001)

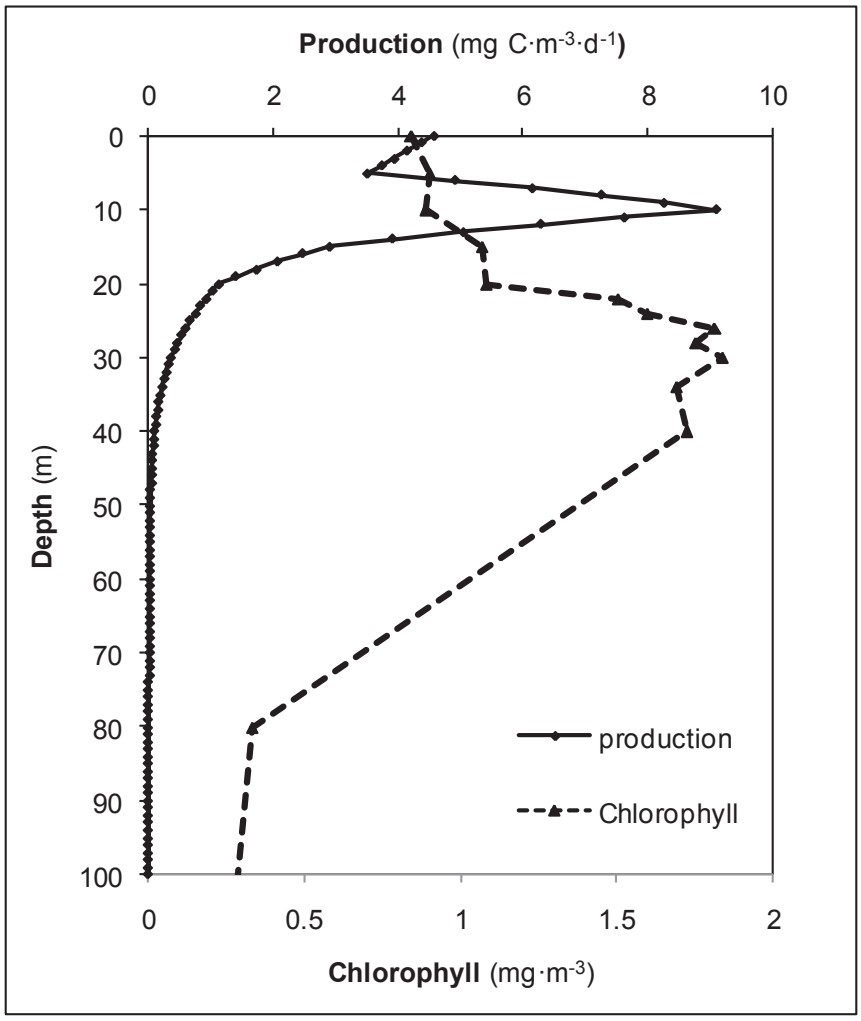

Figure 2.6 Chlorophyll and primary production profile at station HN 210, 8-25-2000 (Data adapted from Bub 2001)

obtained by Sterner (2010), with the production maximum at 10 m and the DCM located 30 m below.

2.5 Evidence from the Bacterioplankton Community

While it is difficult to support a paradigm where the DCM is conceived as a favorable environment for phytoplankton growth, such is not the case with respect to bacterioplankton. Peaks in heterotrophic bacterial production within the DCM (Figure 2.7a) observed by Elenbaas (2001), suggest a localized source of soluble organic carbon. It is noteworthy that the bacterioplankton carbon requirement (BCR; Figure 2.7b) within the metalimnion (location of the DCM) significantly exceeds that of the epilimnion and hypolimnion. Determination of phytoplankton carbon excretion rates (Figure 2.7c) indicates that this source is insufficient to meet the BCR, indicating the presence of an alternative supply. This phenomenon has been well described by researchers working in oligotrophic, P-limited waters of the Mediterranean Sea (Alboran Sea, western Mediterranean, Fernández et al. 1994; NW Mediterranean Sea, Van Wambeke et al. 2001; Northern Adriatic Sea, Pugnetti et al. 2005; NW Mediterranean, Alonso-Sáez et al. 2008; Mediterranean Sea, López-Sandoval et al. 2010). These authors suggested that dissolved organic carbon released through senescence and viral-induced lysis of phytoplankton cells and zooplankton grazing could serve as the missing source.

A similar conclusion may be reached through the results of community-level physiological profiling performed by Elenbaas (2001). Here, similarities in

carbon source utilization (i.e. their resource profile) were determined using Biolog assays (color development in reflecting uptake of various organic substrates) of Lake Superior water. A multivariate statistical technique (principal component analysis; PCA) was used to differentiate between groups within the bacterioplankton community (Figure 2.8).

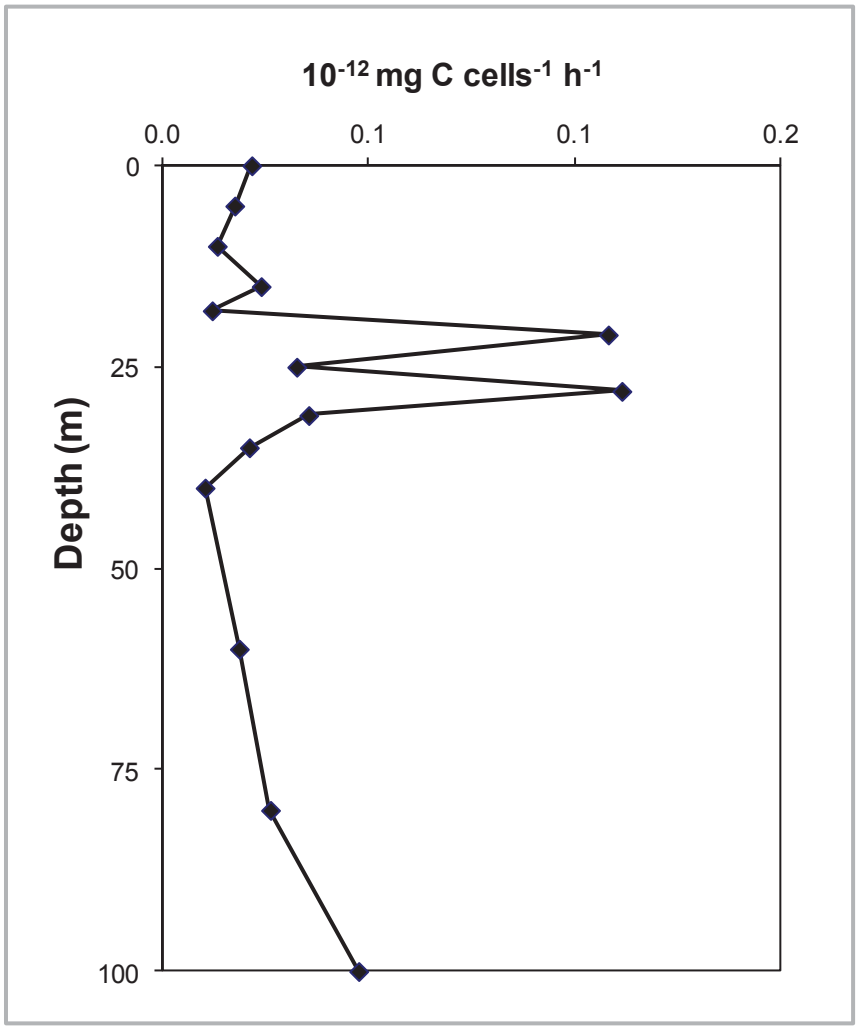

Figure 2.7a Production of bacterioplankton in the water column, HS 170, 7-14-1999, (Data from Elenbaas 2001)

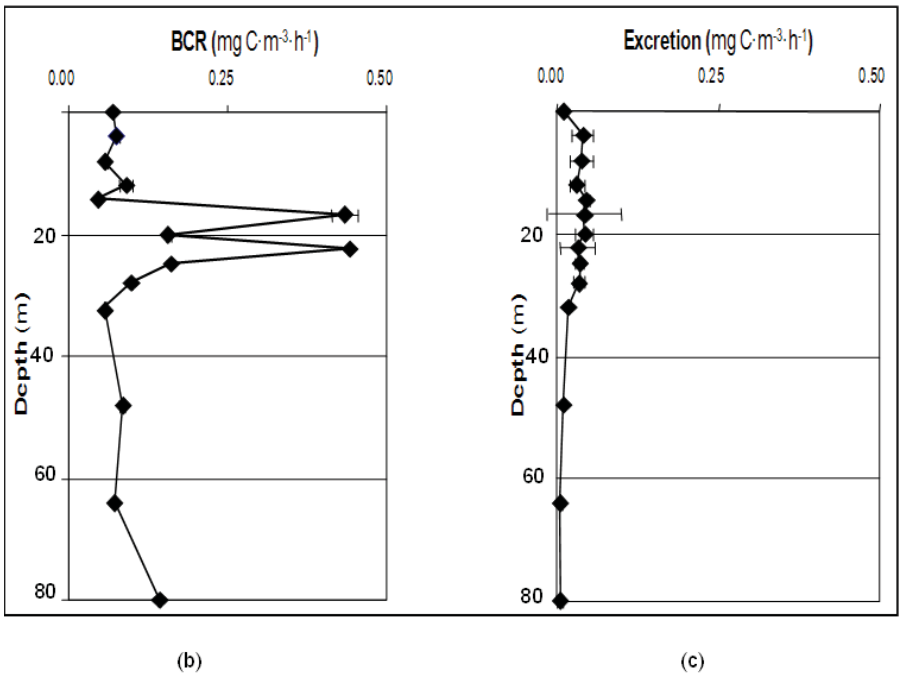

Figure 2.7 Carbon excretion by actively photosynthesizing phytoplankton is able to satisfy the bacterial carbon requirement (BCR) only in the surface waters, HS 170, 7-14-1999 (Data from Elenbaas 2001)

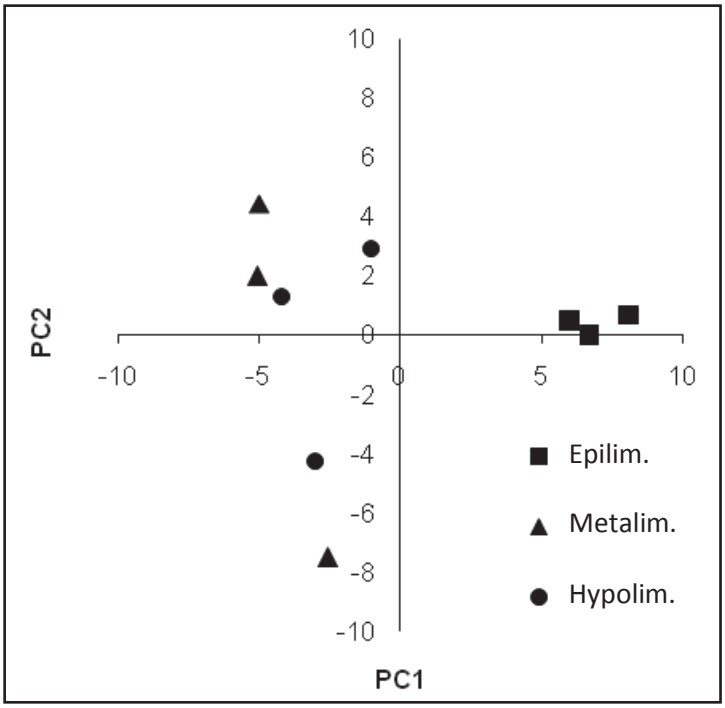

Figure 2.8 DCM (22m) and hypolimnetic (50m) bacteria prefer similar food sources in contrast to bacteria found in the epilimnion (5m), the axis represent principal components 1 and 2 (Biolog HN110, August 1999, data from Elenbaas 2001)

The bacterial carbon resource utilization within the DCM was more closely aligned with that of the hypolimnion (region of algal senescence) than with the epilimnion (region of algal growth). These results point to the DCM, not as a location of active growth, but rather as a region of transition to senescence and death.

2.6 Phytoplankton-Zooplankton Interactions

The phytoflagellates and a significant fraction of the diatoms that dominate the Lake Superior phytoplankton assemblage (Munawar and Munawar 1978) are small forms. For example, Sterner (2010) reports that 50% of the chlorophyll passes a 2 μm filter and 75% passes a 5 μm filter. These forms are susceptible to grazing, and thus losses to grazing pressure have been proposed as a mechanism leading to the characteristic shape of the DCM (Olsen and Odlaug 1966, Fee 1976, Longhurst 1976, Herman et al. 1981, Fahnenstiel and Scavia 1987, Pedrós-Alió et al. 1987, Christensen et al. 1995, Pilati and Wurtsbaugh 2003, Sterner 2010, Khromechek et al. 2010). As in other systems, zooplankton in Lake Superior (dominated by *Calanoids Limnocalanus macrurus and Diaptomus copepodites,* Yurista et al. 2009) exhibit negative phototaxis and migrate vertically during the diel light cycle, over distances of several meters, permitting the zooplankton biomass peak observed in the thermocline region (Figure 2.9) to traverse the DCM (Yurista et al. 2009).

Thus, large numbers of zooplankton are expected to pass through the DCM daily (similar to observations in other systems e.g. Williamson et al. 1996).

Further, since rates of zooplankton grazing are known to be proportional to prey availability (Bierman and Dolan 1981), grazing pressure would reach its maximum within the DCM. Thus grazing pressure should not serve to form the DCM, but rather to attenuate the magnitude of the peak.

The doubling or tripling of chlorophyll levels observed within the DCM is unlikely to have evolved in response to growth as light is approaching compensation levels, the temperature is far below the optimum, and there are no observed nutritional benefits. Further, losses to respiration, sinking and grazing remain, and bacterioplankton dynamics within the DCM suggest a catabolic system. Although not an environment well-suited to support the full phytoplankton assemblage, it has been suggested that some species have adapted to flourish in this environment.

2.7 DCM Formation and Maintenance by evolved algal species

Based on studies conducted in the ELA lakes in northwestern Ontario, Fee (1976) concluded that the observed dominance of a single species in the DCM (*Dinobryon sertularia* var. *protuberans*) occurred because this species was better adapted and thus obtained dominance through competitive exclusion. Similar findings (in this case for *Cyclotella stelligera, C. comensis, and C. ocellata*) were reported by Fahnenstiel and Glime (1983) for samples collected from the Lake Superior water column in 1979. However, sampling conducted in 1978 and 1980 found no differences in the composition of the Lake Superior phytoplankton assemblage over the water column even though chlorophyll in the

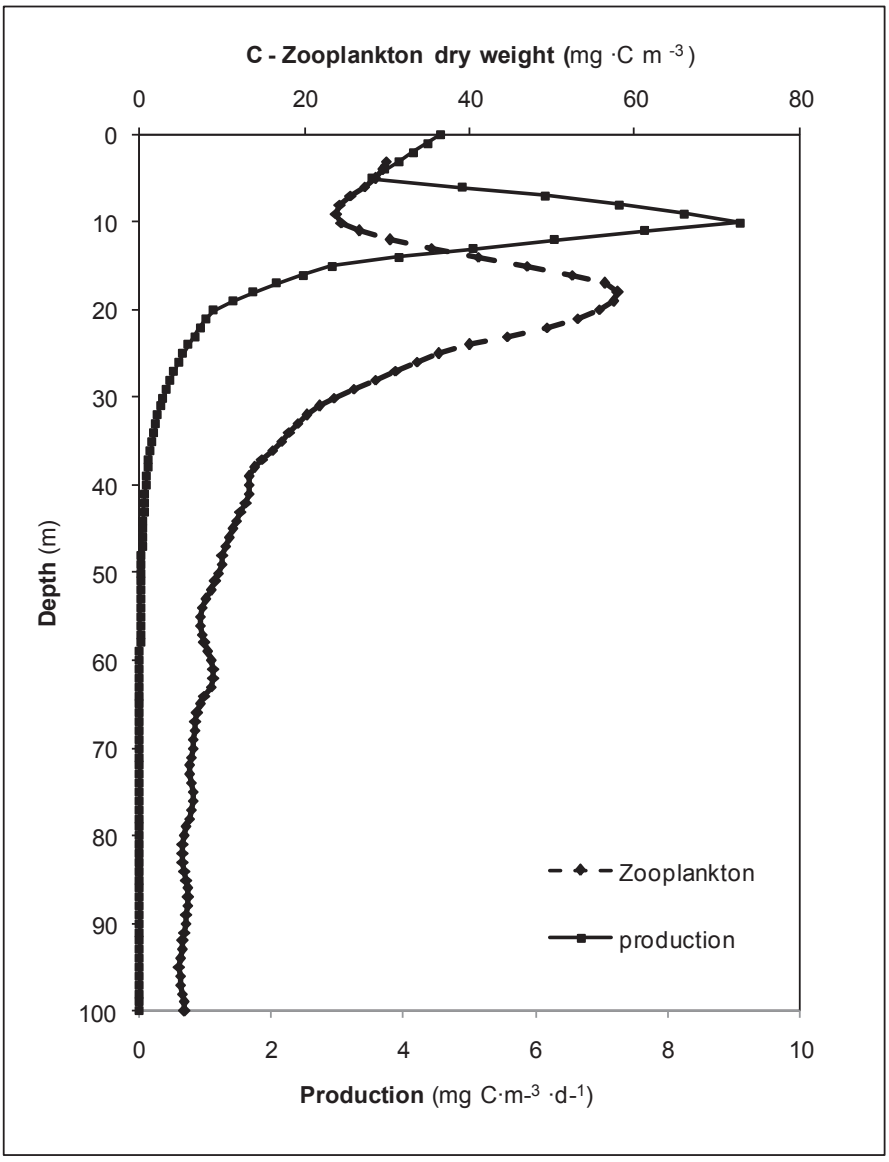

Figure 2.9 Zooplankton distribution in offshore waters of Lake Superior (unpublished data from Yurista)

DCM was 2 to 3 times higher than surface concentrations (Fahnenstiel et al. 1984). Water column sampling conducted in Lake Superior from 1997-1999 (Barbiero and Tuchman 2001, 2004) also failed to reveal the presence of "evolved algae"; only modest increases in DCM species were observed (Utermöhl technique, Lund et al. 1958) compared to the epilimnion assemblage, the largest being 5.3% (1998, *Gymnodinium* spp.). One would expect greater and more consistent deviations from the surface water community structure if "evolved species", better adapted to DCM conditions, were present. Thus the idea that formation and maintenance of the Lake Superior DCM is driven by the growth of more successful algal species seems unsupported.

Consequently, the idea that the DCM depth *a priori* represents a favorable niche for growth needs to be reconsidered, raising the question: which other factors or processes may mediate DCM dynamics? This question is addressed in the next section through a modeling analysis supported by a review of the literature.

3.0 Modeling DCM Dynamics

Explanations for the formation and maintenance of the DCM in Lake Superior have traditionally been sought by examining the impact of niche exploitation or reduced grazing on algal growth rates. After careful analysis, however (see discussion above), these mechanisms are seen to be inadequate in explaining the formation and maintenance of the DCM. Additional processes need to be considered. In this regard, settling and photoadaptation have been suggested as possible mechanisms contributing to the DCM formation.

3.1 Effects of Mass Transport

The increase in water column stability due to thermal stratification is regarded as a necessary condition for DCM formation (Camacho 2006); however, turbulent diffusion associated with eddies remains present and tends to modify vertical structure by reducing concentration gradients (Crank 1979). Therefore diffusive mass transport merits consideration as an agent mediating DCM dynamics.

Mass transport also occurs via settling. In marine environments, settling particles accumulate at certain locations in the water column, with maxima occurring just below the pycnocline, a major density discontinuity. MacIntyre et al. (1995) suggested that accumulation of this marine snow (aggregates of diverse particle types; Alldredge 2002) correlates well with density gradients. An analog for this phenomenon in freshwater systems may be found where reductions in settling velocity are mediated by the thermal structure. As

phytoplankton sink from the epilimnion, their density relative to the ambient environment decreases and their settling velocity becomes less. In thermally-stratified systems, water reaches its maximum density near the bottom of the metalimnion, a depth coincident with that of the DCM. This mechanism was invoked as a means of DCM formation and maintenance decades ago by Steele and Yentsch (1960) and continues to be popular (e.g. Brooks and Thorke 1977, Cullen 1982, Priscu and Goldman 1983, Takahashi and Hori 1984, Shortreed and Stockner 1990, Condie 1999, Hiroshi Serizawa et al. 2010).

3.2 Effects of Photoadaptation

When algae experience a sustained change in light regime, optimization of their photosynthetic capacity will follow. In low light environments, this optimization leads to the formation of additional chlorophyll, effectively decreasing the carbon to chlorophyll ratio (Geider et al. 1997). The concept that chlorophyll levels at depth increase through photoadaptation (peaking at compensation depth) is frequently suggested in explaining the DCM as well (Steele 1964, Kiefer et al. 1976, Fahnenstiel et al. 1984, Taguchi et al. 1988, Fennel and Boss 2003, Barbiero and Tuchman 2004, Hamilton et al. 2010).

Although the development and manifestation of the DCM in various lakes and oceans seem to behave similarly, the relative importance of governing mechanisms is likely to vary due to the unique and intrinsic properties of each system (Camacho 2006). Thus attention now turns to identifying and quantifying the key mechanisms driving DCM dynamics in Lake Superior. A carbon-based

mathematical model for algal growth (photosynthesis, respiration, excretion) will be utilized for this purpose, sequentially introducing functionalities describing photoadaptation, grazing and settling.

4.0 Development of a 1-D Model for the DCM in Lake Superior

4.1 Model Segmentation

The spatial homogeneity of the DCM in Lake Superior (Munawar and Munawar 1978, Barbiero and Tuchman 2001) suggests that a one dimensional (vertical) framework is adequate for modeling the phenomenon. Here, the water column is represented by 100, 1m-thick completely-mixed cells.

4.2 Mass Balance and Solution

A differential equation describing the mass balance on particulate organic carbon (POC; algal biomass) is written for each cell. The equation accommodates exchange via mass transport (diffusion and settling), gains through growth and losses through grazing. In general terms:

Change in mass of particulate organic carbon = diffusion ± settling + growth - grazing (3)

Expressed mathematically,

$$V_i \frac{dC_i}{dt} = \frac{EA_c}{l} \cdot \left(C_{i+1} - C_{(i-1)}\right) + \frac{v_s}{l}\left(C_{i-1} - C_{i+1}\right) + \mu_{Max} \cdot \left(f_T \cdot f_I \cdot f_P\right) \cdot C_i - k_{grazing} \cdot C_i \qquad (4)$$

where

V_i =	volume (remains constant)	m^3
C_i =	POC concentration in cell i	$mg \cdot L^{-1}$
t =	Time	d
E =	diffusion coefficient	$m^2 \cdot d^{-1}$
A_c =	cross sectional area of the interface	m^2

l =	mixing length	m
v_s =	settling velocity	$m \cdot d^{-1}$
i =	target cell	
μ_{max} =	maximum growth rate	d^{-1}
f_T =	temperature attenuation function	-
f_I =	light attenuation function	-
f_P =	nutrient attenuation function	-
$k_{grazing}$ =	zooplankton grazing rate	d^{-1}

This system of linked ordinary differential equations written over the water column is solved using numerical integration (explicit Euler method). As applied here, the model is implemented in a linear fashion, starting with diffusion and settling and then sequentially introducing growth as mediated by temperature, light and grazing, to permit isolation and examination of the processes potentially contributing to water column dynamics.

Mass Transport

As described above, terms in the mass balance (Equation 4) are introduced in the model sequentially to elucidate their individual roles in the formation of the DCM. Here, the role of mass transport, i.e. diffusion and settling, on DCM structure is examined.

4.2.1 Mass Transport: Diffusion

Mass is exchanged between model cells through turbulent diffusion. The magnitude of that exchange varies with the value for the turbulent diffusion coefficient (E; mixing strength) and the concentration gradient:

$$V \cdot \frac{dC}{dt} = \frac{EA_c}{h} \cdot \left(C_{i+1} - C_{(i-1)} \right) \quad (5)$$

The net flux for a particular cell will be in the direction of the concentration gradient (high to low). Equation (5) is simplified by substitution of the model values for cell height (h; 1m) and area (A_c; 1 m^2), which changes the turbulent diffusion coefficient (E) to the bulk diffusion coefficient (E'):

$$V \cdot \frac{dC}{dt} = E' \cdot \left(C_{i+1} - C_{(i-1)} \right) \quad (6)$$

Where: E' Bulk diffusion coefficient $m^3 \cdot d^{-1}$

Reported values for E' by Denman and Gargett (1983), fluctuate with wind conditions and depth. The values found in literature are as follows; epilimnion (3.5 $m^2 \cdot d^{-1}$ to 960 $m^2 \cdot d^{-1}$), base of the mixed layer (0.7 $m^2 \cdot d^{-1}$ to 14.7 $m^2 \cdot d^{-1}$) and thermocline (0.4 $m^2 \cdot d^{-1}$ to 1.7 $m^2 \cdot d^{-1}$); no values for the hypolimnion were reported. The findings suggest that the bulk diffusion coefficient decreases with depth, and typical values are applied in this model. E' decreases linearly from the surface to the base of the mixed layer (10 $m^2 \cdot d^{-1}$ decreasing to 1 $m^2 \cdot d^{-1}$) and reaches its lowest value in the thermocline (0.4 $m^2 \cdot d^{-1}$). The value for E' in the hypolimnion remains constant (1 $m^2 \cdot d^{-1}$), in the order of that reported by Chapra (1997), variations of E' with depth are shown in Figure 4.1.

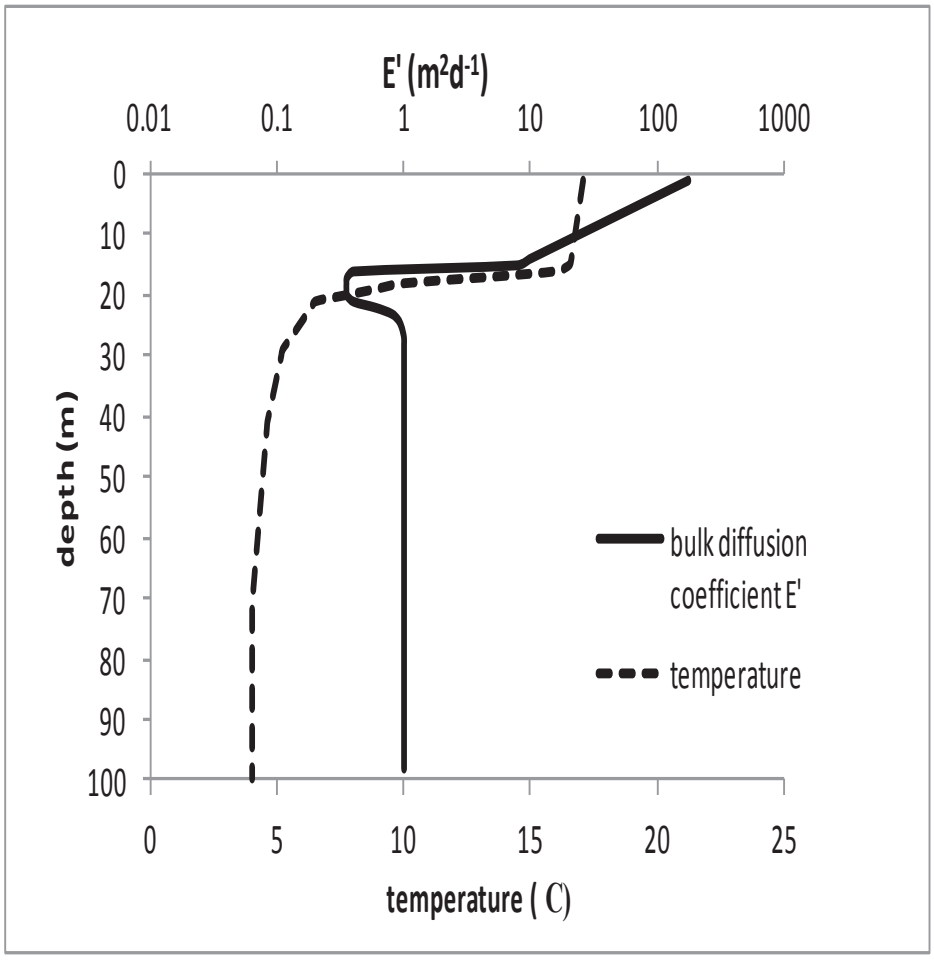

Figure 4.1 Bulk diffusion coefficient (E') in relation to depth.

4.2.2 Mass Transport: Settling

Settling results in a downward flux of mass, with the net transport in each model cell equal to the difference between mass in and mass out:

$$V \cdot \frac{dC}{dt} = \frac{v_s}{h}\left(C_{i-1} - C_{i+1}\right) \quad (7)$$

Settling velocity, as described by Stokes' law for discrete particle settling, is impacted by features of both the water and the particle:

$$v_s = \frac{g}{18}\left(\frac{\rho_s - \rho_w}{\mu}\right) \times d^2 \quad (8)$$

where

g =	acceleration due to gravity	$m \cdot s^2$
ρ_s =	particle density	$g \cdot L^{-1}$
ρ_w =	water density	$g \cdot L^{-1}$
μ =	dynamic viscosity	$m^2 \cdot d^{-1}$
d =	particle diameter	µm

Variations in water density (ρ_w) and viscosity (μ) over the water column are accommodated by incorporating Stokes' Law in the model. Settling velocity is also impacted by the diameter (d) and density (ρ_s) of the algal particles. The majority of the algae in Lake Superior are small forms (< 5 µm, Sterner 2010), and application of such diameters to Stokes' Law yields velocities much less than those calculated from sediment trap experiments performed above and below the thermocline (0.36 $m \cdot d^{-1}$ and 0.14 $m \cdot d^{-1}$, Fahnenstiel and Scavia 1987; 0.27 $m \cdot d^{-1}$ to 0.46 $m \cdot d^{-1}$ measured at 31 m depth, Baker 1991). This suggests that particle aggregation is occurring, leading to more rapidly settling entities. In the model, a

particle diameter of 12 μm and a density of 1050 g·L^{-1} is applied to Stokes' Law, yielding depth variable settling velocities on the order of those reported from sediment trap measurements (Baker 1991) (Figure 4.2). Model coefficients, developed as described here, are summarized in Table 4.1.

4.2.3 Kinetics: Growth

Previous sections have focused on mass transport phenomena. The process continues with the examination of the effect of growth on the DCM structure. In the POC mass balance (Equation (4)),

$$V_i \frac{dC_i}{dt} = \frac{EA_c}{l} \cdot \left(C_{i+1} - C_{(i-1)}\right) + \frac{v_s}{l}\left(C_{i-1} - C_{i+1}\right) + \mu_{Max} \cdot \left(f_T \cdot f_I \cdot f_P\right) \cdot C_i - k_{grazing} \cdot C_i \quad (9)$$

the growth term (highlighted), accommodates the mediating effects of temperature, light and nutrients. The coefficient μ_{max} refers to the maximum specific growth rate (d^{-1}), i.e. the rate expected under optimum conditions of temperature, light and nutrient availability. Mediating effects are introduced here sequentially.

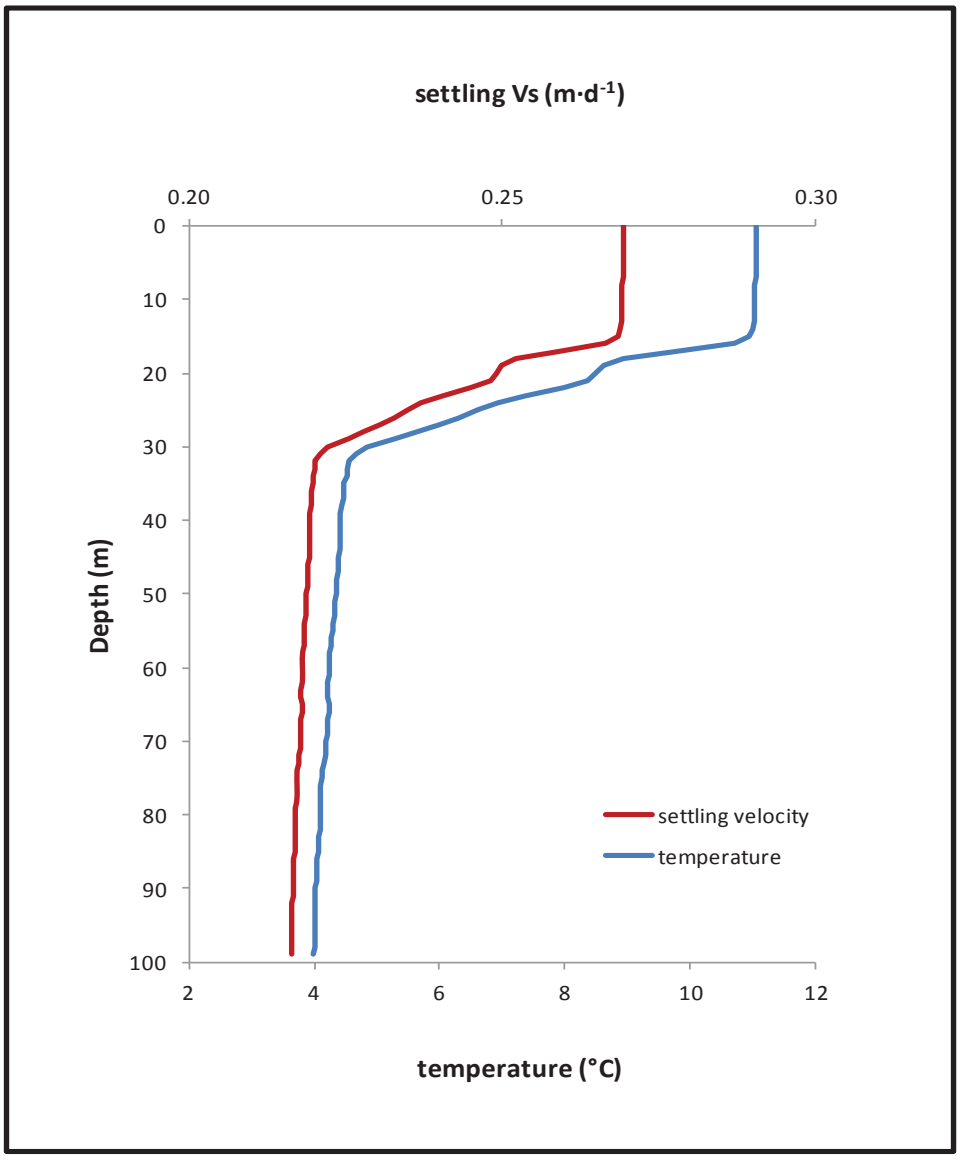

Figure 4.2 Depth variable settling velocity

4.2.3.1 Temperature

The term f_T in Equation (4) describes the effects of temperature and is a concave function with an optimal temperature $T_{opt,}$ (Cero and Cole 1994),

$$f_T = e^{-\alpha_T (T_z - T_{opt})^2} \qquad \alpha_T = \alpha_{T1} \; if \; T \le T_{opt} \; or \; \alpha_T = \alpha_{T2} \; if \; T > T_{opt} \tag{10}$$

where

α_{T1} =	fitting parameter	dimensionless
α_{T2} =	fitting parameter	dimensionless
T_z =	temperature at depth	°C
T_{opt} =	optimum growth temperature	°C

This concave function serves to attenuate growth rates at temperatures above and below the optimum, where K_1 governs the slope of the ascending limb and K_2 that of the descending limb. Bub (2001) measured chlorophyll-specific growth rates for the epilimnetic algal assemblage of Lake Superior over a range of temperatures with saturating light conditions and ambient nutrient levels. Those rates are converted here to a carbon-specific basis by multiplying by the Chl:C ratio (MacIntyre et al. 2002). Four results for closely clustered temperatures (14-16°C; Figure 4.3a) were pooled and averaged, yielding the final carbon-specific data set (Figure 4.3b).

These data were then normalized to the observed (experimental) maximum specific growth rate and fit using the model presented as Equation (10) to yield values of α (0.0195 for $T<T_{opt}$ and α 0.0151 for $T>T_{opt}$) and T_{opt} (13.5°C; Figure 4.3c).

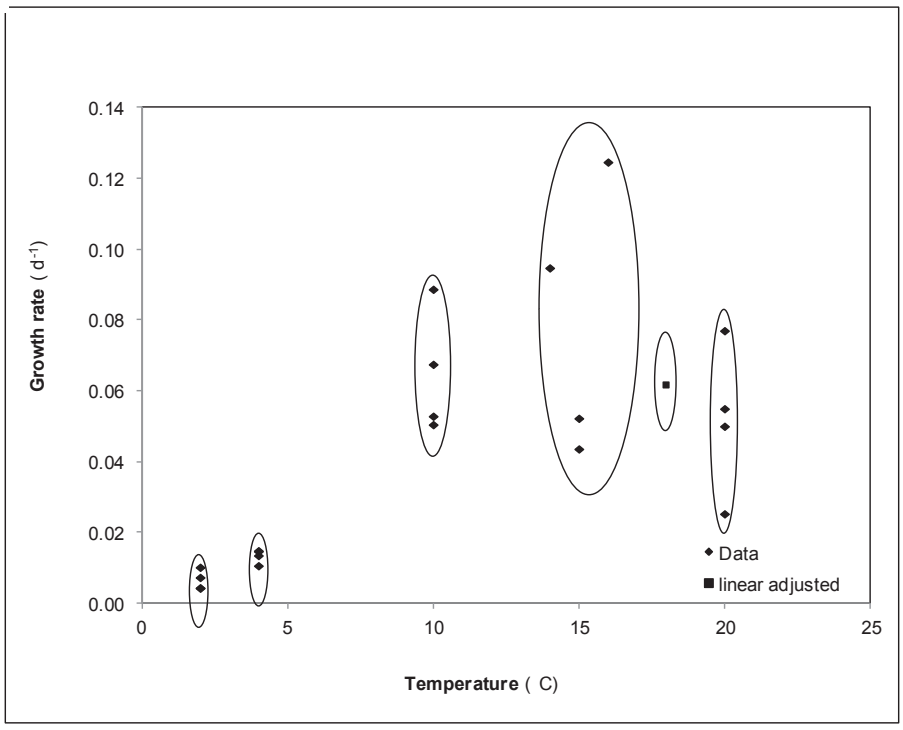

Figure 4.3a Clustered growth data (Data adapted from Bub 2001)

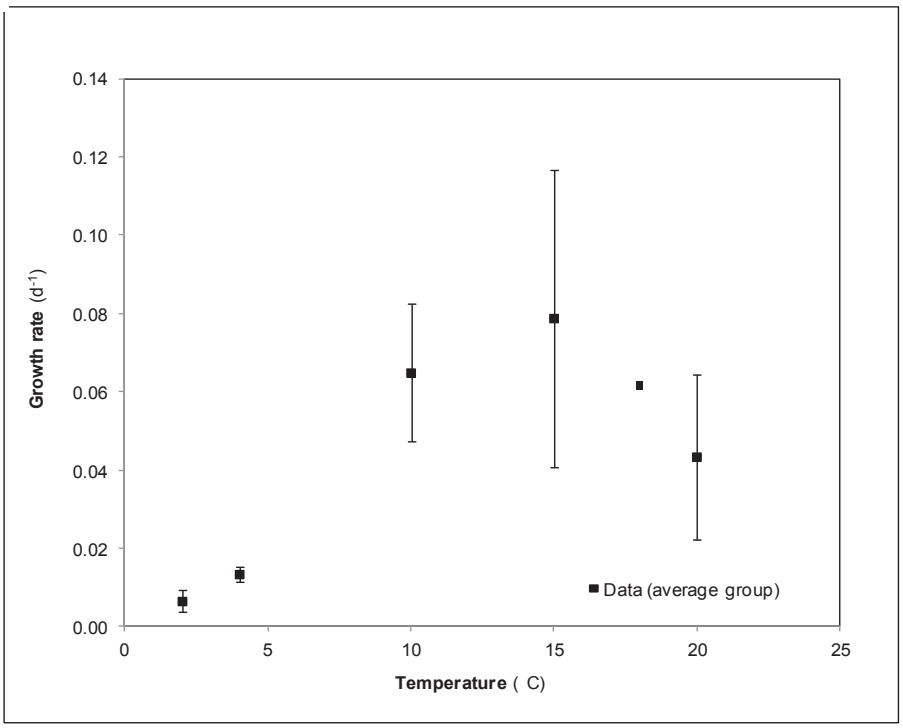

Figure 4.3b Average growth data, error bars represent one standard deviation (Data adapted from Bub 2001)

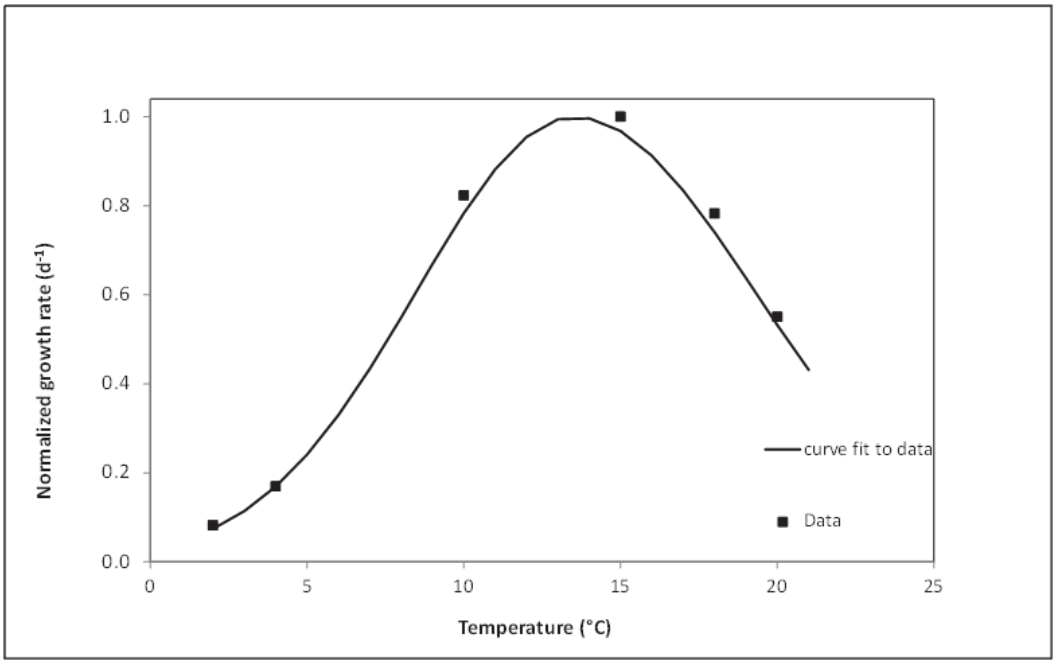

Figure 4.3c Normalized average growth response f_T and model curve (Data adapted from Bub 2001)

4.2.3.2 Light

The f_I term in equation (4) expresses the attenuation of algal growth due to sub optimal light conditions, described in the model by the light response function (PI curve) presented previously (Platt et al. 1980),

$$f_I = \left(1 - e^{\frac{-\alpha^C \cdot I_z}{\mu_{Max}}}\right) \cdot e^{\frac{-\beta^C \cdot I_z}{\mu_{Max}}} \tag{11}$$

Chlorophyll-specific PI curves were developed by Bub (2001) for the epilimnetic (0 m sample) and DCM (30 m sample) phytoplankton assemblages of Lake Superior under ambient conditions of nutrients and temperature. The growth response corresponds to net production as all measurements were made after an incubation period of 8 hours so to include respiration and excretion losses. Here, these rates are normalized to temperature (Equation (10) with values of α and T_{opt} for Lake Superior). The temperature-normalized rates were then multiplied by the depth specific Chl:C ratio to convert them to a carbon-specific basis (MacIntyre et al. 2002) followed by normalization to the average maximum growth rate and fit to the Equation (11) to yield PI curves for the epilimnion (Figure 4.4a) and the DCM (Figure 4.4b).

The value of the maximum specific growth rate derived for the epilimnion (μ_{max} = 0.071 d^{-1}) corresponds well with that noted in the temperature experiments described above (μ_{max} = 0.082 d^{-1}; Figure 4.3b) and to values calculated from the data of Sterner (2010; μ_{max} = 0.096d^{-1} ± 0.025 d^{-1}) for five observations made in Lake Superior at a depth of 10 m in summer. The

anticipated effects of shade adaptation are apparent in comparing PI-curves for epilimnetic and DCM (shade-adapted) algae (Figure 4.4c). The shade adapted assemblage has higher rates of photosynthesis under low light conditions and exhibits a higher degree of photoinhibition under high light conditions than does the epilimnetic community (see also Anning 2000).

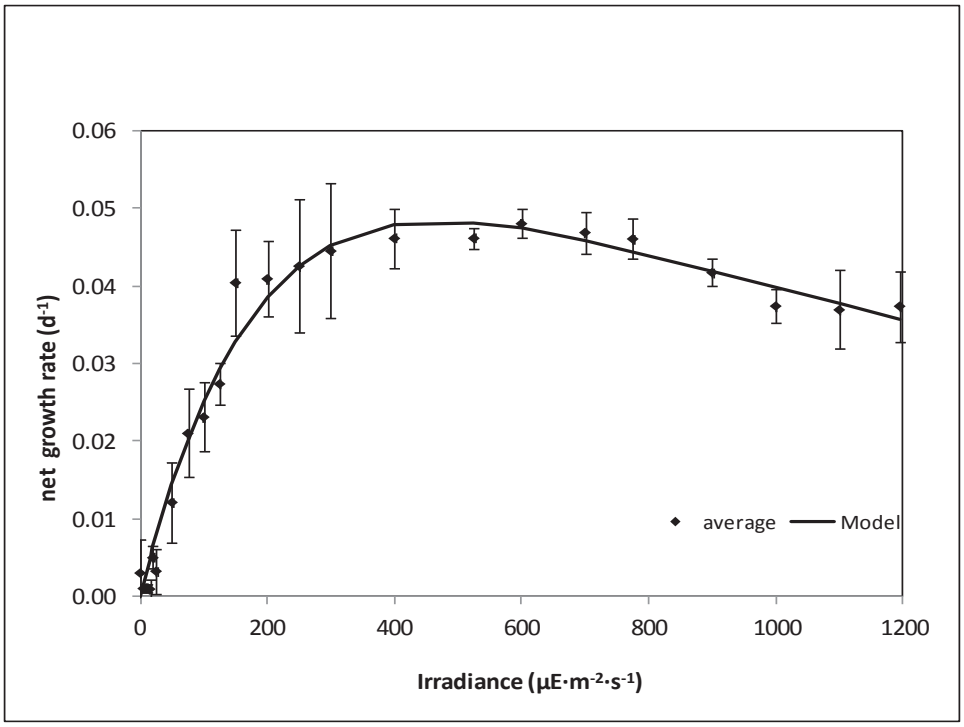

Figure 4.4a PI-response curve for the epilimnion (Data adapted from Bub 2001)

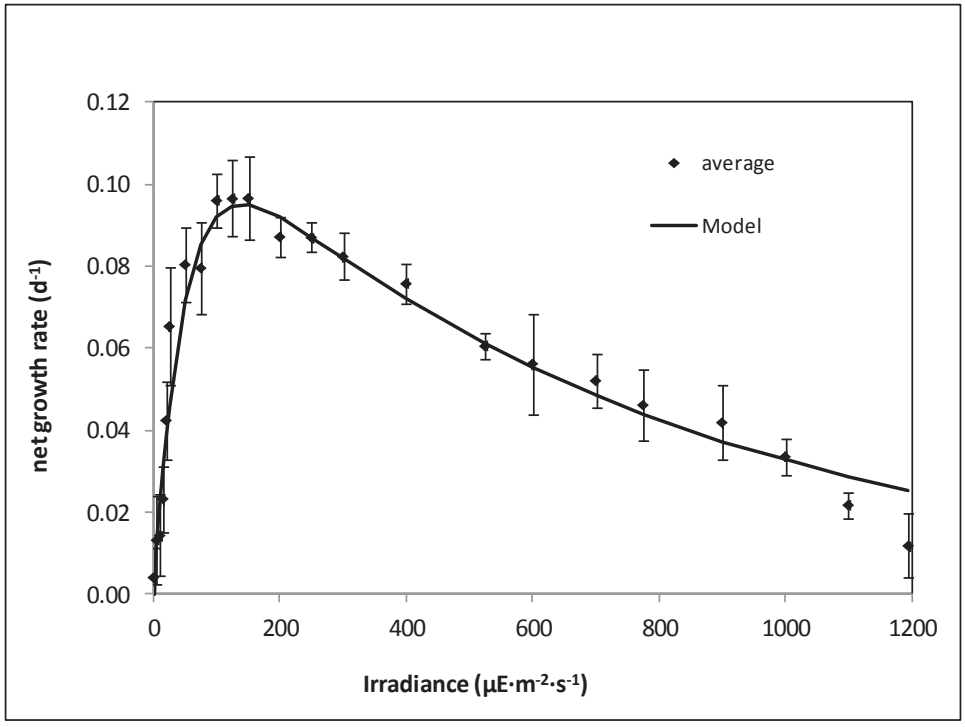

Figure 4.4b PI-response curve for the DCM (Data adapted from Bub 2001)

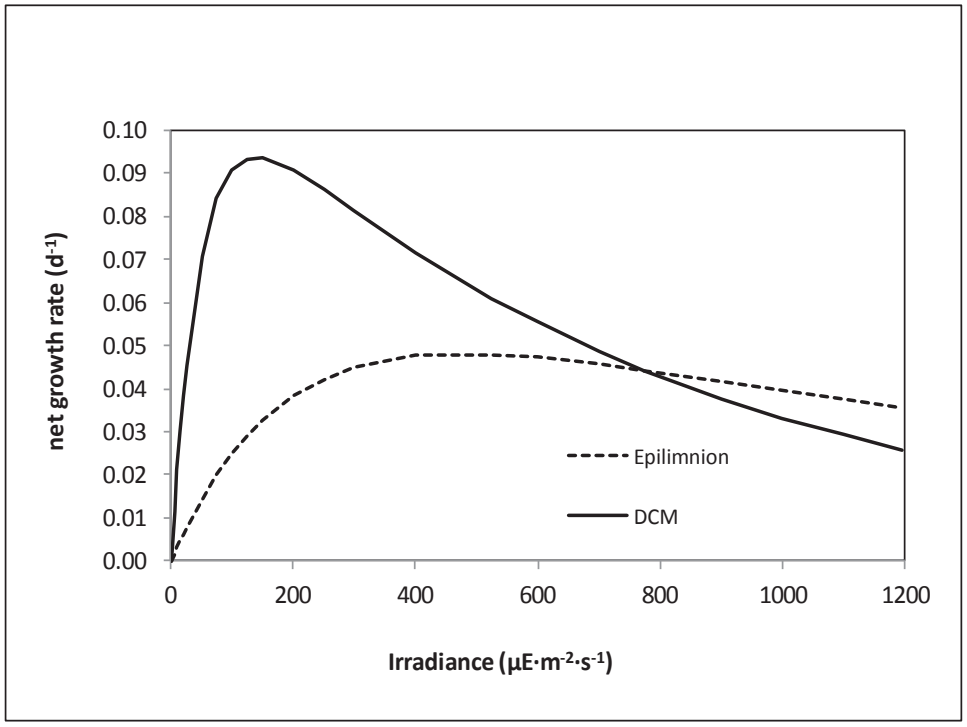

Figure 4.4c High Chl:C , DCM; low Chl:C , epilimnion (Data adapted from Bub 2001)

4.2.3.3 Nutrients

Lake Superior is phosphorus limited (Sterner et al. 2004), and gradients during thermal stratification are rarely observed in the water column either in space (SRP; Baehr and McManus 2003) or in time (TDP; Siew 2003). Although not considered in this work, it is possible, even likely, that spatiotemporal variation in algal stored phosphorus reserves occurs. This homogeneity in the water column suggests that phosphorus availability need not be accommodated in modeling DCM formation (Sterner 2010). This path is supported by the findings of Sterner (2011) that predictions of primary productivity, based solely on light and temperature, were well correlated with measurements (r^2=0.93). In the work reported here, the effects of phosphorus limitation are accommodated implicitly through the use of site-specific growth rate estimates developed for the Lake Superior phytoplankton assemblage under ambient nutrient conditions.

4.2.3.4 Respiration

The effects of respiration in the photic zone are implied in the growth rate; below the photic zone a background loss of biomass with a rate of 0.01 d^{-1} is assumed similar to Diehl (2002).

4.2.4 Kinetics: Zooplankton Grazing

Here, the effect of grazing on the DCM structure is considered. In the POC mass balance (Equation (4)), the grazing term (highlighted),

$$V_i \frac{dC_i}{dt} = \frac{EA_c}{l} \cdot \left(C_{i+1} - C_{(i-1)}\right) + \frac{v_s}{l}\left(C_{i-1} - C_{i+1}\right) + \mu_{Max} \cdot \left(f_T \cdot f_I \cdot f_P\right) \cdot C_i - k_{grazing} \cdot C_i \quad (12)$$

accommodates the mediating effect of grazing .

Losses due to zooplankton grazing can be described using a relationship that accommodates the effects of filtering rate, zooplankton density and temperature (Chapra 1997),

$$k_{grazing} = \frac{C_i}{K_{sa} + C_i} \cdot F_{zoo} \cdot \theta^{T_z - 20} \cdot C_{zoo} \quad (13)$$

Where

$k_{grazing}$ =	grazing rate	d^{-1}
K_{sa} =	Half saturation constant grazing	$\mu C \cdot L^{-1}$
F_{zoo} =	zooplankton filtering rate	$L \cdot mgC^{-1} \cdot d^{-1}$
Θ =	temperature correction factor for grazing	dimensionless
T_z =	temperature at depth z	°C
C_{zoo} =	zooplankton concentration	$mg \cdot L^{-1}$

The zooplankton assemblage in Lake Superior is dominated by calanoids (Fahnenstiel et al. 1984, Yurista 2009). Peters and Downing (1984) report that the filtration rate for zooplankton assemblages dominated by calanoids is insensitive to variations in food concentration and has a median value of 1.73 $L \cdot mgC^{-1} \cdot d^{-1}$. This rate falls in the general range reported by Chapra (1 to 2 $L \cdot mgC^{-1} \cdot d^{-1}$, 1997) and is applied in this model. The sensitivity of grazing rates to temperature is calculated here using a value of θ = 1.08 (Chapra 1997). Zooplankton concentrations in the water column are more consistent in space and in time in the offshore waters of Lake Superior (where the DCM is observed)

than in the nearshore. A zooplankton density maximum is typically observed in the vicinity of the thermocline, and diel vertical migration is limited to a distance of several meters (Yurista 2009). In this model, zooplankton concentrations are put in as an average sampling season water column profile for offshore stations (total depth >150 m; 2004-2006, Yurista, unpublished data). See Figure 2.9

4.3 Model Inputs: Environmental Forcing Conditions and Initial Conditions

Environmental forcing conditions include light and temperature, two features important in mediating phytoplankton growth. Incident irradiance (I_o) over the June-August interval when the DCM is observed varies only by about 15%, thus a constant value may be utilized.

Surface irradiance is assumed to vary between 0 and 1000 $\mu E \cdot m^{-2} \cdot s^{-1}$, following a sinusoidal function reflecting diel changes. The light regime algae experience at depth z is calculated on an hourly basis according to the Beer-Lambert law:

$$I_{z,t} = I_{0,t} \times e^{-k_e \cdot z} \qquad (14)$$

where

$I_{o,t}$ = surface irradiance $\mu E \cdot m^{-2} \cdot s^{-1}$

k_e = light extinction coefficient m^{-1}

The magnitude of the extinction coefficient varies with levels of CDOM, phytoplankton, organic detritus and nonvolatile suspended solids. Values for the extinction coefficient vary only minimally in Lake Superior, with values ranging from 0.15 m^{-1} to 0.25 m^{-1} (Sterner 2011). A value of 0.16 m^{-1}, is applied in this

model, similar to late summer extinction rates reported by Sterner (2010). This combination of incident radiation and extinction coefficient values results in a compensation depth (~ 1% of surface irradiance) of 29m and an irradiance at that depth of 10 $\mu E \cdot m^{-2} \cdot s^{-1}$. The model uses a constant temperature profile, reflecting typical water column structure during the target period: a well mixed, 17 meter deep epilimnion having a temperature of 11°C, a 17m thick metalimnion with a thermocline at 25m, and a 66-m deep hypolimnion with a temperature of 4°C (see Figure 4.5).

The initial condition for model simulations is provided by the water column particulate organic carbon distribution, assumed to be homogenous at 0.125 $mgC \cdot L^{-1}$ (a value similar that reported by Sterner 2010 for the period prior to stratification). See table 4.1.

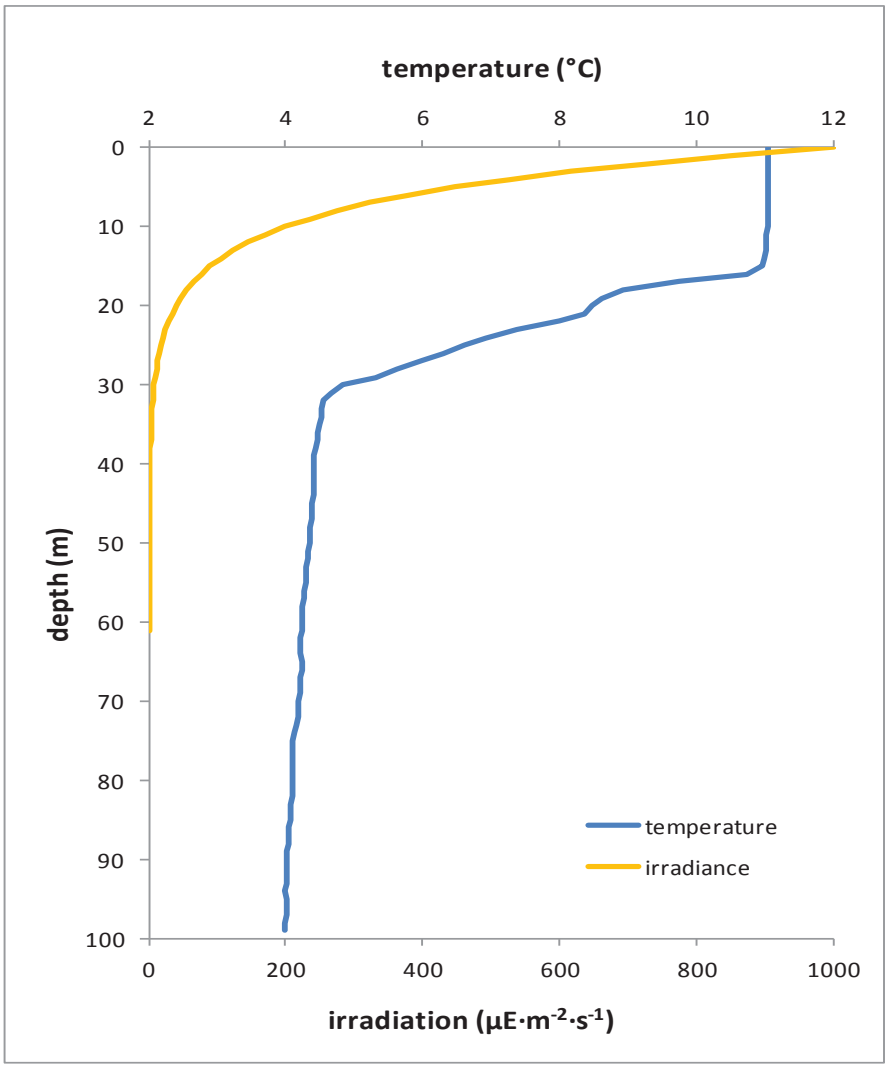

Figure 4.5 Light extinction and temperature profile

TABLE 4.1

Summary of model parameters and data

Para-meter	Description	Value		Units
α^{chl}	chlorophyll-specific initial slope of the PI curve	Epilimnion 0.002	DCM 0.004	$m^2 \cdot \mu E^{-1}$
α^{C}	carbon-specific initial slope of the PI curve	Epilimnion 0.00033	DCM 0.0024	$m^2 \cdot \mu E^{-1}$
β^{chl}	chlorophyll-specific curve fitting parameter photo inhibition	Epilimnion 0.001	DCM 0.0003-0.00004	$m^2 \cdot \mu E^{-1}$
β^{C}	carbon-specific curve fitting parameter photo inhibition	Epilimnion 0.00004	DCM 0.00016	$m^2 \cdot \mu E^{-1}$
Γ	fitting parameter photoadaptation	4.5		$gChl \cdot C^{-1}$
ϴ	temperature correction factor for grazing	1.08		-
μ_{Max}	carbon specific growth rate	Epilimnion 0.07	DCM 0.12	d^{-1}
M	dynamic viscosity	temperature variable		$cm^2 \cdot s^{-1}$
ρ_w	water density	temperature variable		$g \cdot L^{-1}$
A_c	cross sectional area of the interface	1		m^2
C_i	particulate organic carbon at depth i	0.125		$mgC \cdot L^{-1}$
$Chl:C_{min}$	minimum ratio Chlorophyll to Carbon	4.4		$\mu g\ Chl:mg\ C^{-1}$
C_{zoo}	zooplankton concentration	depth variable		$mg \cdot L^{-1}$
D	particle diameter	5		μm
E	diffusion coefficient	depth variable		$m^2 \cdot d^{-1}$

Table 4.1 (*continued*)

Para-meter	Description	Value		Units
E'	turbulent diffusion coefficient	depth variable		$m^3 \cdot d^{-1}$
G	acceleration due to gravity	9.81		$m \cdot s^2$
I_o	surface light energy	1000		$\mu E \cdot m^{-2} \cdot s^{-1}$
L	mixing length	1		m
I_{zmax}	maximum irradiance at depth	variable		$\mu E \cdot m^{-2} \cdot s^{-1}$
$I_{z,t}$	irradiance at depth z and time t	variable		$\mu E \cdot m^{-2} \cdot s^{-1}$
K_1	fitting parameter, ascending limb	0.0200		-
K_2	fitting parameter, descending limb	0.0103		-
K_e	light extinction	0.20		m^{-1}
$k_{grazing}$	grazing rate	depth variable		d^{-1}
Kg_{Topt}	maximum growth rate temperature function	0.081		d^{-1}
K_{photo}	half saturation constant irradiance	Epilimnion 100	DCM 25	$\mu E \cdot m^{-2} \cdot s^{-1}$
k_r	chlorophyll degradation rate	0.05		d^{-1}
K_{sa}	Half saturation constant grazing	1.5		$\mu C \cdot L^{-1}$
F_{zoo}	zooplankton filtering rate	3.0		$L \cdot mgC^{-1} \cdot d^{-1}$
P_s	particle density	1050		$g \cdot L^{-1}$
T	Time			d
T_{opt}	temperature optimum	13.4		°C
T_z	temperature at dept z	depth variable		°C
V_i	Volume	1		m^3
v_s	settling velocity	depth variable		$m \cdot d^{-1}$

5.0 Model Results

In the following section, mechanisms described earlier (mass transport, growth and grazing) are evaluated in isolation and in concert through application of the model. Simulations are performed over a period of 50 days, representing the period from early stratification until late summer, with model parameter values presented in Table 4.1, unless otherwise specified. The effects of physical processes are presented first, followed by those with a biological origin.

5.1 Diffusion

Under completely-mixed conditions, the turbulent diffusion coefficient is the same over the water column. For a homogenous initial condition, constant vertical profiles of temperature, solutes and particulate matter would be maintained. With initially higher levels of material present in the epilimnion, gradients would be relaxed over time. Under thermally-stratified conditions the turbulent diffusion coefficient is reduced at the thermocline. A homogenous initial condition and a case where POC concentrations are doubled in the upper 16 meters of the water column (a step function) are analyzed (Figures 5.1a and 5.1b). Diffusive forces, as expected, are not able to create an accrual of carbon at any depth and relax concentration gradients analog to dynamics in the thermal structure. Diffusion is thus not a mechanism that can contribute to the formation of a carbon maximum.

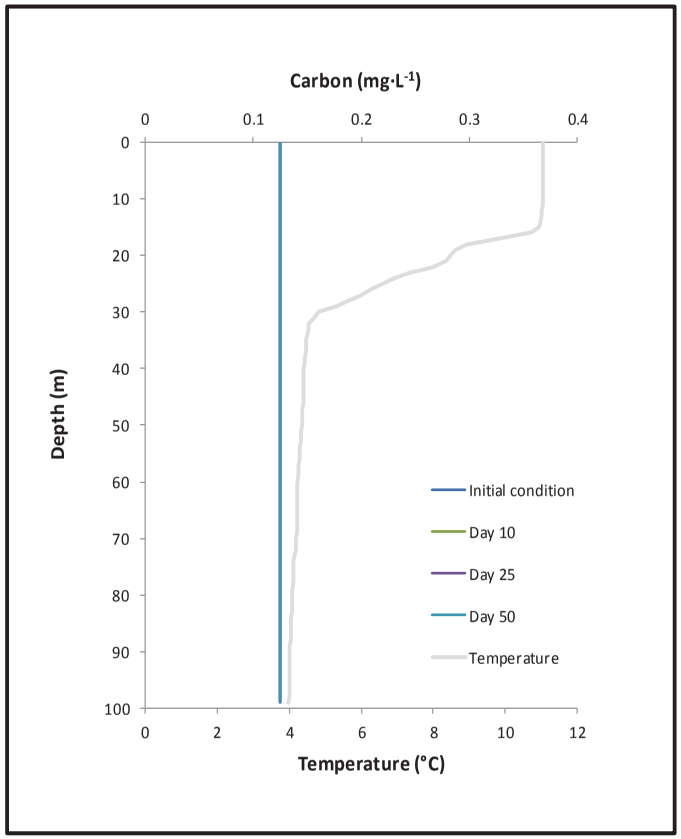

Figure 5.1a Turbulent diffusion acting on a homogeneous carbon distribution in a stratified water column.

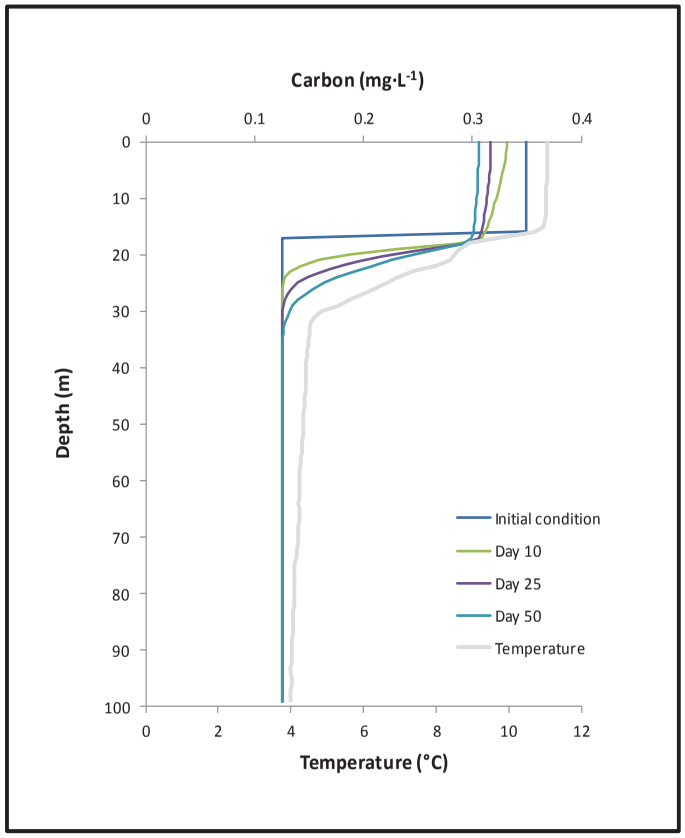

Figure 5.1b Turbulent diffusion acting on a step increase in carbon concentration (initial POC concentration is doubled in the top 16 meters of the water column)

5.2 Settling

In the absence of other mechanisms, mass transport of the characteristic particle through settling results in the accumulation of cells at metalimnetic depths for extended periods (Figure 5.2a). The algal assemblage consists of phytoplankton with varying physical characteristics, and the effect of settling therefore is also evaluated for smaller and larger than average particles (*ceteris paribus*). A decrease of particle diameter to 7 µm increases the residence time in the metalimnion dramatically (Figure 5.2b). The smaller sized phytoplankton retained on the density gradient could be a reason for the occasionally observed increase in abundance of certain smaller algal species at this depth (e.g. *Cyclotella* species; Fahnenstiel and Glime 1983).

The effect of settling on larger and/or denser particles, here simulated by increasing the particle diameter to 17 µm, is shown in Figure 5.2c. Larger particles are less influenced by the density gradient, resulting in a shorter residence time in the metalimnion on their way to the sediments. Benthic organisms would therefore receive a greater proportion of large and dense algal cells up to several months after production in the epilimnion (e.g. lipid rich diatoms).

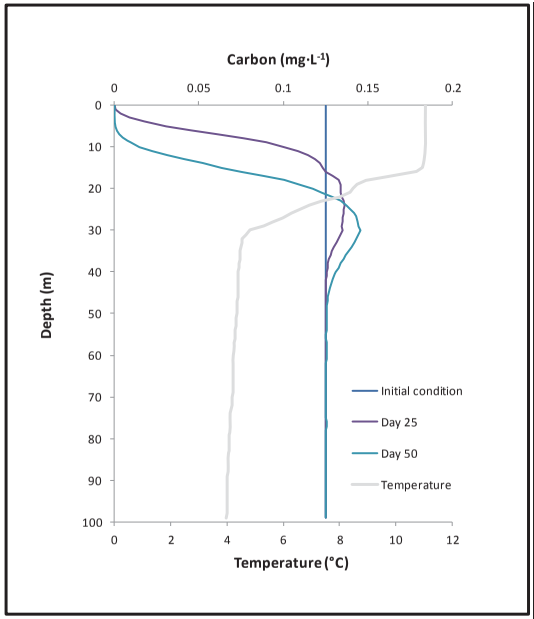

Figure 5.2a Carbon profile simulating the settling of particles with a diameter of 12 µm and a density of 1050 mg·L^{-1}

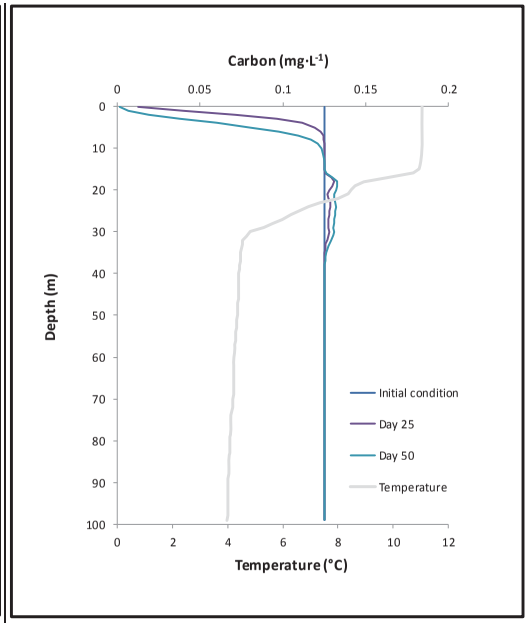

Figure 5.2b Carbon profile simulating the settling of particles with a diameter of 7µm and density of 1050 mg·L^{-1}

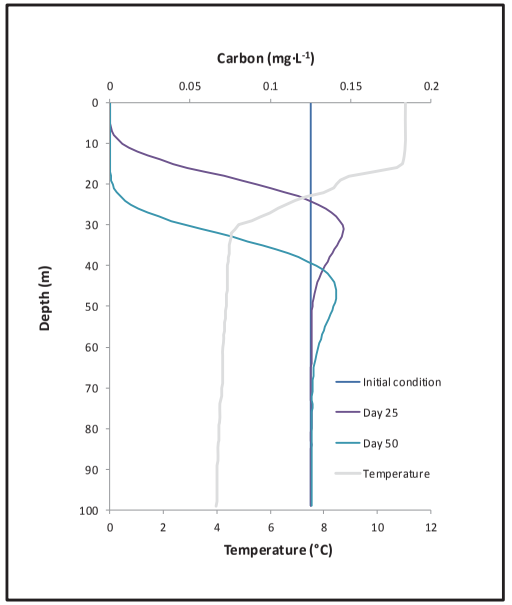

Figure 5.2c Profile simulating the settling of particles with a diameter of 17µm and density of 1050 mg·L^{-1}

5.3 Diffusion and Settling

The combination of diffusion and settling leads to a smoother, more continuous result with gradually changing concentration over the profile and a carbon maximum similar to that observed in Lake Superior (Figure 5.3a and b). Concentrations in the upper water column are lower than those observed. However, simulated concentrations in the metalimnion are expected to increase when the model incorporates growth dynamics. The modeled concentrations at deeper levels in the water column are higher than those observed but will be reduced by application of biological processes like respiration and decay. Mechanisms of mass transport are able to create the accumulation of carbon in the metalimnion similar to observed carbon profiles, but additional mechanisms are needed to match observed profiles more closely. The effects of biological mechanisms (growth and grazing) on the carbon profile are discussed in the following sections.

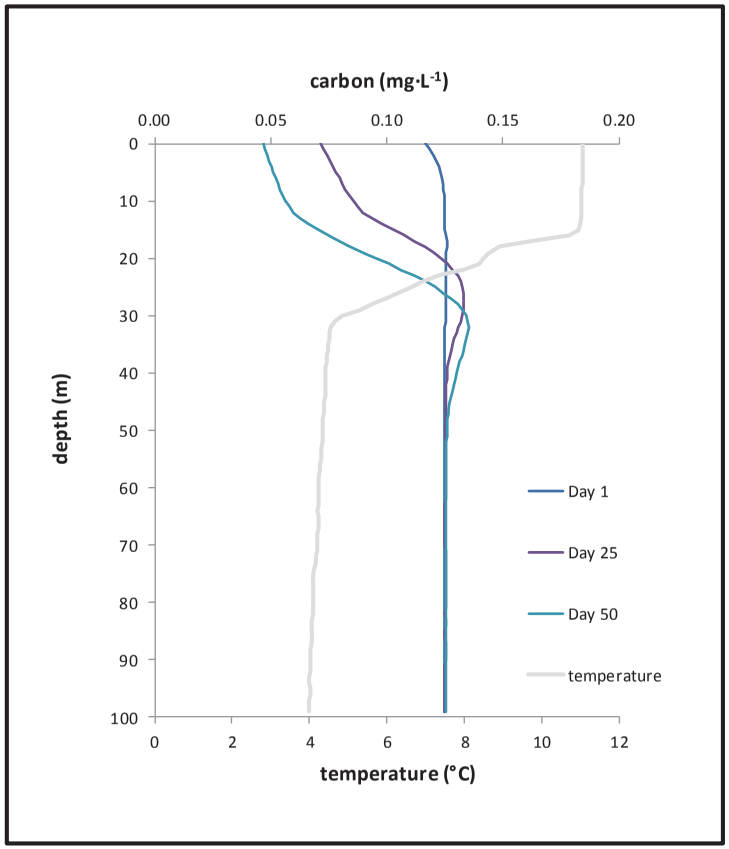

Figure 5.3a Effects of mass transport (settling and diffusion) on a particle with a diameter of 12 μm and a density of 1050 mg·L^{-1}

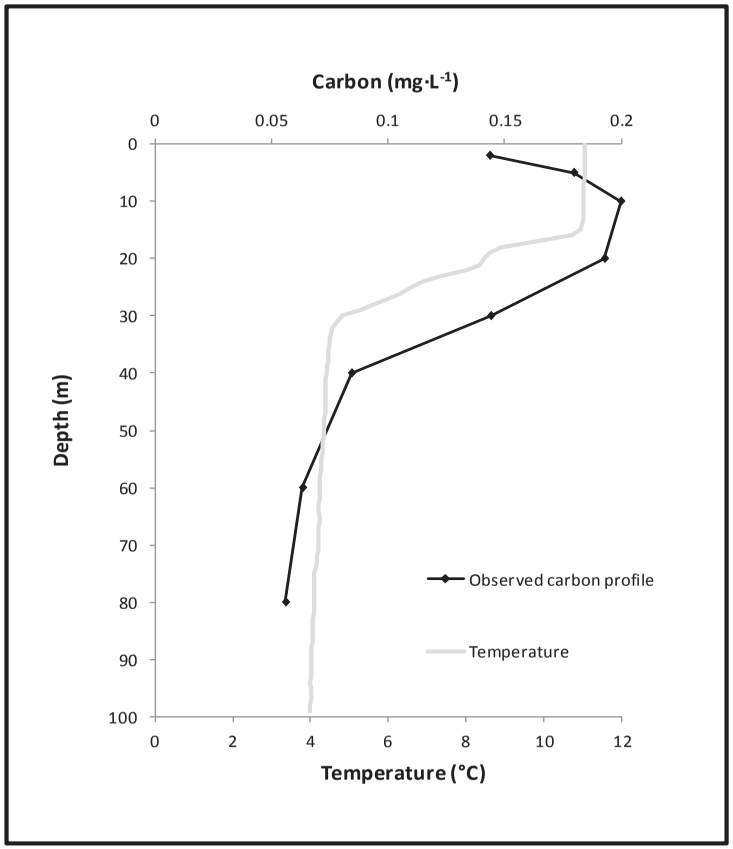

Figure 5.3b Observed carbon profile (Sterner 2010)

5.4 Growth

Growth (in the absence of shade adaptation, discussed later) is strongest in the upper layer of the epilimnion, similar to findings by Sterner (2010). Photo inhibition in the surface layer of the water column is minimal due to the applied kinetics and in reality can vary significantly depending on the antecedent conditions. Algal growth decreases as conditions at depth become less favorable (photosynthetic radiation and temperature). Growth in the absence of respiration, mass transport and grazing is shown in Figure 5.4a. When growth and respiration are activated, simulation shows that carbon is supplied to the epilimnion and reduced in the hypolimnion (Figure 5.4b). The effect of losses due to zooplankton grazing is discussed next.

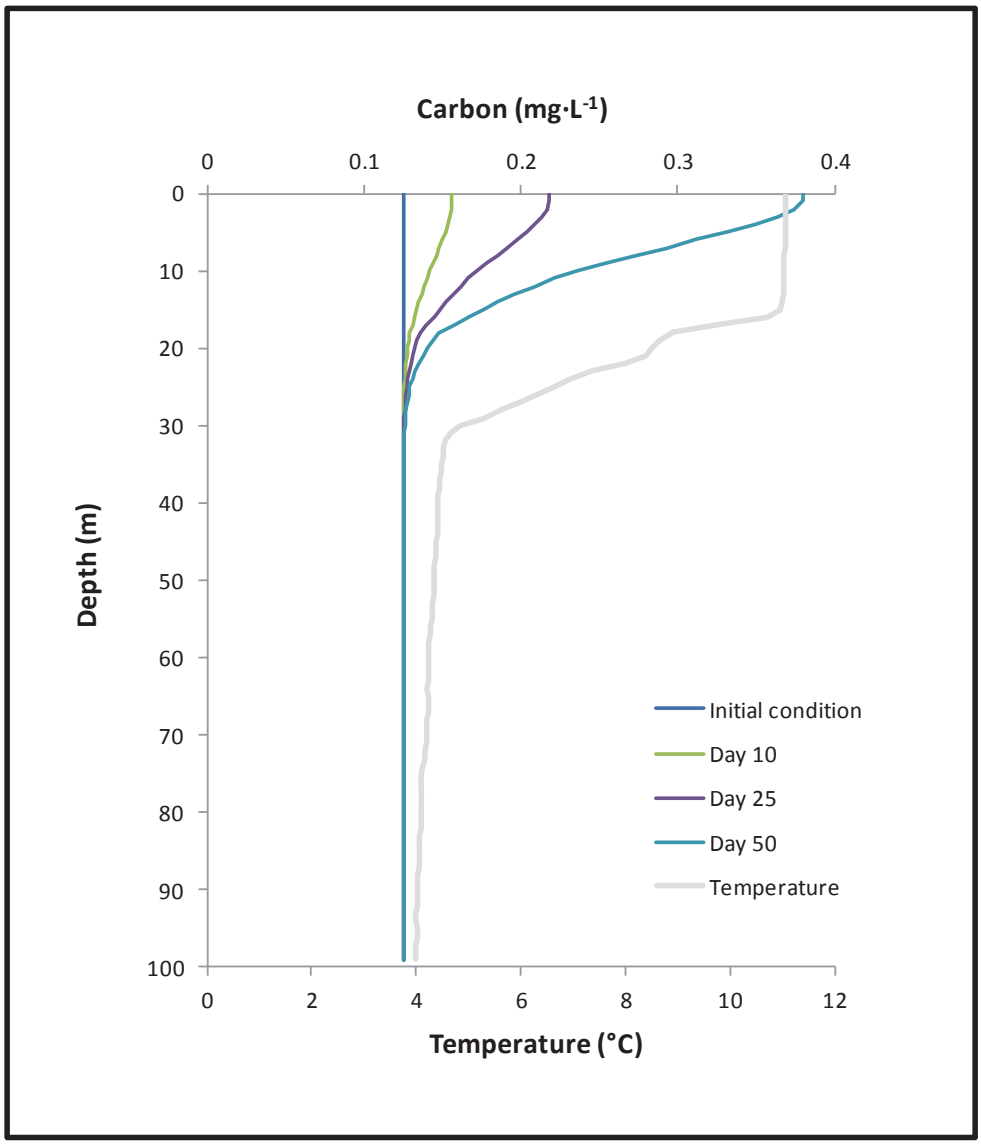

Figure 5.4a Effect of growth without basal respiration below the photic zone

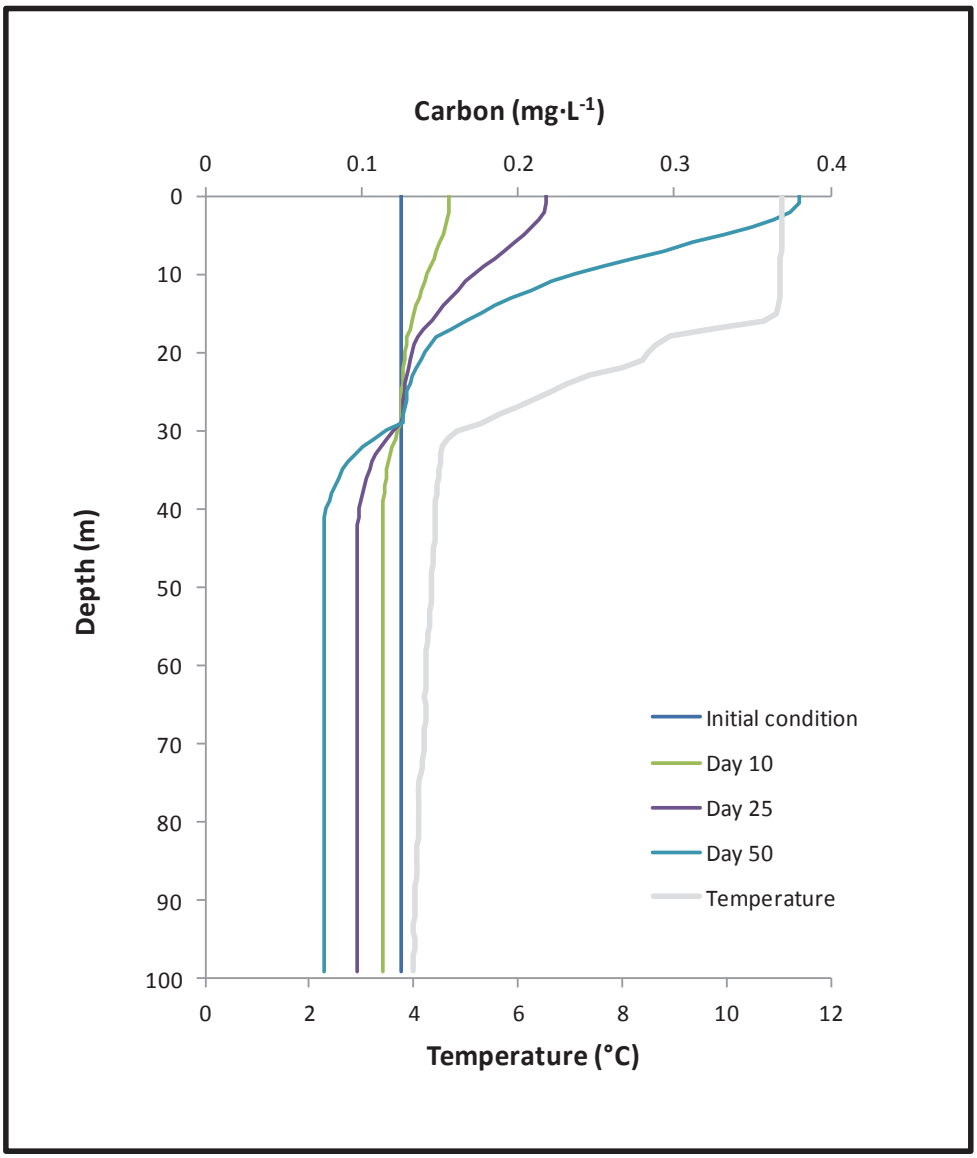

Figure 5.4b Effects of growth with basal respiration below the photic zone

5.5 Zooplankton grazing

Carbon loss due to zooplankton grazing is primarily determined by the distribution of zooplankton in the water column and secondarily by temperature. Losses, therefore, reflect the reverse image of the zooplankton distribution, with greatest losses at the zooplankton biomass maximum (Figure 5.5a). Temperature induced changes in the ingestion rates follow the thermal structure, showing elevated rates in warmer water (Figure 5.5b). Ingestion rates relative to zooplankton biomass suggest supplementation with alternative carbon sources (e.g. bacteria; Auer and Powell, 2004). The location of the zooplankton biomass maximum in the water column coincides with a depth approximately where algal accumulation occurs under calm conditions, signified by low turbulent mixing (Figure 5.5c). Zooplankton response (migration) to a change in depth of the algal biomass maximum falls outside the scope of this model. The interaction of all previously described mechanisms is discussed in the next section.

5.6 Growth, Settling, Diffusion and Zooplankton Grazing

When all mechanisms are applied in symphony with kinetics described in Table 4.1 a carbon profile results with a slowly descending maximum maintaining its presence in the metalimnion for an extended period of time. Higher growth rates in the epilimnion will result in a more pronounced maximum at a higher depth (discussed in section 6) (Figure 5.6).

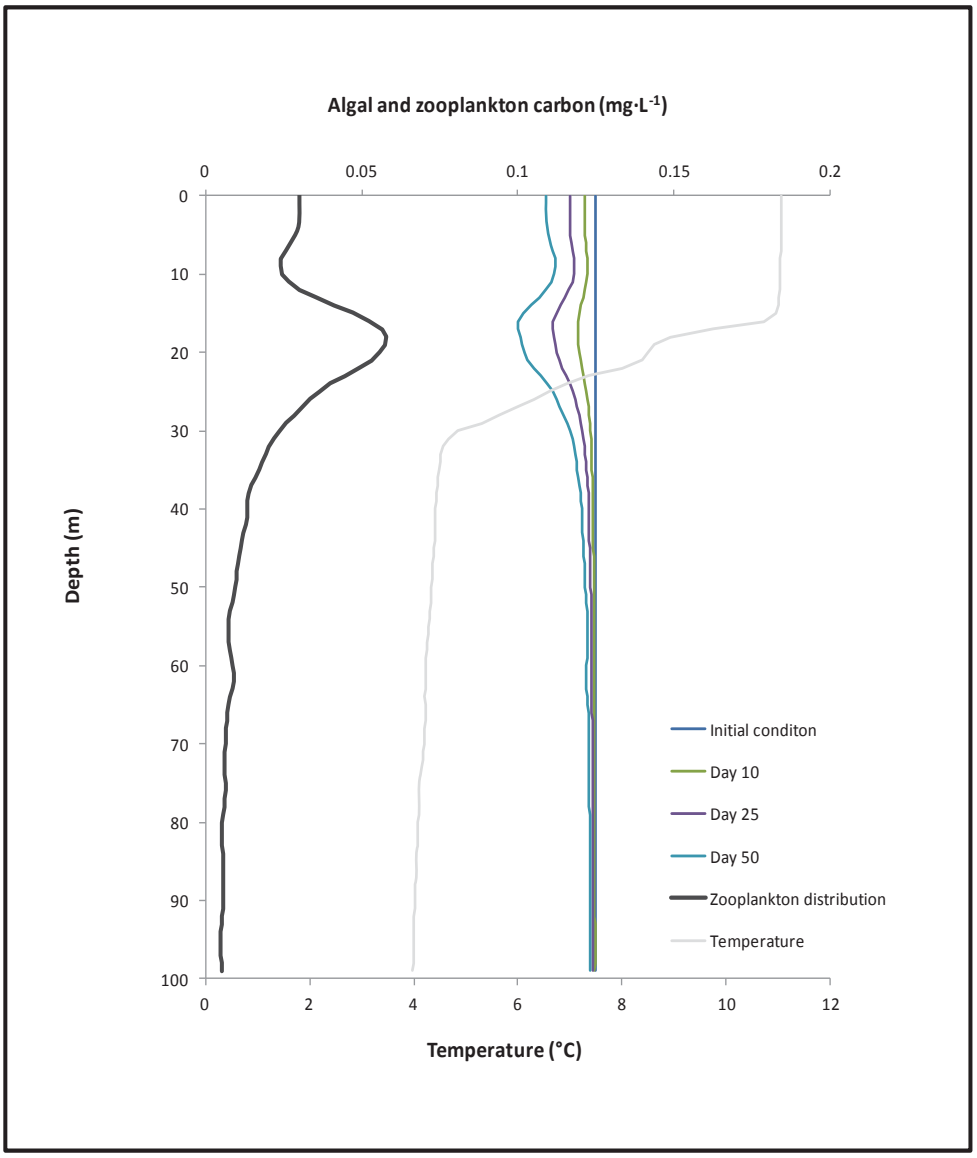

Figure 5.5a Effects of zooplankton grazing

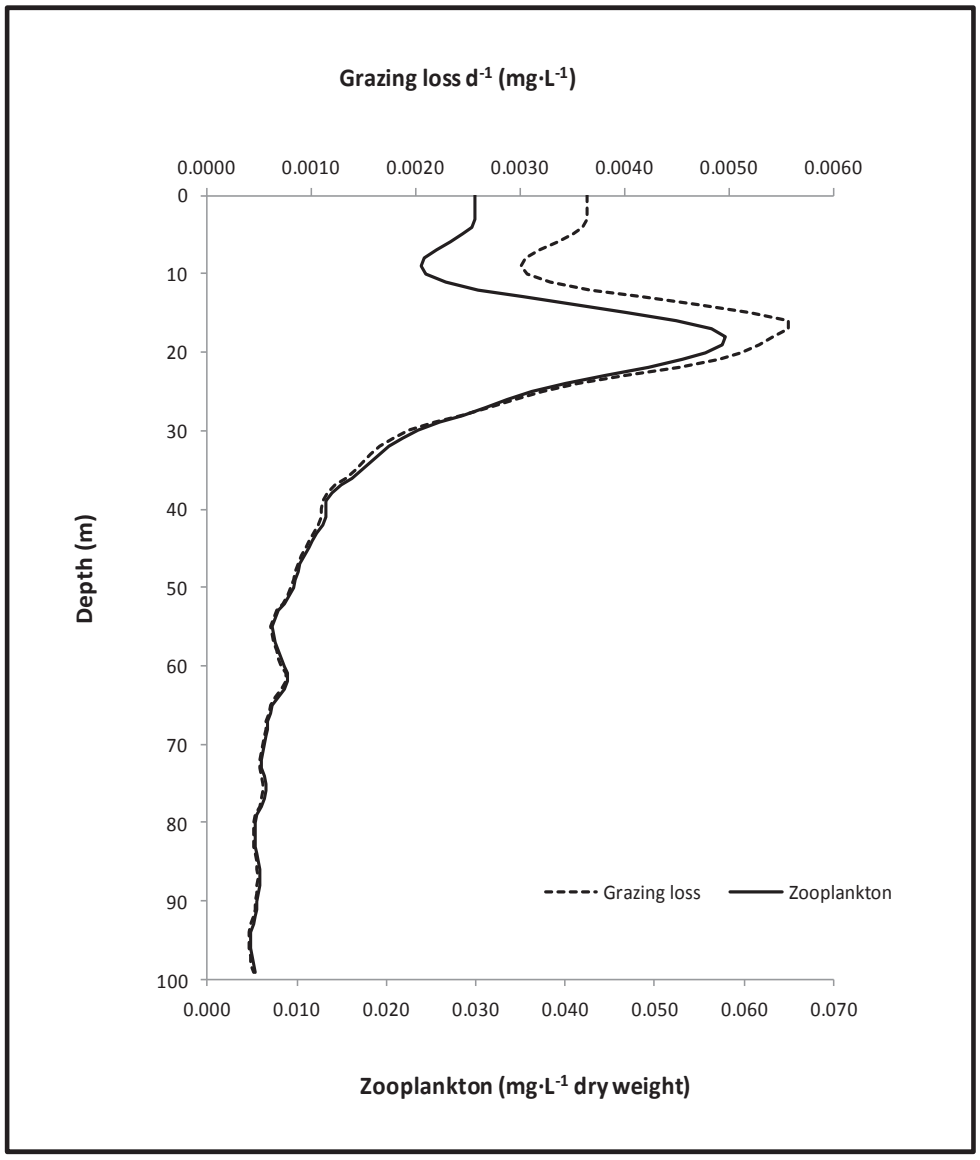

Figure 5.5b Grazing losses in relation to the zooplankton distribution

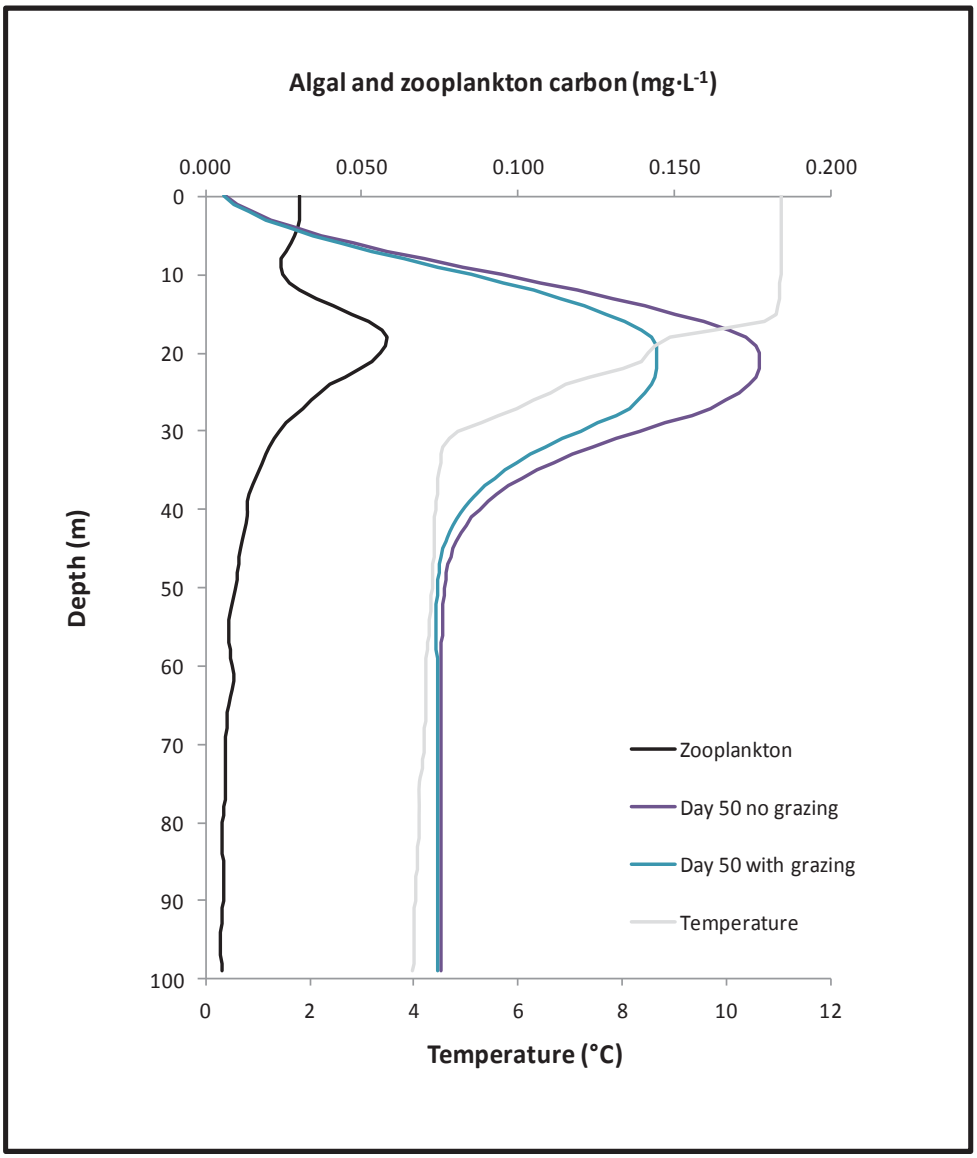

Figure 5.5c Effect of grazing losses (low diffusion, settling, growth and respiration)

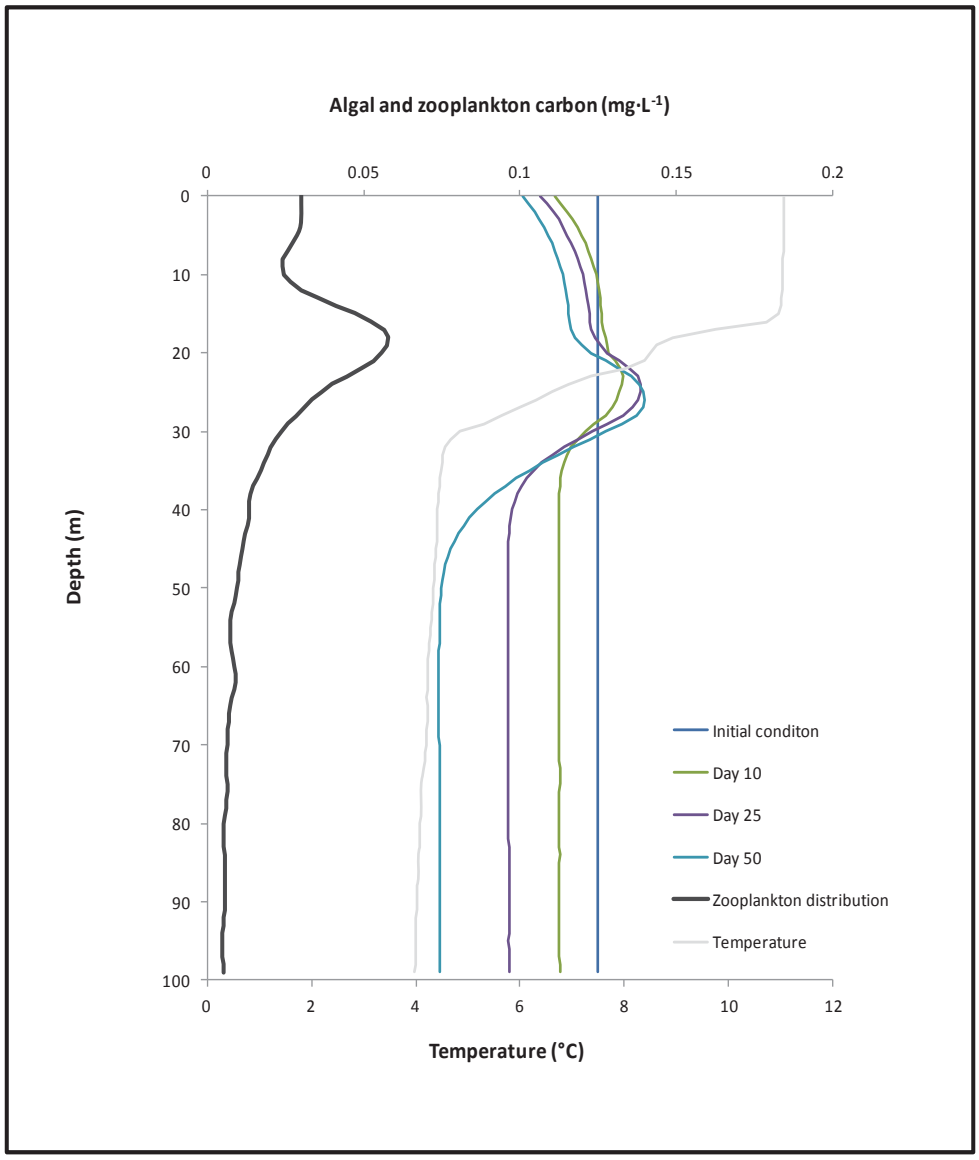

Figure 5.6 Carbon profile with all mechanisms (diffusion, settling, grazing growth and respiration) applied.

6.0 Model Comparison to Measured POC and Chlorophyll Data

Modeling efforts in the previous section, based on derived kinetic coefficients as described in Table 4.1, confirm the accumulation of algal biomass in the metalimnion and the impact different mechanisms have in its creation. In the following section algal biomass (measured as particulate organic carbon (POC)), chlorophyll, temperature and growth rate data reported by Sterner (taken at the CARGO6 cruise on September 17 2008; 2010) are used to calibrate the model for further analysis of mechanisms responsible for the formation and maintenance of the DCM. As the calibration data was taken in late summer, a 50 day simulation period is applied to obtain comparable results. In order to match the modeled carbon profile with the measured POC profile, turbulent mixing is decreased to 2.2 $m^3 \cdot d^{-1}$at the surface and reduced in a linear fashion to the thermocline and kept constant past this depth at 0.4 $m^3 \cdot d^{-1}$. The maximum growth rate is increased to 0.45 d^{-1} to match measured growth rates. The resulting model generated carbon profile is able to match the measured POC profile closely, as shown in Figure 6.1.

6.1 Sensitivity analysis of model

The potential variability in model derived biomass at a depth of 10 m (the maximum in carbon biomass) is evaluated by a sensitivity analysis where the maximum growth rate, grazing rate, turbulent diffusion coefficient, particle diameter and optimum growth temperature are independently increased and decreased by 20% (Table 6.1).

TABLE 6.1

Model Sensitivity Analysis

Parameter	Percent change in carbon biomass at 10m depth with a parameter increases of +20%	Percent change in carbon biomass at 10m depth with a parameter decreases of -20%
Turbulent diffusion	-3%	3%
Particle diameter	-44%	43%
μ_{Max}	4%	-6%
α^C	31%	-24%
β^C	-1%	1%
$k_{grazing}$	0%	-1%
K_{sa}	2%	-3%
T^{opt}	-41%	22%

The model is particular sensitive to α^C and T_{opt} which were determined on a site specific basis (Figures 4.3c and 4.4c). The model is also highly sensitive to particle diameter which can be properly estimated from Baker's work (1991).

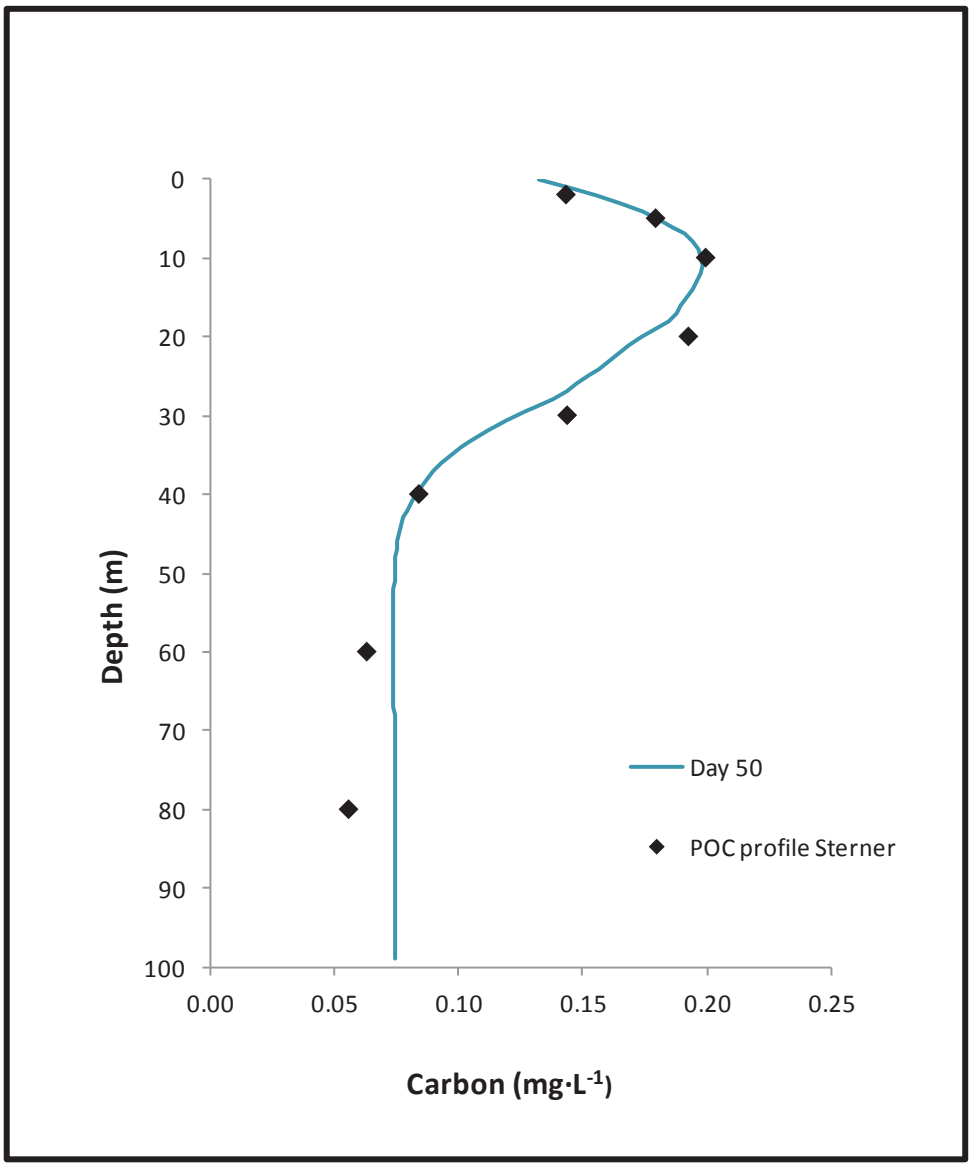

Figure 6.1 Model generated carbon profile and measured data Sterner (2010)

6.2 Constant Chlorophyll to Carbon Ratio

This work, however, focuses on the vertical distribution of chlorophyll in the water column, and model output expressed in units of carbon needs to be expressed in units of chlorophyll. Conversion of carbon to units of chlorophyll in water quality models is often done using an average chlorophyll to carbon (Chl:C) ratio (e.g. Ambrose et al. 1993). When the model generated carbon profile is converted to a chlorophyll profile using an average Chl:C ratio of 6 μg Chl:mg C^{-1}, a comparison can be made with measured chlorophyll data (Figure 6.2a). The resulting chlorophyll profile shows a poor fit, and a closer look at the applied and measured Chl:C ratios reveals that using an average Chl:C ratio for conversion is not appropriate (Figure 6.2b). Algae respond to limiting light conditions by expanding their photosynthetic apparatus with additional chlorophyll (i.e. Chl:C ratio is not constant with depth); this process, referred to as photo adaptation, is discussed in the next section.

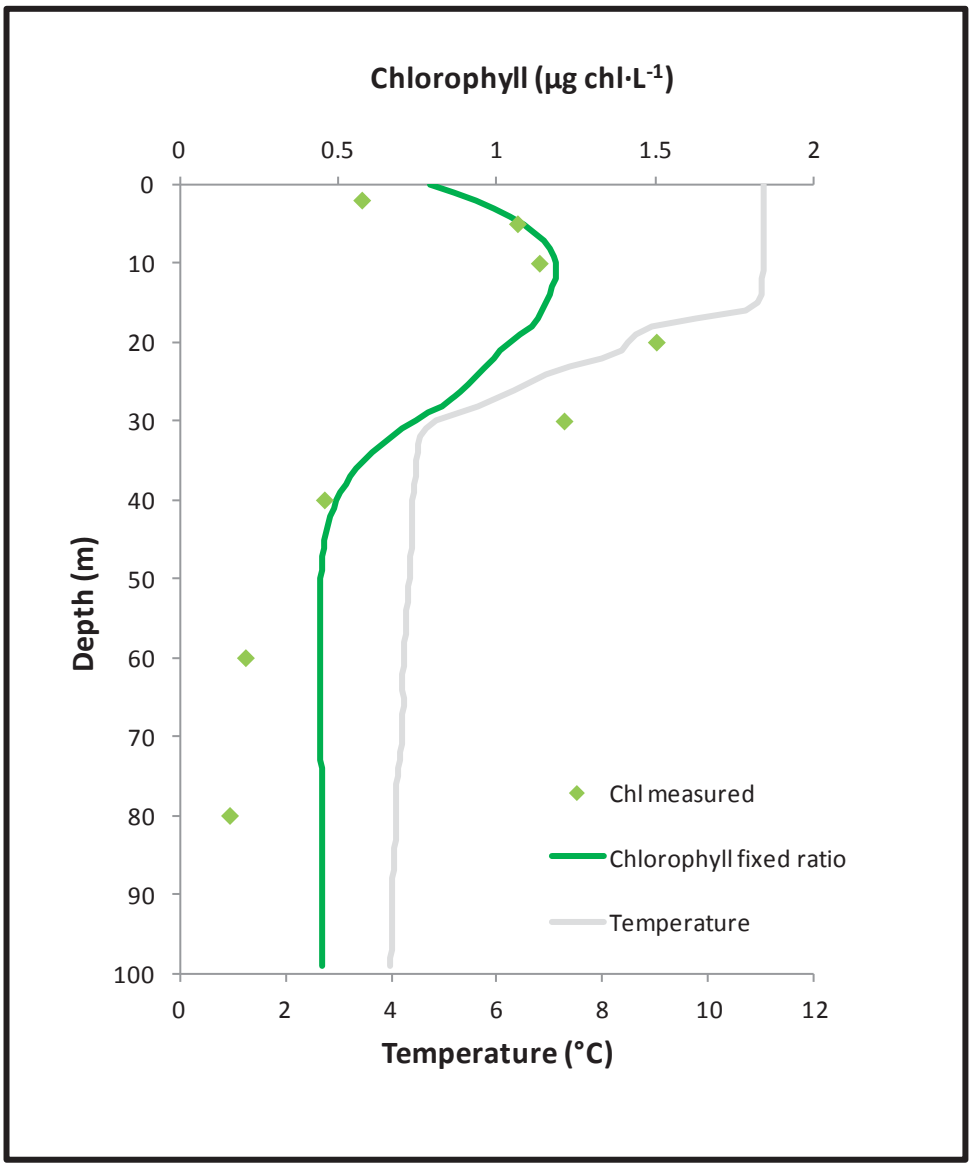

Figure 6.2a Model generated chlorophyll profile with fixed Chl:C ratio and measured chlorophyll profile

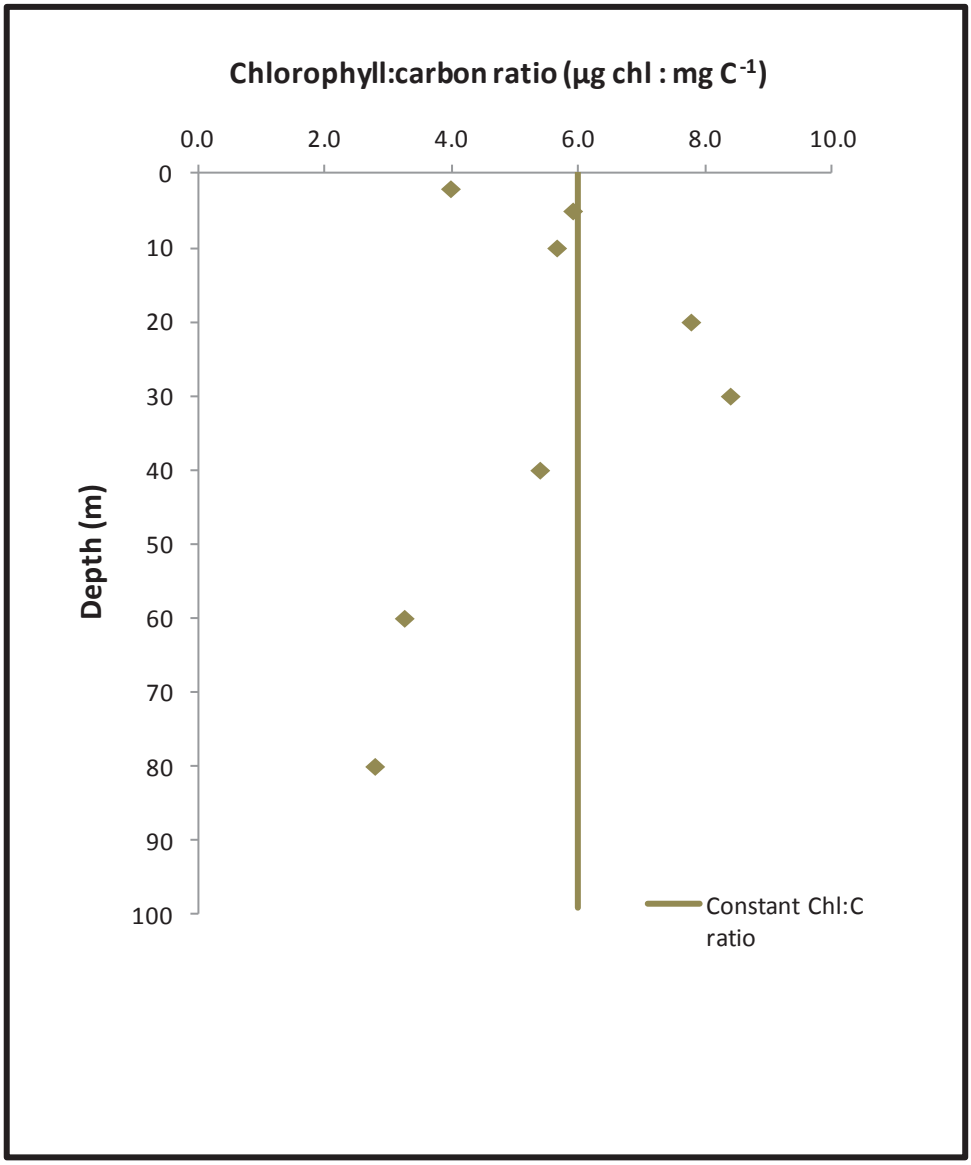

Figure 6.2b Constant Chl:C ratio compared to measured ratios

6.3 Variable Chlorophyll to Carbon Ratio

The need to use variable chlorophyll to carbon ratios became apparent from the previous figures. However, the significance of variable ratios in converting from chlorophyll to carbon, and *vice versa*, is not acknowledged by all researchers. Kruskopf and Flynn (2006), for example, caution that chlorophyll concentration should not *de facto* be regarded as phytoplankton biomass., a practice still encountered, even though it has long been known by phycologists that chlorophyll is not a good indicator for biomass (Steel and Baird, 1961) because Chl:C ratios can fluctuate (e.g. Flemer 1969).

The time scale of photoadaptation (hours rather than days, Cullen and Lewis 1988, Geider et al. 1998) is fast relative to that of algal growth, thus negating the need for a high degree of temporal resolution (Flynn 2003) and permitting the application of an empirical conversion function in this model, e.g. that of Laws and Chalup (1990) and Chapra (1997),

$$\mathrm{Chl{:}C}_z = \mathrm{Chl{:}C}_{\min} + \gamma \cdot \frac{K_{photo}}{K_{photo} + I_z} \qquad (15)$$

where

$\mathrm{Chl{:}C}_z$ =	Chlorophyll to carbon ratio at depth z	$\mu gChl \cdot mgC^{-1}$
$\mathrm{Chl{:}C}_{min}$ =	Minimum chlorophyll to carbon ratio	$\mu gChl \cdot mgC^{-1}$
γ =	Fitting parameter	dimensionless
K_{photo} =	Half saturation constant for photoadaptation	$\mu E \cdot m^{-2} \cdot s^{-1}$
I_z =	Irradiance at depth	$\mu E \cdot m^{-2} \cdot s^{-1}$

Alternatively a function proposed by Flynn (2003) may be used:

$$\mathrm{Chl{:}C}_z = \mathrm{Chl{:}C}_{\min} + \frac{\mu_z}{I_z \cdot \alpha^{chl}} \quad (16)$$

where

μ_z = Carbon growth rate at depth z — d^{-1}

α^{chl} = Chlorophyll-specific initial slope of growth-irradiance curve — $\mu gC \cdot \mu gChl^{-1} \cdot \mu E \cdot m^{-2} \cdot s^{-1}$

Chlorophyll to carbon ratios in Lake Superior range from 2.6 to 6.2 μgChl·mgC^{-1} in the epilimnion and from 4.7 to 13.1 μgChl·mgC^{-1} within the DCM (Barbiero and Tuchman 2004), a variation consistent with the expected photoadaptation response. Spatiotemporal differences in nutrient regime, known to shift ratios over the whole water column (Chapra 1997), may explain the spread in the chlorophyll to carbon ratios cited above. Here, average values over these ranges are used in parameterizing Equation (15). Taking the average epilimnion value (4.4 μgChl·mgC^{-1}) as Chl:C $_{min}$, and recognizing that the average DCM value (8.9 μgChl·mgC^{-1}) represents Chl:C $_z$ for $I_z \sim 0$, yields γ as the difference between Chl:C $_z$ and Chl:C $_{min}$, 4.5 μgChl·mgC^{-1}. In simulating photoadaptation, Chapra (1997) suggests that the coefficient K_{photo} is well represented by the half-saturation constant in a Monod-based photosynthesis-irradiance relationship, here 100 $\mu E \cdot m^{-2} \cdot s^{-1}$ for the epilimnion and 50 $\mu E \cdot m^{-2} \cdot s^{-1}$ at DCM depth.

Below the compensation depth, photoadaptation ceases and Chl:C ratios fall as chlorophyll degradation is initiated as a means of internal nutrient

recycling. This pigment catabolism occurs when stable, chlorophyll-containing complexes are broken down to recover proteins, lipids and carotenoids (Matile et al. 1999). The degradation process is well described by a first order decay with the rate coefficient ranging from 0.025 d^{-1} (Geider et al. 1998) to 0.069 d^{-1} (Faugeras et al. 2004); a rate constant of 0.05 d^{-1} is applied here . Degradation proceeds until the minimum Chl:C ratio is reached, and further reductions are assumed to lead to cell lysis. A conceptualization of the impacts of these processes on the Chl:C ratio over the water column underscores the importance of the rarely invoked degradation phenomenon (Figure 6.3a). Here, the amplitude of the maximum ratio is determined by nutrient conditions in the water column (Chapra 1997), and the depth of the maximum ratio is determined by the rate of light attenuation. Fluctuations in the compensation depth and the capacity of turbulent diffusion to reduce gradients are expected to shape the width of the peak. The dynamics of the Chl:C ratio outlined here suggest that the use of an average water column value can seriously bias calculations of (carbon biomass) growth and production.

The functions described by Chapra and Flynn lead to depth variable Chl:C ratios, and both functions are compared to measured Chl:C values to determine their accuracy (Figures 6.3b and c). The best fit to the data is obtained by the function described by Chapra and is applied hereafter for conversions between carbon and chlorophyll. The conversion of the model generated carbon profile to a chlorophyll based profile results in a good fit with measured chlorophyll values (Figure 6.3d). The model generated carbon and chlorophyll profile are displayed

side by side in Figures 6.3d and e. Spatial separation of the carbon and chlorophyll maximum is caused by increased Chl:C ratios near the compensation depth, stemming from shade adaptation, and illustrates the reason for applying variable Chl:C ratios.

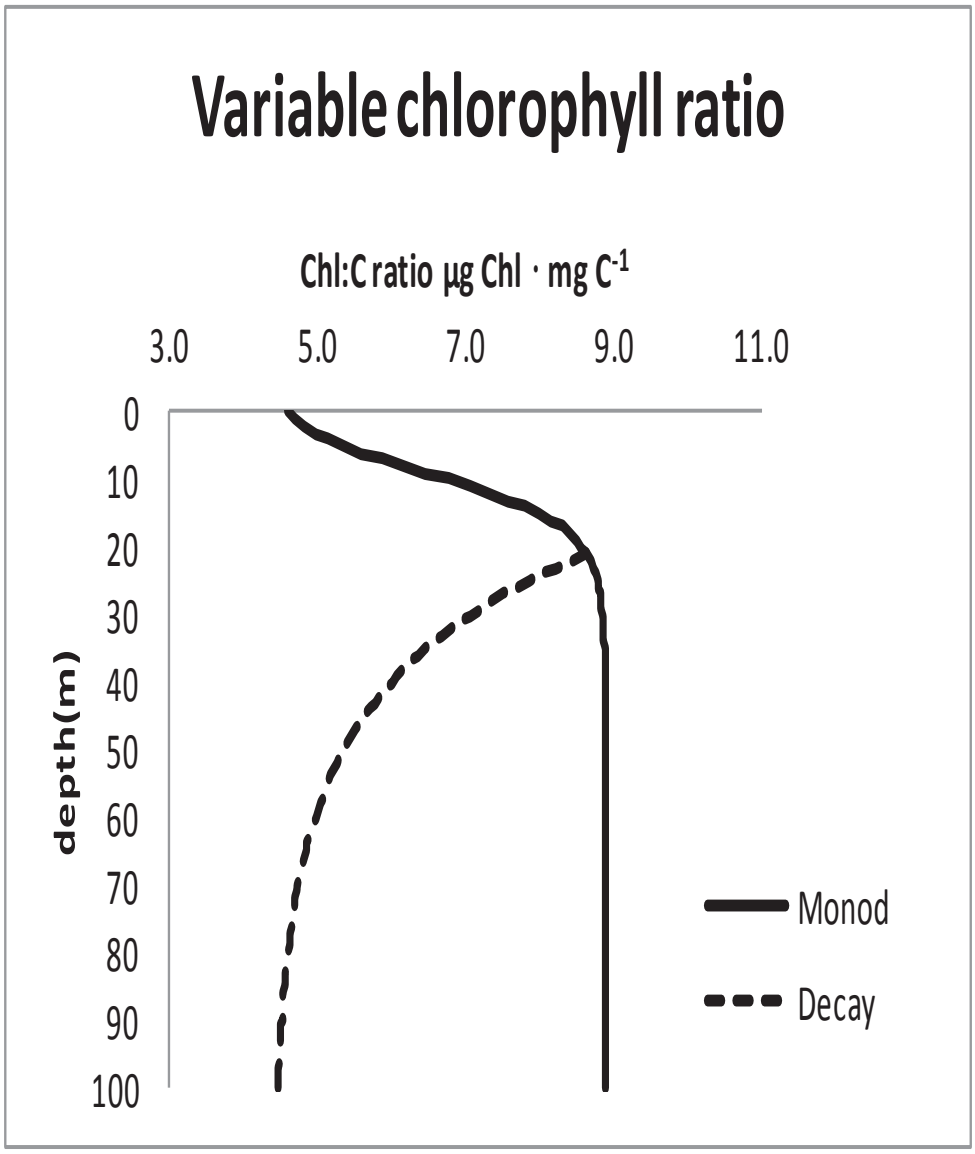

Figure 6.3a Conceptualization of depth variation in chlorophyll to carbon ratios: based on photoadaptation (solid line) and based on photoadaptation with degradation below the compensation depth (dashed line)

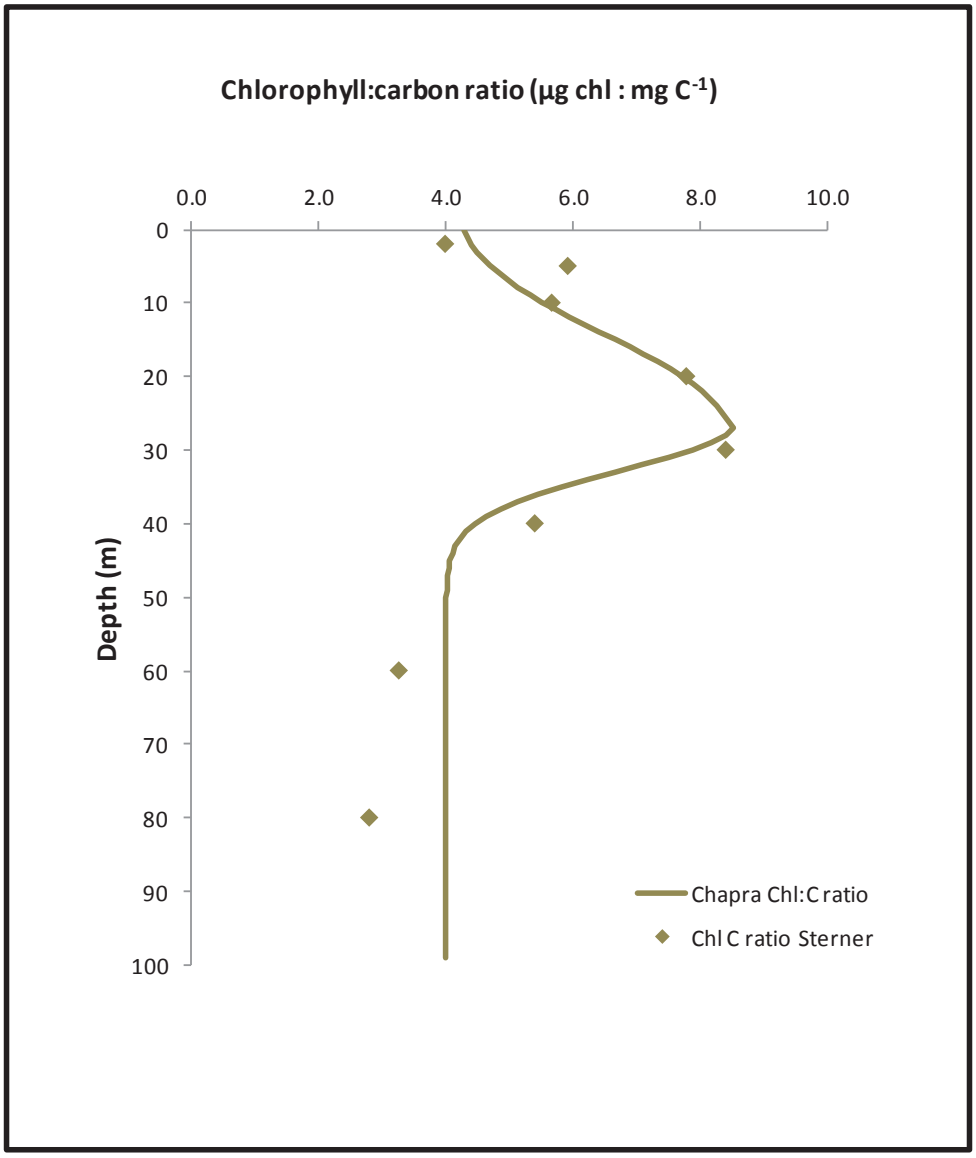

Figure 6.3b Depth variable Chl:C ratio (Chapra function)

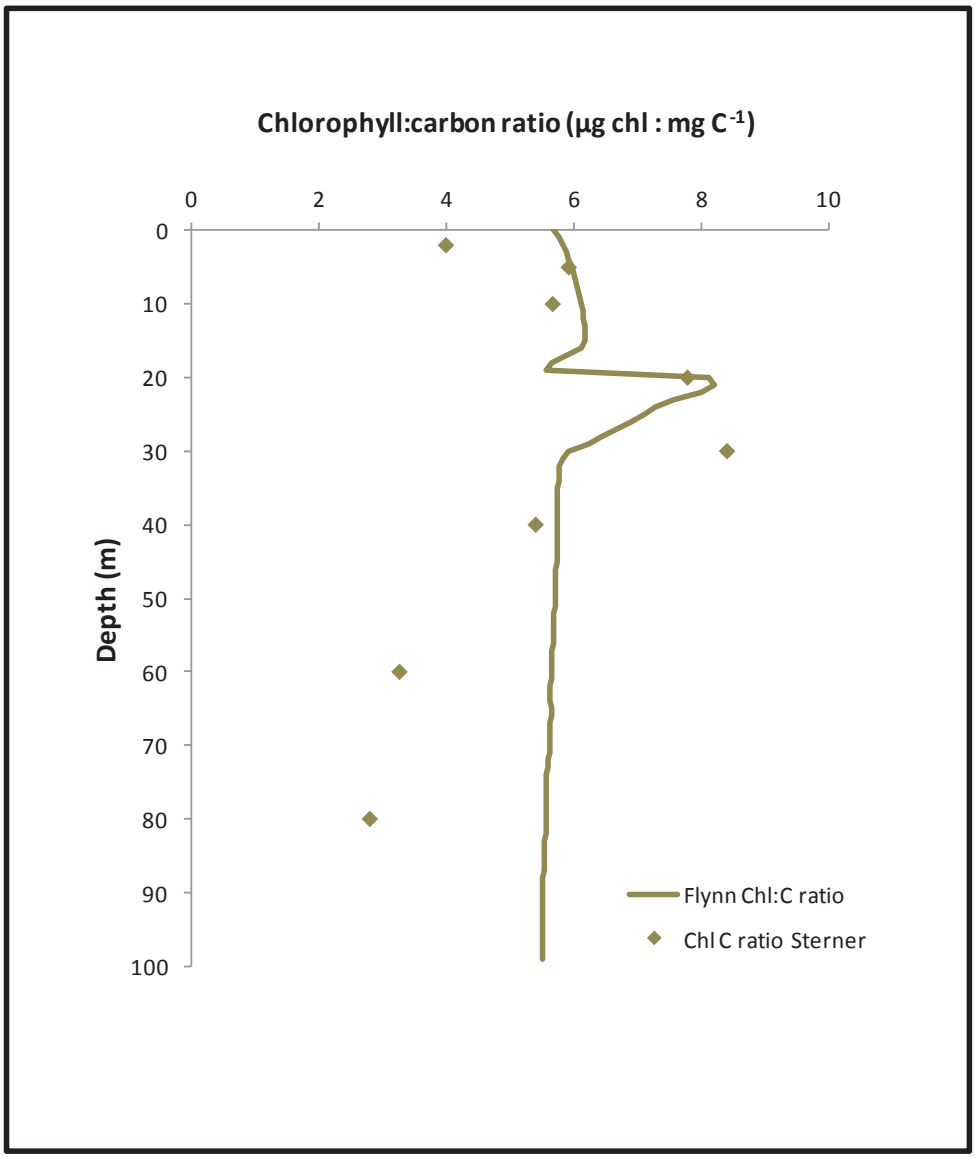

Figure 6.3c Depth variable Chl:C ratio (Flynn function)

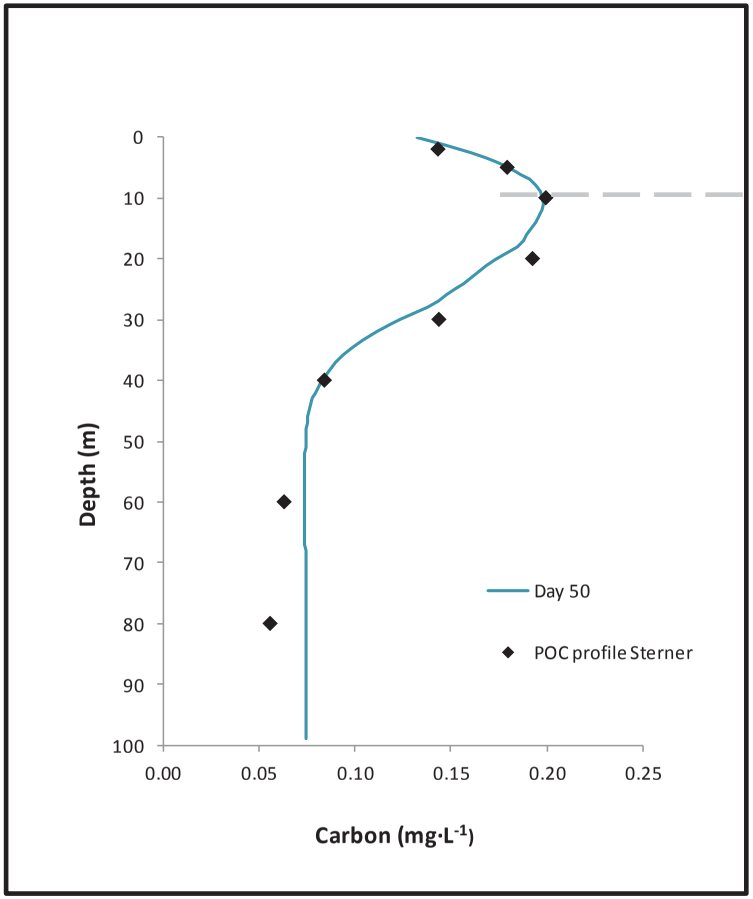

Figure 6.3d Model generated carbon profile and measured POC values (POC data from Sterner 2010)

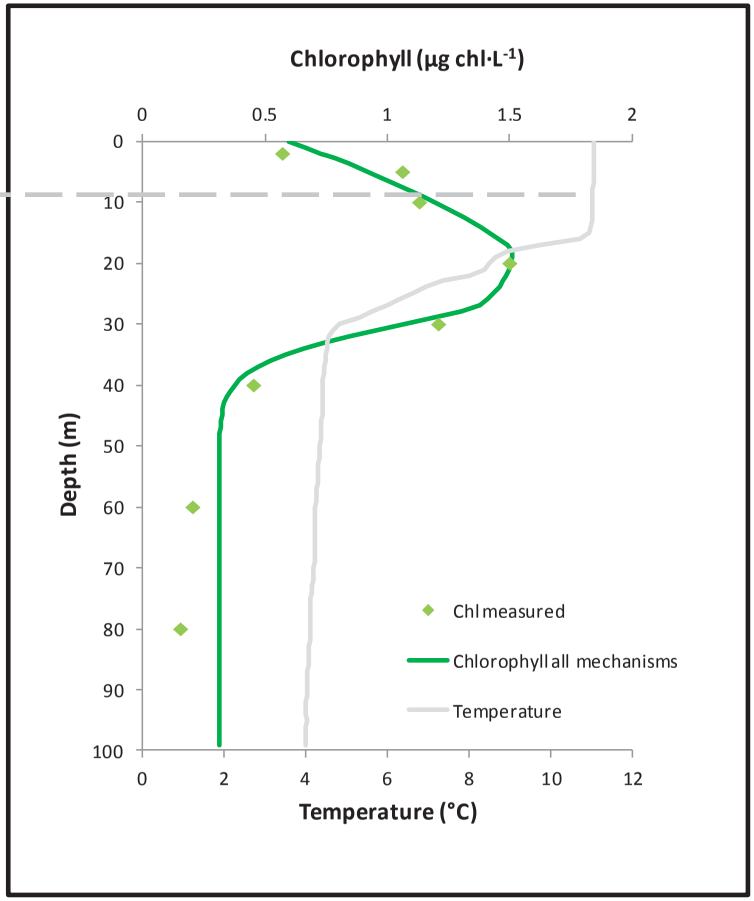

Figure 6.3e Chlorophyll profile based on a conversion with Chapra's function and measured data points (Chlorophyll data from Sterner 2010)

7.0 The Impact of Mechanisms on the DCM in Lake Superior

In the following section the impact on the water column chlorophyll profile by each previously described mechanism (Settling, Growth, Grazing and Shade Adaptation) will be evaluated by eliminating it from the complete model (all other mechanisms applied). Comparison of simulated chlorophyll profiles with and without the application of this mechanism will reveal its contribution to the DCM. Effects of settling are described first, followed by growth, grazing and chlorophyll to carbon ratios.

7.1 Removal of the Depth Variable Settling Velocity

The application of a constant settling velocity in the model results in a chlorophyll distribution differing more in shape than in extent (Figure 7.1). A constant settling velocity eliminates the particle retardation effect associated with the thermally induced, metalimnetic density gradient and results in the formation of a carbon peak at a greater depth. A differential, i.e. variable, settling velocity accommodates the retention and potential loss to grazing of smaller algae, with larger, more rapidly settling forms collecting at the sediment surface.

7.2 Removal of the Settling Mechanism ($v_s = 0$)

When algal cells are not allowed to settle through the elimination of the settling mechanism, the chlorophyll distribution follows the growth profile and the formation of a DCM is completely absent (Figure 7.2).

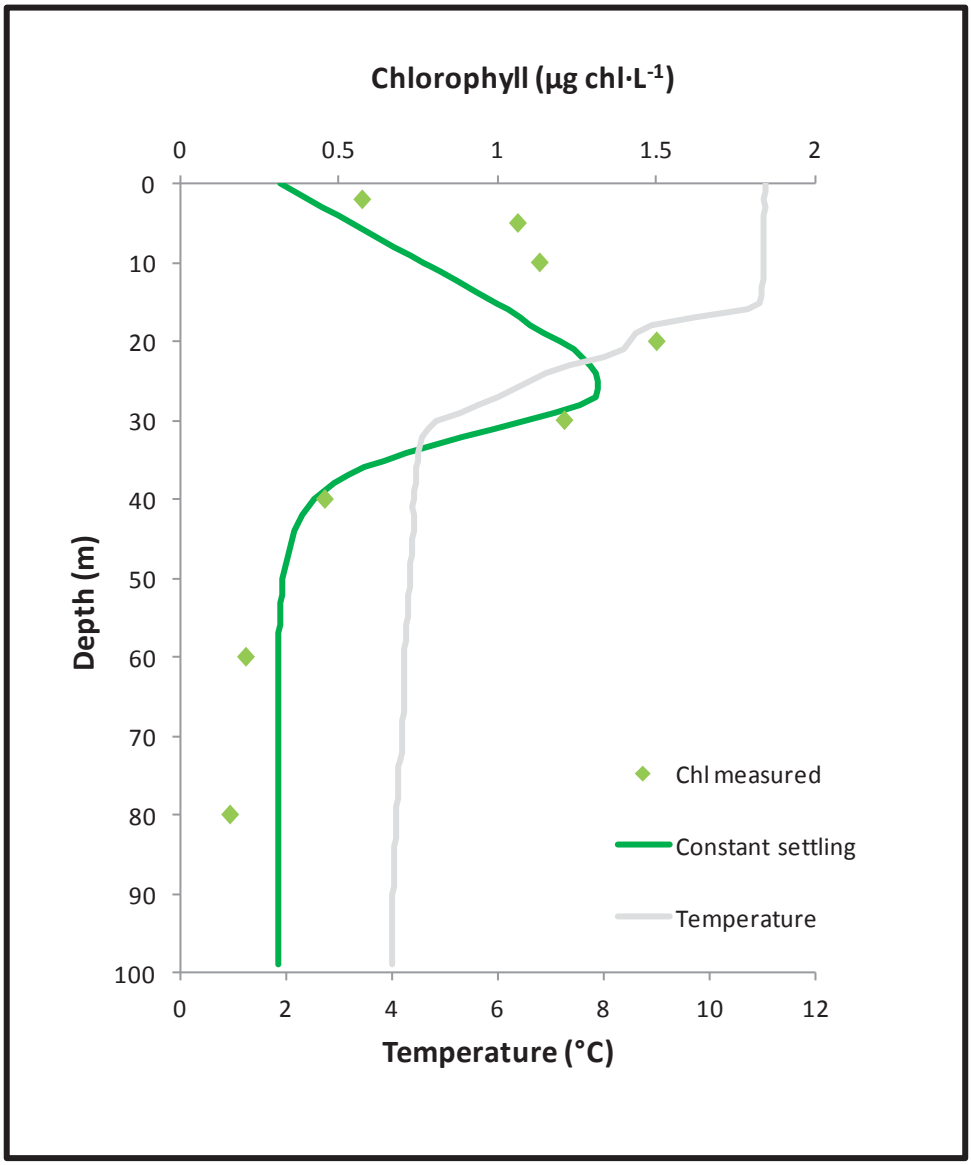

Figure 7.1 Constant settling (0.35 $m.d^{-1}$), all other mechanisms applied

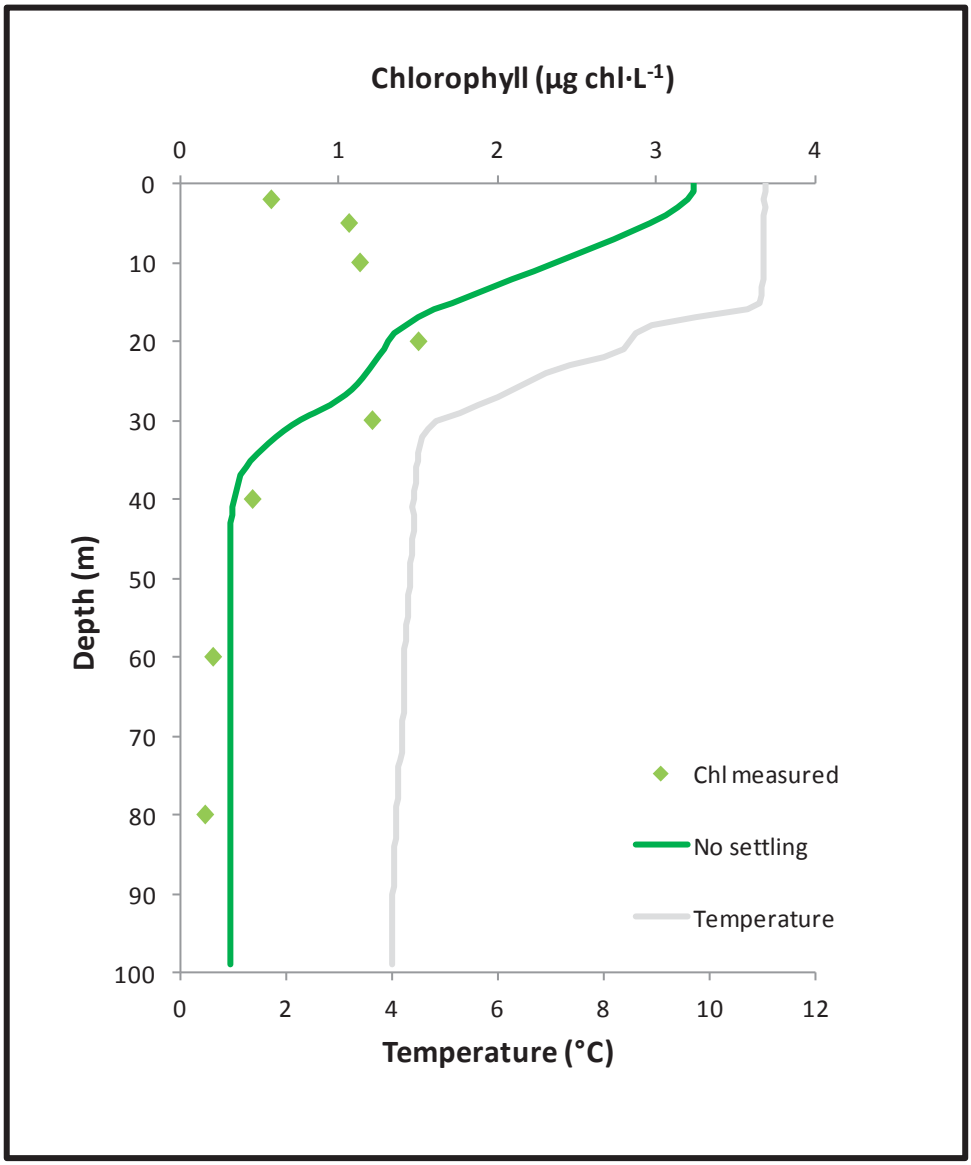

Figure 7.2 No settling, all other mechanisms applied

7.3 Removal of Growth Below the Mixed Layer (17m)

The elimination of growth below the mixed layer simulates the absence of all growth at DCM depth. The effect of growth at DCM depth is marginal and confirms the results from the previous analysis of the widely accepted paradigm (Figure 7.3).

7.4 Removal of All Growth

Even if all growth is absent, a DCM is still able to form by settling of algae present at initial conditions, even maintaining its characteristic shape. The extent of the DCM is severely reduced by lack of growth and signifies that the DCM is supported by algal growth in the epilimnion (Figure 7.4).

7.5 Removal of Zooplankton Grazing

Grazing loss is highest at the zooplankton biomass peak positioned at or close to the depth of maximum algal carbon biomass (previously discussed) and tends to remove elevated algal concentrations. The effect of grazing on the chlorophyll profile is similar and shows a decrease in chlorophyll concentrations at the DCM depth (Figure 7.5).

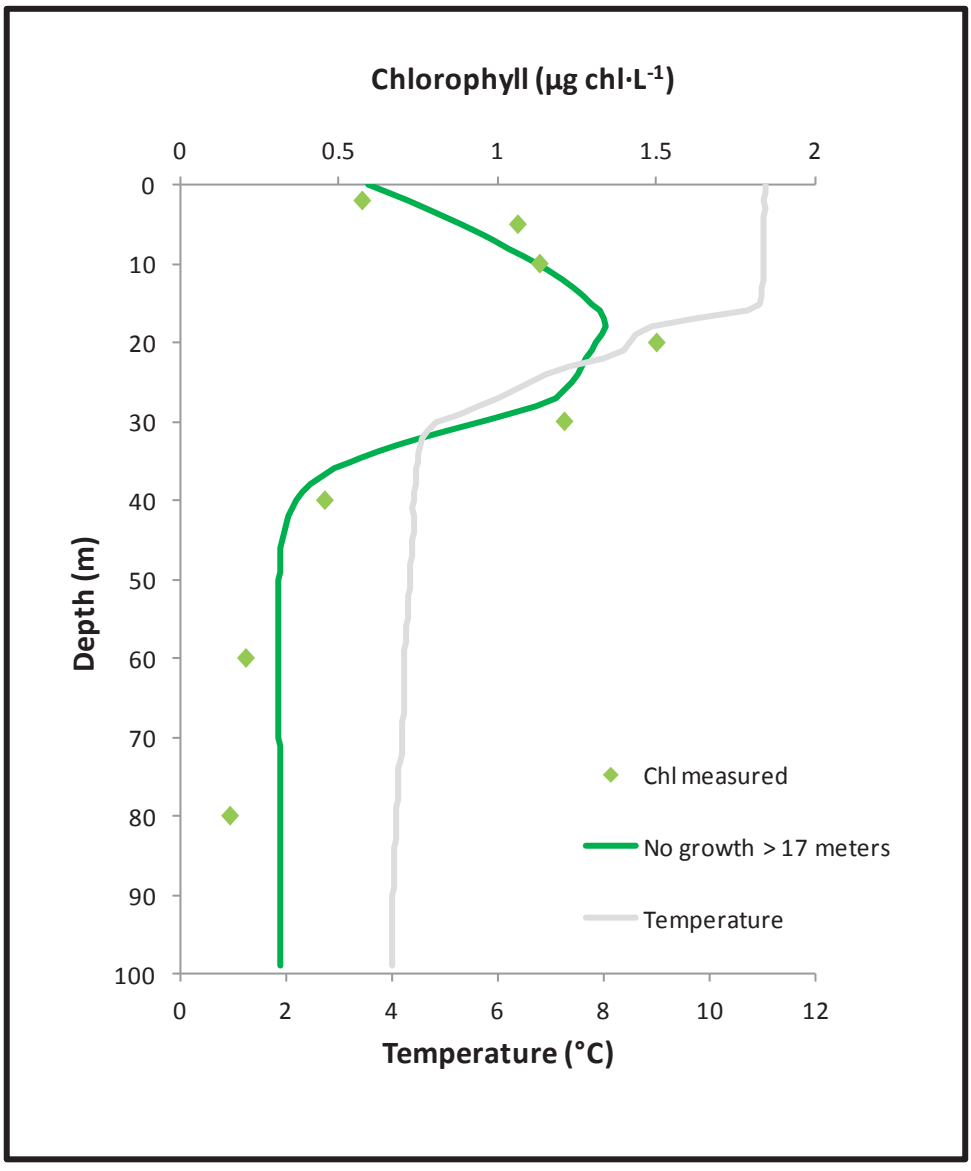

Figure 7.3 No growth below 17 meter depth, all other mechanisms applied

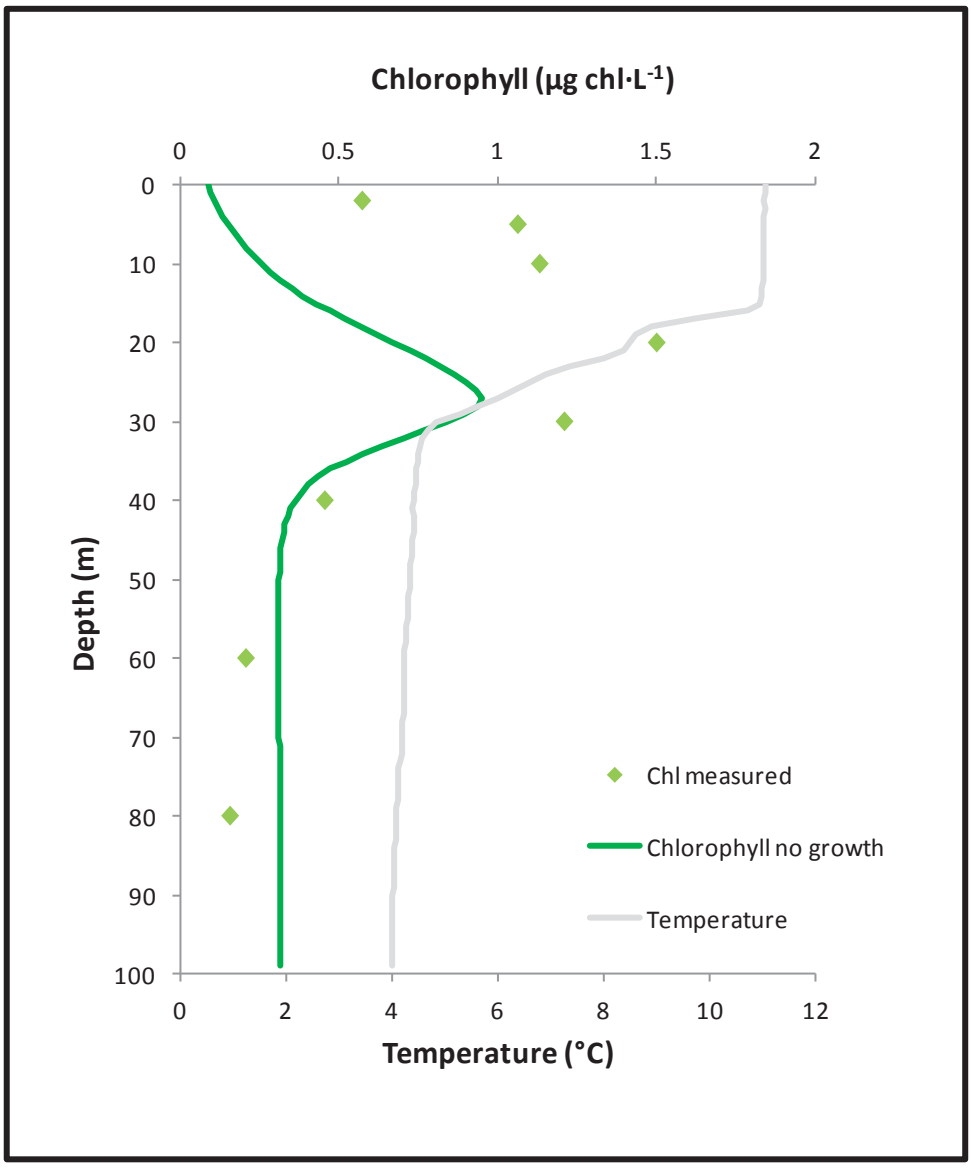

Figure 7.4 No growth, all other mechanisms applied

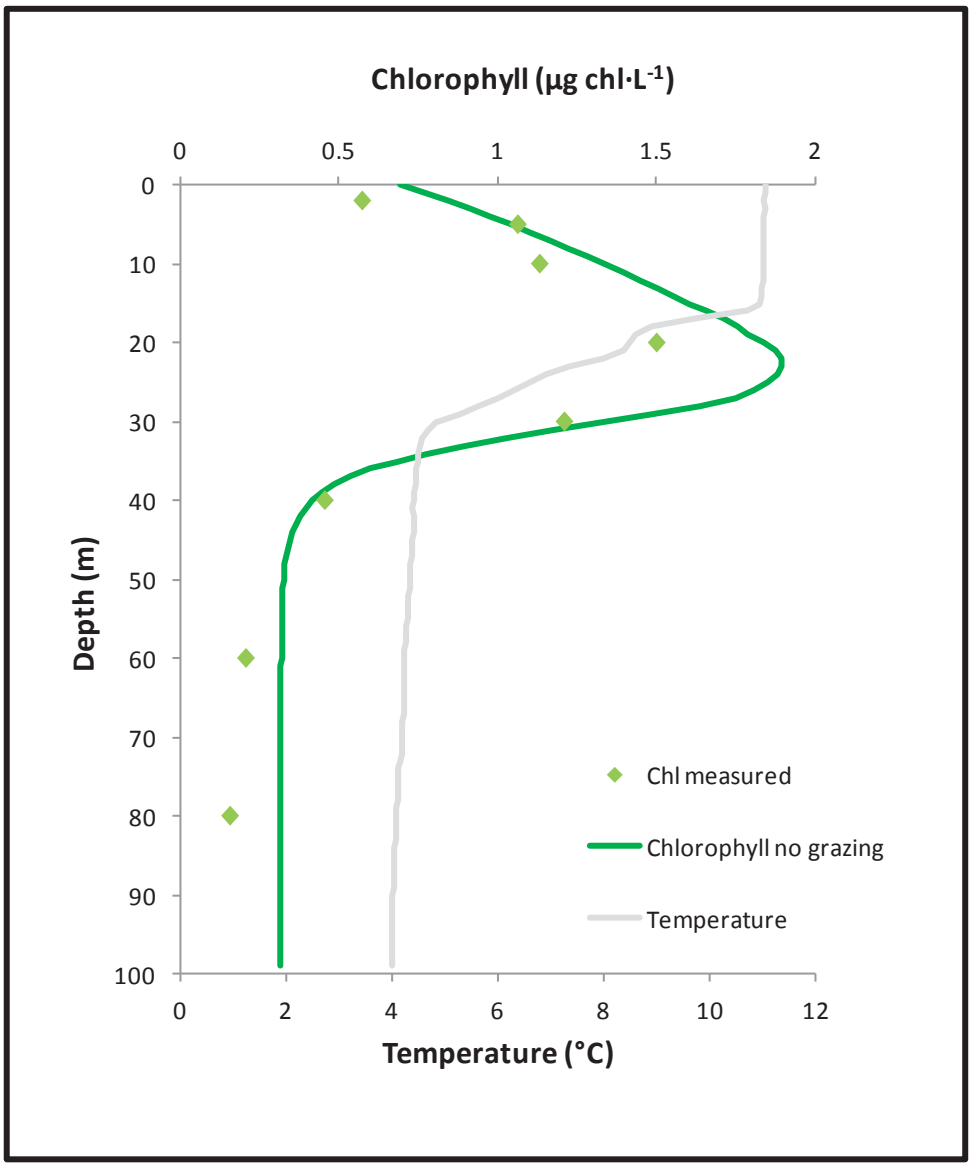

Figure 7.5 No grazing, all other mechanisms applied

7.6 Removal of the Depth Variable Chl:C Ratio

The effects of a depth-variable chlorophyll to carbon ratio was previously discussed and tends to affect the shape of the DCM more than its magnitude (Figure 6.2a).

7.7 Summary of Evaluated Mechanisms

The previously described mechanisms can be classified in two categories, those that primarily affect the shape and those that primarily affect the magnitude of the DCM. Processes of biological origin tend to govern the magnitude of the chlorophyll formation, regulating observed maxima, and those with a physical origin tend to regulate its shape. Depth-varying Chl:C ratios primarily affect the shape of the DCM (Figures 7.6a and b).

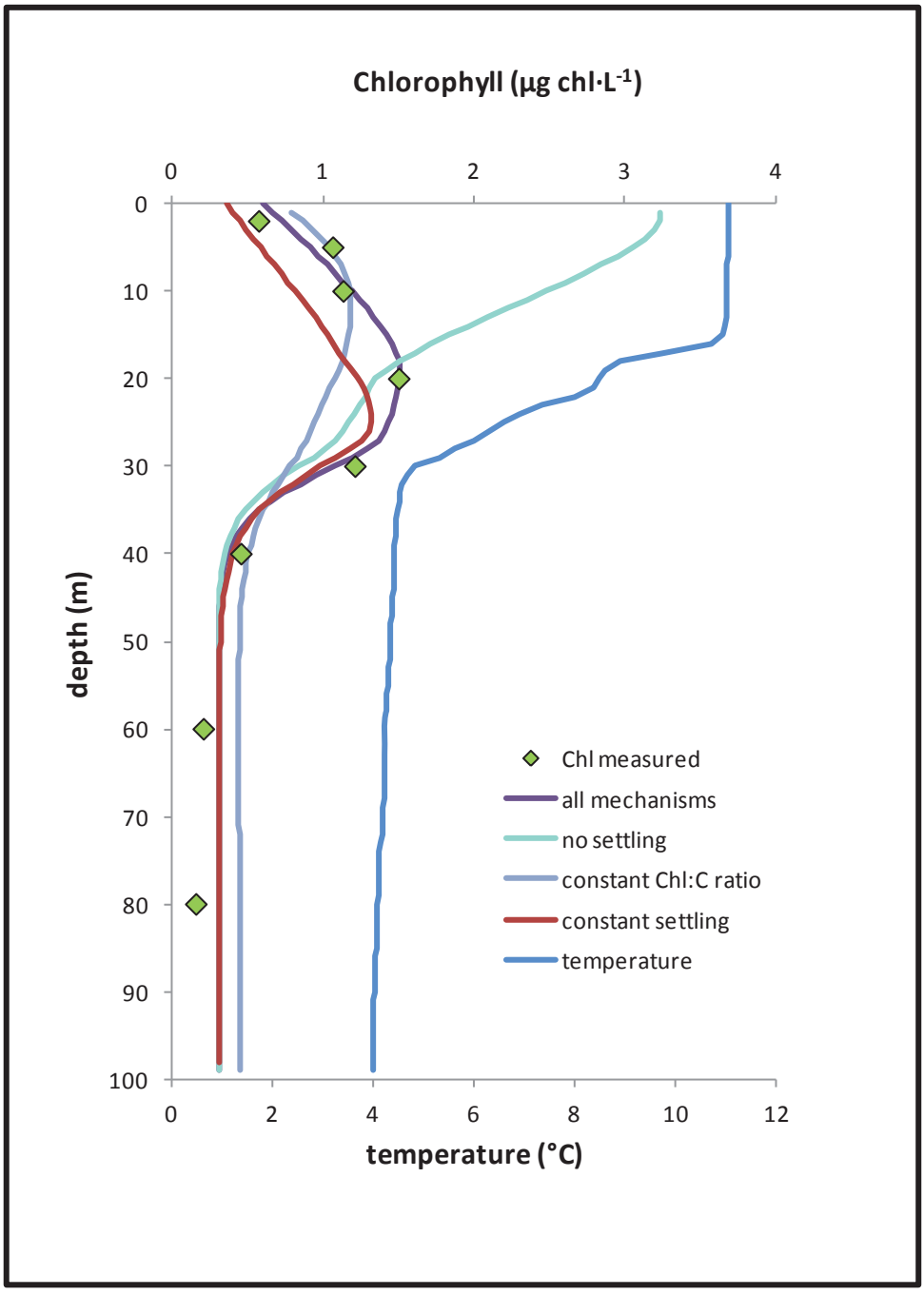

Figure 7.6a Effects of: eliminating settling, maintaining a constant settling velocity, and maintaining a constant Chl:C ratio on the water column chlorophyll profile

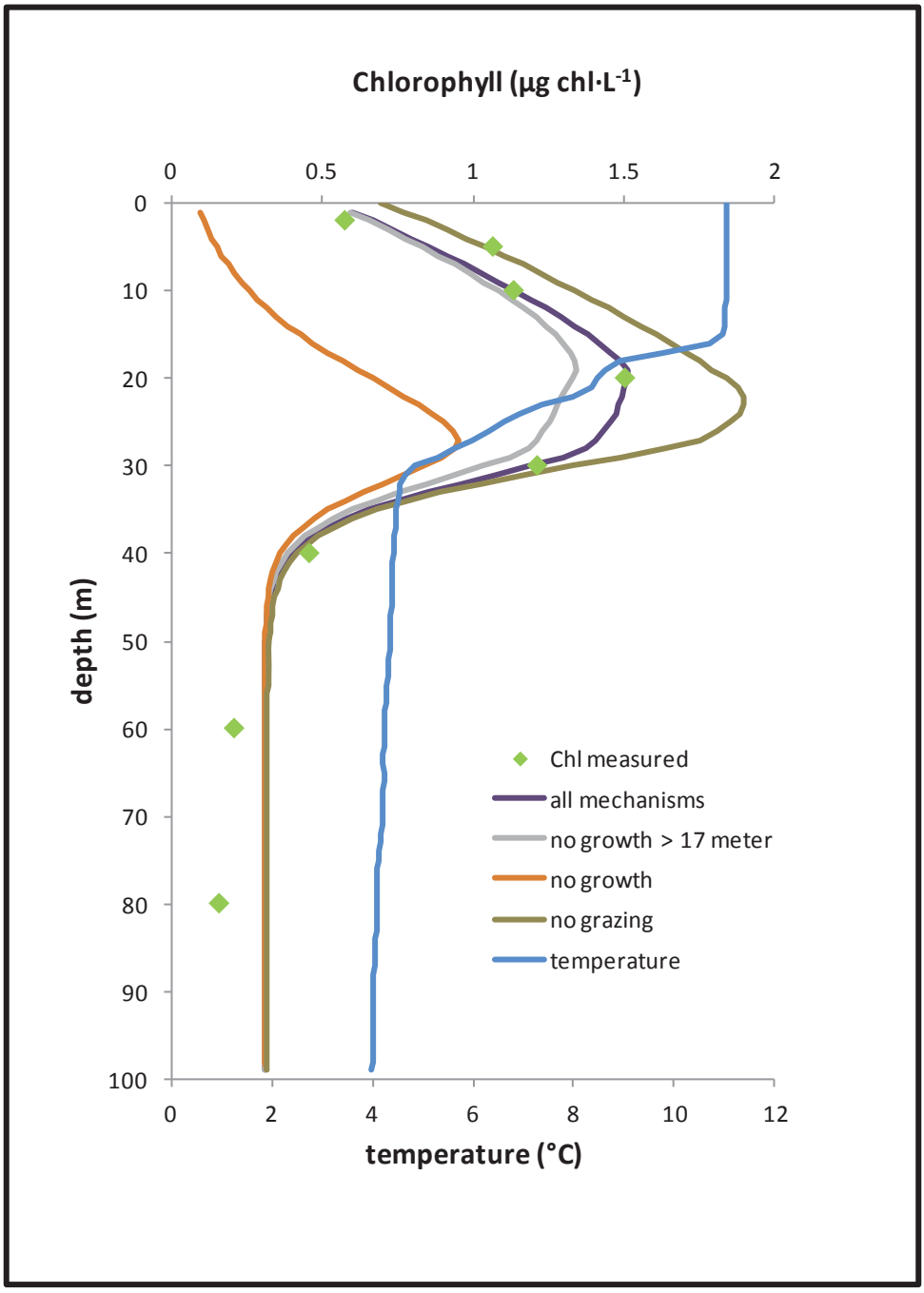

Figure 7.6b Effects of eliminating: growth below 17 meters, all growth, and zooplankton grazing on the water column chlorophyll distribution

8.0 Summary and Conclusions

The deep chlorophyll maximum is a regularly observed phenomenon in Lake Superior, and scientists have proposed a variety of physical and biological mechanisms to explain its dynamics. A numerical model, developed in this study, is applied in testing the impact of each mechanism, resulting in a conceptual understanding of DCM dynamics.

Settling during periods of reduced vertical mixing (induced by thermal stratification) delivers phytoplankton produced in the epilimnion to a low light environment within the metalimnion, favoring the formation of additional photosynthetic capacity (shade adaptation). The increased capacity leads to modest production in the metalimnion; however, growth below the mixed layer (>17m) has only a marginal effect on the DCM. The idea that the DCM stems from growth by algal species adapted to exploit a favorable niche is not supported by this work, and thus the paradigm “the DCM is a great place to live” needs to be abandoned.

Similarly, while zooplankton grazing effectively decreases the magnitude of the DCM peak, no support is developed in the work performed here for the hypothesis that this mechanism contributes to the shape of the DCM. The highest density of zooplankton is essentially coincident with the depth of the phytoplankton biomass (carbon) maximum, a likely result of grazers seeking peak prey levels.

Subsurface peaks in particulate organic carbon are primarily the result of settling of phytoplankton growing in the epilimnion. While chlorophyll

accumulates coincidentally with the carbon, it is shade adaptation near the base of the photic zone that leads to increased cellular chlorophyll content and the development of a pigment maximum below that of the carbon maximum. Where light conditions particularly favor the process, shade adaptation mediates the magnitude, shape and vertical position of the chlorophyll peak. The observed separation of the carbon biomass and chlorophyll maximum should caution scientists to equate the DCM with a large nutrient pool that is available to higher trophic levels.

The variable settling velocity resulting from a temperature induced density gradient has only a minor contributing effect on the DCM formation and maintenance. However, the effects on the algal assemblage are more pronounced, since the larger and denser particles quickly pass through the DCM and smaller cells accumulate along the density gradient, possibly increasing the relative abundance of certain algal species. The domination of the DCM by a single algal species should therefore not immediately be interpreted as the presence of specially adapted algae capable of exploiting a favorable niche.

The ecological significance of the DCM should not be separated from the underlying carbon dynamics. When evaluated in its entirety, the DCM becomes the projected image of a structure that remains elusive to measure but represents the foundation of all higher trophic levels. The results presented here may support a (re)interpretation of chlorophyll profiles in terms of carbon biomass.

These results also offer guidance in examine ecosystem perturbations such as climate change. For example, warming would be expected to prolong the period of thermal stratification, extending the late summer period of suboptimal (phosphorus-limited) growth and attendant transport of phytoplankton to the metalimnion. This reduction in epilimnetic algal production would decrease the supply of algae to the metalimnion, possibly reducing the supply of prey to the grazer community. This work demonstrates the value of modeling to challenge and advance our understanding of ecosystem dynamics, steps vital to reliable testing of management alternatives.

9.0 References

Abbott MR, Denman KL, Powell TM, Richerson PJ, Richards RC, Goldman CR. 1984. Mixing and the dynamics of the deep chlorophyll maximum in Lake Tahoe. Limnology and Oceanography. 29(4):862–878.

Alldredge AL, Cowles TJ, MacIntyre S, Rines JEB, Donaghay PL, Greenlaw CF, Holliday DV, Dekshenieks MM, Sullivan JM, Zaneveld JRV. 2002. Occurrence and mechanisms of formation of a dramatic thin layer of marine snow in a shallow Pacific fjord. Marine Ecology Progress Series. 233:1–12.

Alonso-Sáez L, Vázquez-Domínguez E, Cardelús C, Pinhassi J, Sala MM, Lekunberri I, Balagué V, Vila-Costa M, Unrein F, Massana R, Simó R, Gasol JM. 2008. Factors controlling the year-round variability in carbon flux through bacteria in a coastal marine system. Ecosystems. 11(3):397–409.

Ambrose RB, Wool TA, Martin JL. 1993. The water quality analysis simulation program, WASP5, Part A: Model documentation. Environmental Research Lab, USEPA, Athens, GS.

Anagnostou E, Sherrell RM. 2008. A MAGIC method for sub-nanomolar orthophosphate determination in freshwater. Limnology and Oceanography: Methods. 6:64–74.

Anderson GC. 1969. Subsurface chlorophyll maximum in the northeast Pacific Ocean. Limnology and Oceanography. 14(3):386–391.

Anning T, MacIntyre HL, Pratt SM, Sammes PJ, Gibb S, Geider RJ. 2000. Photoacclimation in the marine diatom Skeletonema costatum. Limnology and Oceanography. 45(8):1807–1817.

Auer MT, Bub LA. 2004. Selected features of the distribution of chlorophyll along the southern shore of Lake Superior. Journal of Great Lakes Research. 30(1): 269–284.

Auer MT, Powell KD. 2004. Heterotrophic bacterioplankton dynamics at a site off the southern shore of Lake Superior. Journal of Great Lakes Research. 30(1):214–229.

Auer MT, Gatzke TL. 2004. The spring runoff event, thermal bar formation, and cross margin transport in Lake Superior. Journal of Great Lakes Research. 30(1):64-81.

Auer MT, Tomlinson LM, Higgins SN, Malkin SY, Howell ET, Bootsma HA. 2010. Great Lakes Cladophora in the 21st century: same algae--different ecosystem. Journal of Great Lakes Research. 36(2):248-255.

Baehr MM, McManus J. 2003. The measurement of phosphorus and its spatial and temporal variability in the western arm of Lake Superior. Journal of Great Lakes Research. 29(3):479-487.

Baker JE, Eisenreich SJ, Eadie BJ. 1991. Sediment trap fluxes and benthic recycling of organic carbon, polycyclic aromatic hydrocarbons, and polychlorobiphenyl congeners in Lake Superior. Environmental Science and Technology. 25(3):500–509.

Barbiero RP, Tuchman ML. 2001. Results from the U.S. EPA's Biological Open Water Surveillance Program of the Laurentian Great Lakes: I. Introduction and Phytoplankton Results. Journal of Great Lakes Research. 27(2):134-154.

Barbiero RP, Tuchman ML. 2004. The deep chlorophyll maximum in Lake Superior. Journal of Great Lakes Research. 30(1):256–268.

Bierman Jr VJ, Dolan DM. 1981. Modeling of phytoplankton-nutrient dynamics in Saginaw Bay, Lake Huron. Journal of Great Lakes Research. 7(4):409–439.

Birge EA, Juday C. 1911. The inland lakes of Wisconsin: The dissolved gases in the water and their biological significance. Wisconsin Geological and Natural History Survey Bulletin. 22:1–259

Brooks AS, Torke BG. 1977. Vertical and seasonal distribution of chlorophyll a in Lake Michigan. Journal of the Fisheries Board of Canada. 34(12):2280–2287.

Bub LA. 2001. Spatial and temporal distribution of phytoplankton in Lake Superior. M.S. Thesis. Michigan Technological University, Houghton, MI.

Burnett L, Moorhead D, Hawes I, Howard-Williams C. 2006. Environmental factors associated with deep chlorophyll maxima in dry valley Lakes, South Victoria Land, Antarctica. Arctic, Antarctic, and Alpine Research. 38(2):179–189.

Camacho A. 2006. On the occurrence and ecological features of deep chlorophyll maxima (DCM) in Spanish stratified lakes. Limnetica. 25(1-2):453–478.

Casotti R, Landolfi A, Brunet C, D'Ortenzio F, Mangoni O, d'Alcalà MR, Denis M. 2003. Composition and dynamics of the phytoplankton of the Ionian Sea (eastern Mediterranean). Journal of Geophysical Research. 108(C9):8116.

Cerco CF, Cole TM. 1994. Three-dimensional eutrophication model of Chesapeake Bay. Volume 1: Main Report. DTIC Document.

Christensen DL, Carpenter SR, Cottingham KL. 1995. Predicting chlorophyll vertical distribution in response to epilimnetic nutrient enrichment in small stratified lakes. Journal of Plankton Research. 17(7):1461–1477.

Cole JJ, Likens GE, Hobbie JE. 1984. Decomposition of planktonic algae in an oligotrophic lake. Oikos. 42(3):257–266.

Condie SA. 1999. Settling regimes for non–motile particles in stratified waters. Deep Sea Research I: Oceanographic Research Papers. 46(4):681–699.

Crank J. 1979. The mathematics of diffusion. Volume 1. Clarendon Press, Oxford.

Cullen JJ. 1982. The deep chlorophyll maximum: comparing vertical profiles of chlorophyll a. Canadian Journal of Fisheries and Aquatic Sciences. 39(5):791–803.

Cullen JJ, Lewis MR. 1988. The kinetics of algal photoadaptation in the context of vertical mixing. Journal of Plankton Research. 10(5):1039–1063.

Denman KL, Gargett AE. 1983. Time and space scales of vertical mixing and advection of phytoplankton in the upper ocean. Limnology and Oceanography. 28(5):801–815.

Diehl S. 2002. Phytoplankton, light, and nutrients in a gradient of mixing depths: Theory. Ecology. 83(2):386–398.

Droop MR. 1983. 25 years of algal growth kinetics: A personal view. Botanica Marina. 26(3):99–112.

Duteil O, Lazar A, Dandonneau Y, Wainer I, Menkes C. 2009. Deep chlorophyll maximum and upper ocean structure interactions: Case of the Guinea Thermal Dome. Journal of Marine Research. 67(2):239–271.

Eadie BJ, Chambers RL, Gardner WS, Bell GL. 1984. Sediment trap studies in Lake Michigan: Resuspension and chemical fluxes in the southern basin. Journal of Great Lakes Research. 10(3):307–321.

Elenbaas KD. 2001. Heterotrophic bacterioplankton and related environmental forcing conditions in Lake Superior. M.S. Thesis. Michigan Technological University, Houghton, MI.

Fahnenstiel GL, Glime J. 1983. Subsurface chlorophyll maximum and associated Cyclotella pulse in Lake Superior. Internationale Revue der gesamten Hydrobiologie und Hydrographie. 68(5):605–616.

Fahnenstiel GL, Scavia D. 1987. Dynamics of Lake Michigan phytoplankton: the deep chlorophyll layer. Journal of Great Lakes Research. 13(3):285–295.

Fahnenstiel GL, Chandler JF, Carrick HJ, Scavia D. 1989. Photosynthetic characteristics of phytoplankton communities in Lakes Huron and Michigan: PI parameters and end-products. Journal of Great Lakes Research. 15(3):394–407.

Fahnenstiel GL, Schelske CL, Moll RA. 1984. *In situ* quantum efficiency of Lake Superior Phytoplankton. Journal of Great Lakes Research. 10(4):399–406.

Faugeras B, Bernard O, Sciandra A, Levy M. 2004. A mechanistic modelling and data assimilation approach to estimate the carbon/chlorophyll and carbon/nitrogen ratios in a coupled hydrodynamical-biological model. Nonlinear Processes in Geophysics. 11:515–533.

Fee EJ. 1976. The vertical and seasonal distribution of chlorophyll in lakes of the Experimental Lakes Area, northwestern Ontario: Implications for primary production estimates. Limnology and Oceanography. 21(6):767–783.

Fennel K, Boss E. 2003. Subsurface maxima of phytoplankton and chlorophyll: Steady-state solutions from a simple model. Limnology and Oceanography. 48(4):1521–1534.

Fernandez M, Bianchi M, Van Wambeke F. 1994. Bacterial biomass, heterotrophic production and utilization of dissolved organic matter photosynthetically produced in the Almeria-Oran front. Journal of Marine Systems. 5(3-5):313–325.

Field CB, Behrenfeld MJ, Randerson JT, Falkowski P. 1998. Primary production of the biosphere: Integrating terrestrial and oceanic components. Science. 281(5374):237–240.

Flemer DA. 1969. Chlorophyll analysis as a method of evaluating the standing crop phytoplankton and primary productivity. Chesapeake Science. 10(3):301–306.

Geider RJ, MacIntyre HL, Kana TM. 1997. Dynamic model of phytoplankton growth and acclimation: responses of the balanced growth rate and the chlorophyll a: carbon ratio to light, nutrient-limitation and temperature. Marine Ecology Progress Series. 148(1-3):187–200.

Geider RJ, MacIntyre HL, Kana TM. 1998. A dynamic regulatory model of phytoplanktonic acclimation to light, nutrients, and temperature. Limnology and Oceanography. 43(4):679–694.

González-Gil S, Keafer BA, Jovine RVM, Aguilera A, Lu S, Anderson DM. 1998. Detection and quantification of alkaline phosphatase in single cells of phosphorus-starved marine phytoplankton. Marine Ecology Progress Series. 164:21–35.

Grigorszky I, Padisák J, Borics G, Schitchen C, Borbély G. 2003. Deep chlorophyll maximum by Ceratium hirundinella (OF Müller) Bergh in a shallow oxbow in Hungary. Hydrobiologia. 506(1):209–212.

Guerrero R, Montesinos E, Pedros-Alio C, Esteve I, Mas J, van Gemerden H, Hofman PAG, Bakker JF. 1985. Phototrophic sulfur bacteria in two Spanish lakes: vertical distribution and limiting factors. Limnology and Oceanography. 30(5):919–931.

Hanson CE, Pesant S, Waite AM, Pattiaratchi CB. 2007. Assessing the magnitude and significance of deep chlorophyll maxima of the coastal eastern Indian Ocean. Deep Sea Research Part II: Topical Studies in Oceanography. 54(8-10):884–901.

Heinen EA, McManus J. 2004. Carbon and nutrient cycling at the sediment-water boundary in western Lake Superior. Journal of Great Lakes Research. 30(1):113–132.

Herman AW, Sameoto DD, Longhurst AR. 1981. Vertical and horizontal distribution patterns of copepods near the shelf break south of Nova Scotia. Canadian Journal of Fisheries and Aquatic Sciences. 38(9):1065–1076.

Holm-Hansen O, Hewes CD. 2004. Deep chlorophyll-a maxima (DCMs) in Antarctic waters. Polar Biology. 27(11):699–710.

Huisman J, Thi NNP, Karl DM, Sommeijer B. 2006. Reduced mixing generates oscillations and chaos in the oceanic deep chlorophyll maximum. Nature. 439:322–325.

Ivanikova NV, McKay RML, Bullerjahn GS, Sterner RW. 2007. Nitrate utilization by phytoplankton in Lake Superior is impaired by low nutrient (P, Fe) availability and seasonal light limitation — A Cyanobacterial bioreporter study. Journal of Phycology. 43(3):475–484.

Kiefer DA, Olson RJ, Holm-Hansen O. 1976. Another look at the nitrite and chlorophyll maxima in the central North Pacific. Deep Sea Research and Oceanographic Abstracts. 23:1199–1208.

Klausmeier CA, Litchman E. 2001. Algal games: The vertical distribution of phytoplankton in poorly mixed water columns. Limnology and Oceanography. 46(8):1998–2007.

Kruskopf M, Flynn KJ. 2006. Chlorophyll content and fluorescence responses cannot be used to gauge reliably phytoplankton biomass, nutrient status or growth rate. New Phytologist. 169(3):525–536.

Letelier RM, Karl DM, Abbott MR, Bidigare RR. 2004. Light driven seasonal patterns of chlorophyll and nitrate in the lower euphotic zone of the North Pacific subtropical gyre. Limnology and Oceanography. 49(2):508–519.

Longhurst AR. 1976. Interactions between zooplankton and phytoplankton profiles in the eastern tropical Pacific Ocean. Deep Sea Research and Oceanographic Abstracts. 23:729–754.

López-Sandoval DC, Fernández A, Marañón E. 2011. Dissolved and particulate primary production along a longitudinal gradient in the Mediterranean Sea. Biogeosciences. 8:815–825.

Lund JW, Kipling C, Lecren ED. 1958. The inverted microscope method of estimating algal numbers and the statistical basis of estimation by counting. Hydrobiologia. 11:143–170.

MacIntyre HL, Kana TM, Anning T, Geider RJ. 2002. Photoacclimation of photosynthesis irradiance response curves and photosynthetic pigments in microalgae and cyanobacteria. Journal of Phycology. 38(1):17–38.

MacIntyre S, Alldredge AL, Gotschalk CC. 1995. Accumulation of marine snow at density discontinuities in the water column. Limnology and Oceanography. 40(3):449–468.

Malkin SY, Guildford SJ, Hecky RE. 2008. Modeling the growth response of Cladophora in a Laurentian Great Lake to the exotic invader Dreissena and to lake warming. Limnology and Oceanography. 53(3):1111–1124.

Matile P, Hörtensteiner S, Thomas H. 1999. Chlorophyll degradation. Annual Review of Plant Biology. 50(1):67–95.

McManus J, Heinen EA, Baehr MM. 2003. Hypolimnetic oxidation rates in Lake Superior: Role of dissolved organic material on the lake's carbon budget. Limnology and Oceanography. 48(4):1624–1632.

Mellard JP, Yoshiyama K, Litchman E, Klausmeier CA. 2011. The vertical distribution of phytoplankton in stratified water columns. Journal of Theoretical Biology. 269(1):16–30.

Moll RA, Stoermer EF. 1982. Hypothesis relating trophic status and subsurface chlorophyll maxima of lakes. Archiv fur Hydrobiologie. 94(4):425–440.

Munawar IF, Munawar M. 2009. Phytoplankton communities of Lake Superior, 2001: Changing species composition and biodiversity of a pristine ecosystem. State of Lake Superior. Goodword Books, New Delhi (India). 319–359.

Munawar M, Munawar IF. 1978. Phytoplankton of Lake Superior 1973. Journal of Great Lakes Research. 4(3):415–442.

Nõges P, Poikane S, Kõiv T, Nõges T. 2010. Effect of chlorophyll sampling design on water quality assessment in thermally stratified lakes. Hydrobiologia. 649(1):157–170.

Olson TA, Odlaug TO. 1966. Limnological observations on western Lake Superior. Proc. 9th Conf. Great Lakes Res.,pp. 109-118 Internat. Assoc. Great Lakes Res.

Pedrós-Alió C, Gasol JM, Guerrero R. 1987. On the ecology of a Cryptomonas phaseolus population forming a metalimnetic bloom in Lake Cisó, Spain: Annual distribution and loss factors. Limnology and Oceanography. 32(2):285–298.

Peters RH, Downing JA. 1984. Empirical analysis of zooplankton filtering and feeding rates. Limnology and Oceanography. 29(4):763–784.

Pettersson K. 1980. Alkaline phosphatase activity and algal surplus phosphorus as phosphorus-deficiency indicators in Lake Erken. Archiv fur Hydrobiologie. 89(1/2):54–87.

Pettersson K, Jansson M. 1978. Determination of phosphatase activity in lake water–a study of methods. Proceedings: 20th Congress, Internationale Vereinigung fur Theoretische und Angewandte Limnologie.

Pilati A, Wurtsbaugh WA. 2003. Importance of zooplankton for the persistence of a deep chlorophyll layer: A limnocorral experiment. Limnology and Oceanography. 48(1):249–260.

Platt T, Gallegos CL, Harrison WG. 1980. Photoinhibition of photosynthesis in natural assemblages of marine phytoplankton. Journal of Marine Research. 38(4):687–701.

Priscu JC, Goldman CR. 1983. Seasonal dynamics of the deep-chlorophyll maximum in Castle Lake, California. Canadian Journal of Fisheries and Aquatic Sciences. 40(2):208–214.

Pugnetti A, Armeni M, Camatti E, Crevatin E, Dell'Anno A, Del Negro P, Milandri A, Socal G, Umani SF, Danovaro R. 2005. Imbalance between phytoplankton production and bacterial carbon demand in relation to mucilage formation in the Northern Adriatic Sea. Science of the Total Environment. 353(1-3):162–177.

Rengefors K, Ruttenberg KC, Haupert CL, Taylor C, Howes BL, Anderson DM. 2003. Experimental investigation of taxon-specific response of alkaline phosphatase activity in natural freshwater phytoplankton. Limnology and Oceanography. 48(3):1167–1175.

Reynolds CS. 1994. The long, the short and the stalled: on the attributes of phytoplankton selected by physical mixing in lakes and rivers. Hydrobiologia. 289(1):9–21.

Rose C, Axler RP. 1997. Uses of alkaline phosphatase activity in evaluating phytoplankton community phosphorus deficiency. Hydrobiologia. 361(1):145–156.

Saros JE, Interlandi SJ, Doyle S, Michel TJ, Williamson CE. 2005. Are the deep chlorophyll maxima in alpine lakes primarily induced by nutrient availability, not UV avoidance? Arctic, Antarctic, and Alpine Research. 37(4):557–563.

Serizawa H, Amemiya T, Itoh K. 2010. Effects of buoyancy, transparency and zooplankton feeding on surface maxima and deep maxima: Comprehensive mathematical model for vertical distribution in cyanobacterial biomass. Ecological Modelling. 221(17):2028–2037.

Shortreed KS, Stockner JG. 1990. Effect of nutrient additions on lower trophic levels of an oligotrophic lake with a seasonal deep chlorophyll maximum. Canadian Journal of Fisheries and Aquatic Sciences. 47(2):262–273.

Siew PF. 2003. Phosphorus distribution and cycling in the Keweenaw Peninsula region of Lake Superior. M.S. Thesis. Michigan Technological University, Houghton, MI.

Steele JH. 1964. A study of production in the Gulf of Mexico. DTIC Document.

Steele JH, Baird IE. 1961. Relations between primary production, chlorophyll and particulate carbon. Limnology and Oceanography. 6(1):68–78.

Steele JH, Yentsch CS. 1960. The vertical distribution of chlorophyll. Journal of the Marine Biological Association of the United Kingdom. 39(02):217–226.

Sterner RW. 2010. In situ-measured primary production in Lake Superior. Journal of Great Lakes Research. 36(1):139–149.

Sterner RW. 2011. C: N: P stoichiometry in Lake Superior: freshwater sea as end member. Inland Waters. 1(1):29–46.

Sterner RW, Smutka TM, McKay RML, Xiaoming Q, Brown ET, Sherrell RM. 2004. Phosphorus and trace metal limitation of algae and bacteria in Lake Superior. Limnology and Oceanography. 49(2):495–507.

Taguchi S, DiTullio GR, Laws EA. 1988. Physiological characteristics and production of mixed layer and chlorophyll maximum phytoplankton populations in the Caribbean Sea and western Atlantic Ocean. Deep Sea Research Part I. Oceanographic Research Papers. 35(8):1363–1377.

Takahashi M, Hori T. 1984. Abundance of picophytoplankton in the subsurface chlorophyll maximum layer in subtropical and tropical waters. Marine Biology. 79(2):177–186.

Takahashi M, Ichimura S. 1970. Photosynthetic properties and growth of photosynthetic sulfur bacteria in lakes. Limnology and Oceanography. 15(6):929–944.

Urban NR, Munawar M, Munawar IF. 2009. Nutrient cycling in Lake Superior: a retrospective and update. State of Lake Superior. Goodword Books, New Delhi (India). 83–115.

Urban NR, Jeong J, Chai Y. 2004. The Benthic Nepheloid Layer (BNL) north of the Keweenaw Peninsula in Lake Superior: Composition, dynamics, and

role in sediment transport. Journal of Great Lakes Research. 30(1):133–146.

Vaillancourt RD, Marra J, Seki MP, Parsons ML, Bidigare RR. 2003. Impact of a cyclonic eddy on phytoplankton community structure and photosynthetic competency in the subtropical North Pacific Ocean. Deep Sea Research Part I: Oceanographic Research Papers. 50(7):829–847.

Varela RA, Cruzado A, Tintore J, Ladona EG. 1992. Modelling the deep-chlorophyll maximum: A coupled physical-biological approach. Journal of Marine Research. 50(3):441–463.

Vili D, Orli M, Jasprica N. 2008. The deep chlorophyll maximum in the coastal north eastern Adriatic Sea, July 2007. Acta Botanica Croatica. 67(1):33–43.

Vincent WF, Wurtsbaugh W, Neale PJ, Richerson PJ. 1986. Polymixis and algal production in a tropical lake: latitudinal effects on the seasonality of photosynthesis. Freshwater Biology. 16(6):781–803.

Van Wambeke F, Goutx M, Striby L, Sempéré R, Vidussi F. 2001. Bacterial dynamics during the transition from spring bloom to oligotrophy in the northwestern Mediterranean Sea: relationships with particulate detritus and dissolved organic matter. Marine Ecology Progress Series. 212:89–105.

Watson NHF, Thomson KPB, Elder FC. 1975. Sub-thermocline biomass concentration detected by transmissometer in Lake Superior. Verhandlungen Internationale Vereinigung Limnologie. 19:682–688.

Williamson CE, Sanders RW, Moeller RE, Stutzman PL. 1996. Utilization of subsurface food resources for zooplankton reproduction: Implications for diel vertical migration theory. Limnology and Oceanography. 41(2):224–233.

Williamson R, Field JG, Shillington FA, Jarre A, Potgieter A. 2010. A Bayesian approach for estimating vertical chlorophyll profiles from satellite remote sensing: proof-of-concept. ICES Journal of Marine Science. 68(4):792–799.

Yurista PM, Kelly JR, Miller SE. 2009. Lake Superior zooplankton biomass: Alternate estimates from a probability-based net survey and spatially extensive LOPC surveys. Journal of Great Lakes Research. 35(3):337–346.